



UNIVERSITEIT VAN PRETORIA
UNIVERSITY OF PRETORIA
YUNIBESITHI YA PRETORIA

Comparison of metabolome attenuation in monolayer and three dimensional hepatocyte cultures

Gerben de Koker

A dissertation submitted in fulfilment of the requirements for the degree

Magister Scientiae

in

Pharmacology

Department of Pharmacology, Faculty of Health Sciences,
School of Medicine, University of Pretoria

Supervisor: Prof AD Cromarty, Department of Pharmacology, UP
Co-supervisor: Dr T Hurrell, Department of Physiology and Pharmacology,
Karolinska Institutet

Co-supervisor: Mr JC Cardeano, Department of Pharmacology, UP

2019

Declaration of originality

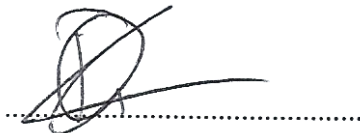
University of Pretoria
School of Medicine
Faculty of Health Sciences
Department of Pharmacology

I,	Gerben de Koker
Student number	11145375
Subject of work	Dissertation
Title	“Comparison of metabolome attenuation in monolayer and three dimensional hepatocyte cultures”

Declaration

1. I understand what plagiarism is and am aware of the University’s policy in this regard
2. I declare that this dissertation is my own original work. Where other people’s work has been used, this has been properly acknowledged and referenced in accordance with applicable requirements
3. I have not used work previously produced by another student or any other person to hand in as my own
4. I have not allowed, and will not allow, anyone to copy my work with the intention of passing it off as his or her own work

Signature



A handwritten signature in black ink, consisting of a large, stylized 'G' followed by a horizontal line, is written over a dotted line.

Acknowledgements

I would like to acknowledge the following people for their contribution and support:

My supervisor Dr Tracey Hurrell, for her mentorship in the lab and during the writing process, as well as believing in me when I lost hope. Thank you for being the inspiring researcher that I needed you to be.

My supervisor Prof Duncan Cromarty for his endless pool of knowledge to provide advice, support and influence my growing interest in LC-MS based research. "Thank you for the fish"

My supervisor Joao Cardeano, who helped spark my interest in LC-MS based research, providing knowledge and advice for the LC-MS process. Thank you for always making the lab a fun and welcoming environment.

The National Research Foundation and through my supervisor Dr Tracey Hurrell's Thuthuka Funding, whose financial contribution allowed this project to be undertaken and completed.

To the Department of Pharmacology, thank you for providing me opportunities to grow as a researcher and helping to shape me with invaluable knowledge.

To friends and colleagues at the Department of Pharmacology for all their support. Especially Margo Nel, whose assistance in the cell culturing lab taught me skills I will be able to apply in any cell culturing lab. As well as Machel Leuschner, for her invaluable insight into LC-MS and her continuous positive mental attitude.

Lastly to my friends and family, who continuously supported me through this journey. Thank you for celebrating the highs as well as holding me up when I was feeling low. Your love and support helped me on this journey and will always be cherished.

Abstract

Keywords: HepG2, Cytochrome P450, Spheroid, Monolayer, Induction cocktail, Metabolome

Introduction:

Drugs have been removed from the market for years due to toxicity screening. The highest attrition from the market can be seen by drugs that cause hepatotoxicity. Most drugs are metabolised by phase I cytochrome enzymes with five cytochromes metabolising approximately 95% of drugs. One of the most used screening platforms is the immortalised hepatocyte cancer cell line: HepG2. As the common model displays almost no phase I metabolomic competency, HepG2 cells are under investigation for prediction of hepatotoxicity via phase I enzymes using both an affordable and reliable methodology. Multicellular spheroid cell models have been shown to be closer to physiological conditions than monolayer cell cultures. Thus, the aim of the study was to determine the degree to which long term exposure to a tailored cytochrome inducing drug cocktail could enhance cytochrome P450 activity, in both traditional monolayer and spheroid cell cultures, at the level of the metabolome

Methods and materials

A suspension spheroid model was used with an agarose mould which, post-optimization, formed 81 spheroids per well. Protein quantification, live-dead microscopy and cell cycle analysis was used to determine the cell viability and culture time. The sulfurhodamine B assay was used to determine the IC₅₀ of each drug individually as well as the combined IC₅₀ of the cocktail for induction. Cells were cultured in presence of an induction cocktail, containing five prototypical cytochrome inducers, continuously for three weeks in monolayers. Cells were then cultured in monolayer and spheroid formats for a further six days. The liquid chromatography mass spectrometry method was optimised by first optimising the chromatography then the mass spectrometer parameters. A single method was developed for liquid chromatography tandem mass spectrometry analysis of 10 analytes in one consecutive run. Cell culture supernatant was collected, and the developed method used to determine the change in parent drug versus metabolites.

Results and discussion

During the optimisation of the spheroids, cells were shown to be compromised by day seven. Therefore, the cells were only cultured for a total time of six days within the spheroid format, to ensure viability. Only two of the drugs appeared to be metabolised. Dextromethorphan was metabolised more in the monolayer format and midazolam was metabolised more in the spheroid format. The overall phase I metabolic capacity of the HepG2 cells were not increased by long-term culture in the presence of a drug cocktail when cultured in either the monolayer or the three-dimensional spheroid format.

Conclusion

Exposure to the drug cocktail containing phenacetin, dextromethorphan, diclofenac, midazolam and bupropion was assessed using the validated method established during this study.

Metabolism was not consistent for the enzyme-combination, as implemented in this study, as only certain drugs were metabolised sufficiently to quantitate the metabolites. It remains unclear whether or not the measured metabolism is because of actual enzyme induction, from inherent metabolism potential or from further problems regarding abnormalities of other inherent metabolism (such as possible phase III transporter inactivity) of the cells.

Table of Contents

Acknowledgements	ii
Abstract	iii
Introduction:	iii
Methods and materials	iii
Results and discussion	iii
Conclusion	iii
Table of Contents	v
Chapter 1: Literature review	1
1.1. Drug screening process	1
1.2. Biotransformation	2
1.2.1. Cytochrome P450 enzyme system	3
1.2.2. <i>In vitro</i> hepatotoxicity testing	6
1.2.3. Induction of metabolism	8
1.3. Monolayer vs. spheroid cultures	11
1.4. OMICS based biology	13
1.5 Aim and objectives	15
Chapter 2: Cell culture and spheroid optimization	16
2.1. Methods and materials	16
2.1.1. Cell culture maintenance	16
2.1.2. Spheroid culture	16
2.1.3. Spheroid morphology and viability	17
2.1.4. Cell cycle analysis	18
2.1.5. Protein analysis	18
2.1.6. Study drugs and preparation of stocks	19
2.1.7. Sulforhodamine B (SRB) assay of HepG2 monolayer cells	19
2.1.8. Exposure of cells to the drug cocktail for induction	20
2.2 Results	21
2.2.1. Spheroid culturing	21
2.2.2. Protein analysis	21
2.2.3. Live-dead microscopy	24
2.2.4. Cell cycle analysis	25
2.2.5. SRB assay	25
Chapter 3: LC-MS/MS method development and cocktail analysis	30
3.1 Materials and methods	30
3.1.1. Standards	30
3.1.2 Sample preparation and LC-MS/MS instrumentation	30
3.1.2.1. Chromatographic conditions	30
3.1.2.2. Mass spectrometer conditions	31
3.1.2.3. Method validation	31
3.2. Results	32

3.2.1. Mass spectrometer optimization -----	32
3.2.2. Chromatography -----	33
3.2.3. Recovery -----	39
3.2.4 Calibration curves -----	40
3.2.5. Induction results -----	46
Chapter 4: Discussion and Conclusion -----	49
4.1. Discussion -----	49
4.2. Conclusion -----	59
4.3 Considerations -----	60
Chapter 5: References -----	63
Chapter 6: Addendum -----	69
Addendum 1: Original ethics letter -----	69
Addendum 2: Ethics extension letter -----	70

Abbreviations, symbols and units

AUC	-	Area under the curve
BCA	-	Bicinchoninic acid
°C	-	Degree celsius
cm ²	-	Centimetre squared
CO ₂	-	Carbon dioxide
CYP	-	Cytochrome
CYP450	-	Cytochrome P450
CE	-	Capillary electrophoresis
Da	-	Dalton
DDI	-	Drug-drug interactions
DNA	-	Deoxyribonucleic acid
DMSO	-	Dimethyl sulfoxide
dH ₂ O	-	Deionised water
EC50	-	50% Effective concentration
ECM	-	Extracellular matrix
EMEM	-	Eagle's minimum essential medium
EDTA	-	Ethylenediaminetetraacetic acid
ER	-	Endoplasmic reticulum
ESI	-	Electrospray ionisation
FA	-	Formic acid
US FDA	-	US food and drug administration
FDA	-	Fluorescein diacetate
FMO	-	Flavin-containing mono-oxygenases
FCS	-	Foetal calf serum
<i>g</i>	-	G-force
GC	-	Gas chromatography
h	-	Hour
HPLC	-	High performance liquid chromatography
HSA	-	Human serum albumin
IC ₅₀	-	50% inhibitory concentration
ICH	-	International conference on harmonization
IS	-	Internal standard
LADME	-	Liberation, absorption, distribution, metabolism, elimination
LC	-	Liquid chromatography
LC-MS	-	Liquid chromatography mass spectrometry
LC-MS/MS	-	Liquid chromatography tandem mass spectrometry
LLOQ	-	Lower limit of quantitation
max	-	Maximum
MeOH	-	Methanol
MeCN	-	Acetonitrile
mg/ml	-	Milligram per millilitre
ml	-	Millilitre
ml/well	-	Millilitre per well
mM	-	Millimolar
MRM	-	Multiple reaction monitoring
MRP	-	Multidrug resistance associated protein
mRNA	-	Messenger ribonucleic acid
MS	-	Mass spectrometry
m/z	-	Mass to charge ratio
NaCl	-	Sodium chloride

NADPH	-	Nicotinamide adenine dinucleotide phosphate
nM	-	Nanomolar
nm	-	Nanometer
NSAID	-	Non-steroidal anti-inflammatory drugs
NMDA	-	N-methyl-D-aspartate
NMR	-	Nuclear magnetic resonance spectroscopy
OATP-2	-	Organic anion transporting polypeptide 2
P-gp	-	P-glycoprotein
PHH	-	Primary human hepatocytes
PBS	-	Phosphate buffered saline
PI	-	Propidium iodide
r	-	Correlation coefficient
r ²	-	Coefficient of determination
RNA	-	Ribonucleic acid
SDS	-	Sodium dodecyl sulfate
SEM	-	Standard error of the mean
s/n	-	Signal to noise ratio
SRB	-	Sulforhodamine B
StDev	-	Standard deviation
TCA	-	Trichloroacetic acid
U/ml	-	Units per millilitre
μl	-	Microlitre
μm	-	Micrometre
μg/ml	-	Microgram per millilitre
UPLC	-	Ultra performance liquid chromatography
v/v	-	Volume to volume
w/v	-	Weight to volume
2D	-	Two-dimensional
3D	-	Three-dimensional
\$	-	United States dollar
%	-	Percentage
*	-	Above compound to indicate the main metabolites of the study

Chapter 1: Literature review

1.1. Drug screening process

The drug development process (Figure 1.1), as defined by the United States Food and Drug Administration (US FDA), is a five-stage process which must be undertaken before a drug is approved for commercial use. The first stage is drug discovery and development. The discovery stage involves both new chemical entities and novel investigational drugs with the main objective of reducing the thousands of screened compounds to a few potential lead compounds for further testing. Development occurs subsequent to identification of the lead compounds and experiments are performed to provide information on compound stability, drugability, absorption, distribution, metabolism, excretion, potential benefits, safety pharmacology, mechanism of action, possible adverse or pharmacogenetic effects, drug interactions and determination of bioequivalence in reference to similar compounds or drugs

1.

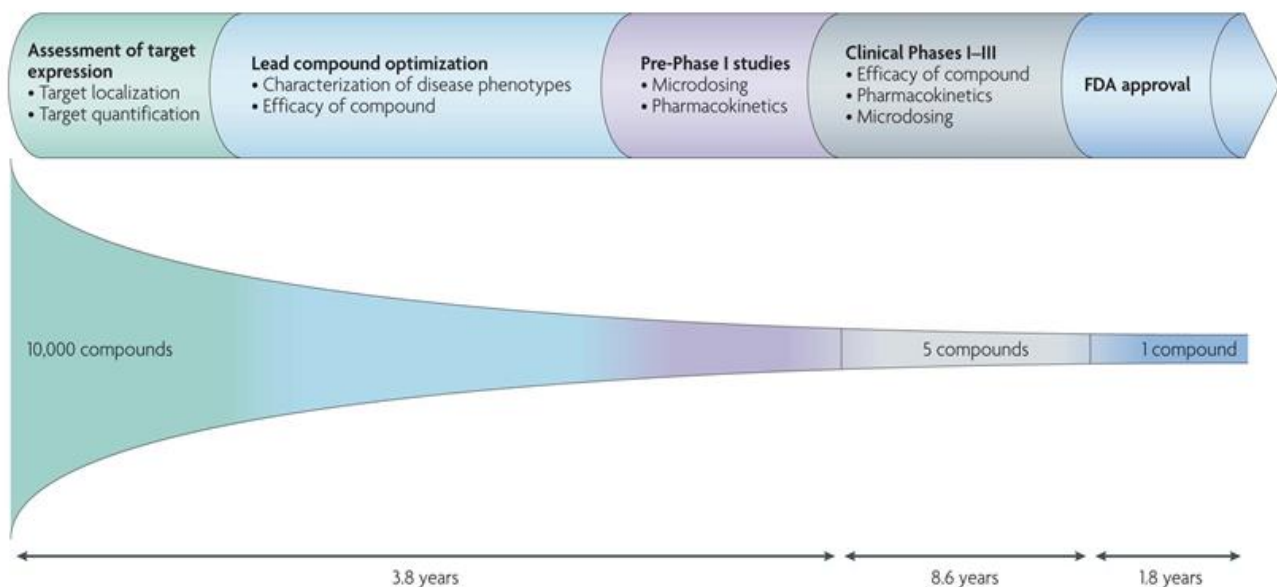


Figure 1.1: The research and development process from pre-discovery where thousands of compounds are considered through the subsequent phases prior to US FDA approval of one compound. Reprinted with permission, licence number 4317030508987 ².

The second stage in the drug development process encompasses preclinical research. This is when *in vitro* and *in vivo* tests are conducted to assess safety and efficacy. Relative safety and efficacy is determined in animal models including but not limited to rats, mice and rabbits. The outcome of these animal studies guide the decision of whether or not to proceed with human clinical trials. This second stage provides *in vivo* related information on absorption, distribution, metabolism and excretion as well as applicable pharmacological safety parameters for an investigational compound in living animals where all the biological systems

can indicate an influence on the lead compound. Before any lead compound can enter clinical trials, it must be registered as a new drug entity ¹.

The third stage is a series of human clinical trials, which are used to further determine efficacy, mechanism of action, dose range, suitable administration procedures, possible adverse effects, pharmacokinetics, pharmacodynamics and drug interactions. Stage four is when the US FDA, or other regulatory agency, receives an application from a company for registration of a drug. Safety and efficacy data, from preclinical and clinical studies, is reviewed for the approval or rejection of the drug application. Stage five involves post-marketing surveillance, whereby the safety profile of marketed drugs is monitored ¹.

The entire process, from initiation to final approval, may take up to 15 years. In America, estimations indicate that the total cost can amount up to \$ 1.8 billion ³. The evaluation of a compound or drug lead can be terminated at any point during of the five stages, which is of special concern in the late stages due to progressive financial implications and investments. If a drug is withdrawn from the market due to incomplete safety data, derived from inadequate safety profiling tests and technical incompetence, a company may suffer a detrimentally significant loss. Despite a comprehensive development process, undesirable safety and pharmacokinetic properties are a major reason for the attrition of candidate drugs ⁴.

From 1953 to 2013, 462 medicinal products were withdrawn from the market in response to the reporting of adverse side effects. Hepatotoxicity contributed to 18% of these withdrawals, making it the most reported adverse effect motivating drug withdrawal ⁵. Therefore, the importance of hepatotoxicity predictions in the early selection and optimization of drug candidates is increasingly being recognized.

1.2. Biotransformation

Pharmacokinetics, originating from the combination of “pharmakon” (drug) and “kinesis” (movement), defines what actions the body exerts on a drug ⁶. Pharmacokinetics describes the multi-step model which includes drug liberation, absorption, distribution, metabolism and excretion (LADME) ⁷. Liberation is defined as drug release from its dosage form prior to absorption into the bloodstream. The drug is then distributed from the bloodstream to enter body tissue. Metabolism and excretion target the elimination of foreign substances, such as these distributed drugs, from the body which reduces the risk for toxicity. Efficient elimination of lipophilic drugs requires transformation to a more hydrophilic form. The liver is the principle site of this drug metabolism which typically inactivates drugs and prepares them for excretion. However, some drugs, known as prodrugs, are converted into active compounds by such metabolic processes. In addition, drug metabolites can be pharmacologically active, resulting in direct toxicity ⁸.

Enzyme systems that metabolize drugs can be separated into two primary groups. Phase I metabolism increases the polarity of a compound in order to increase its solubility in aqueous

environments. This occurs through oxidation, reduction and/or hydrolysis by cytochrome P450 (CYP450), flavin-containing mono-oxygenases (FMO), monoamine oxidases, esterases, amidases, alcohol- and aldehyde dehydrogenase enzymes. Phase II metabolism adds a hydrophilic functional group to the compound, increasing the molecular weight and water solubility of the compound. The reaction occurs through conjugation (acetylation, glucuronidation, sulfation and glutathione binding) by enzymes such as glucuronyl-transferases, sulfotransferases, and glutathione-S-transferases⁹⁻¹⁰. In addition to these two classifications, although phase III metabolism does not directly metabolize drugs, but is rather involved in the transport mechanisms, it is critical to the excretion process as it is responsible for drug efflux. Phase III enzymes include multidrug resistance associated protein (MRP), organic anion transporting polypeptide 2 (OATP2) and P-glycoprotein (P-gp). These transporter enzymes work in unison with phase I and II enzymes for the facilitation of drug metabolism¹⁰⁻¹¹.

1.2.1. Cytochrome P450 enzyme system

Cytochromes are iron containing haemoproteins containing upwards of 500 amino acids with an iron-protoporphyrin IX. CYP450 enzymes were first documented by Martin Klingenberg in 1958¹², who observed an absorption maximum of 450 nm once a reducing agent was added to rat liver fractions. This property is considered unique to CYP450s as it is not observed with other haemoproteins. The identifying characteristic of the CYP450 enzyme system is that the iron prosthetic group forms a thiol bond with a cysteine amino acid, resulting in an electron dense centre for oxygen activation¹³⁻¹⁴.

Cytochromes are classified into different groups based on evolutionary relationships via genomic differentiation. Classification as part of a cytochrome “family”, requires 40% sequence homology whereas subgroups require 55% homology. As genome sequencing for various species is ongoing, the number of enzyme families is still increasing. This has necessitated a change in some nomenclature as capabilities of the initial nomenclature has been surpassed. The great diversity of CYP450s is attributed to plants, insects, fungi and bacteria. However, the nomenclature has not changed for vertebrates as there is no vertebrate CYP450 above the CYP51 family¹⁵. According to the CYP450 database, human cytochromes are classified into 18 families, 47 subfamilies and 136 total CYP450 human sequences¹⁶.

The main catalysing reaction of CYP450 enzymes, involved in phase I metabolism, is an oxidation reaction that introduces oxygen to a non-activated C-H bond from a split molecular oxygen molecule. The catalysis energy needed for the scission of the molecular oxygen is provided by NADPH, serving as a source of electrons ($\text{NADPH} + \text{H}^+ + \text{O}_2 + \text{R} \rightarrow \text{NADP}^+ + \text{H}_2\text{O} + \text{RO}$)¹⁷⁻¹⁸. Numerous complex CYP reactions occur during metabolism and a few of these are illustrated in Figure 1.2.

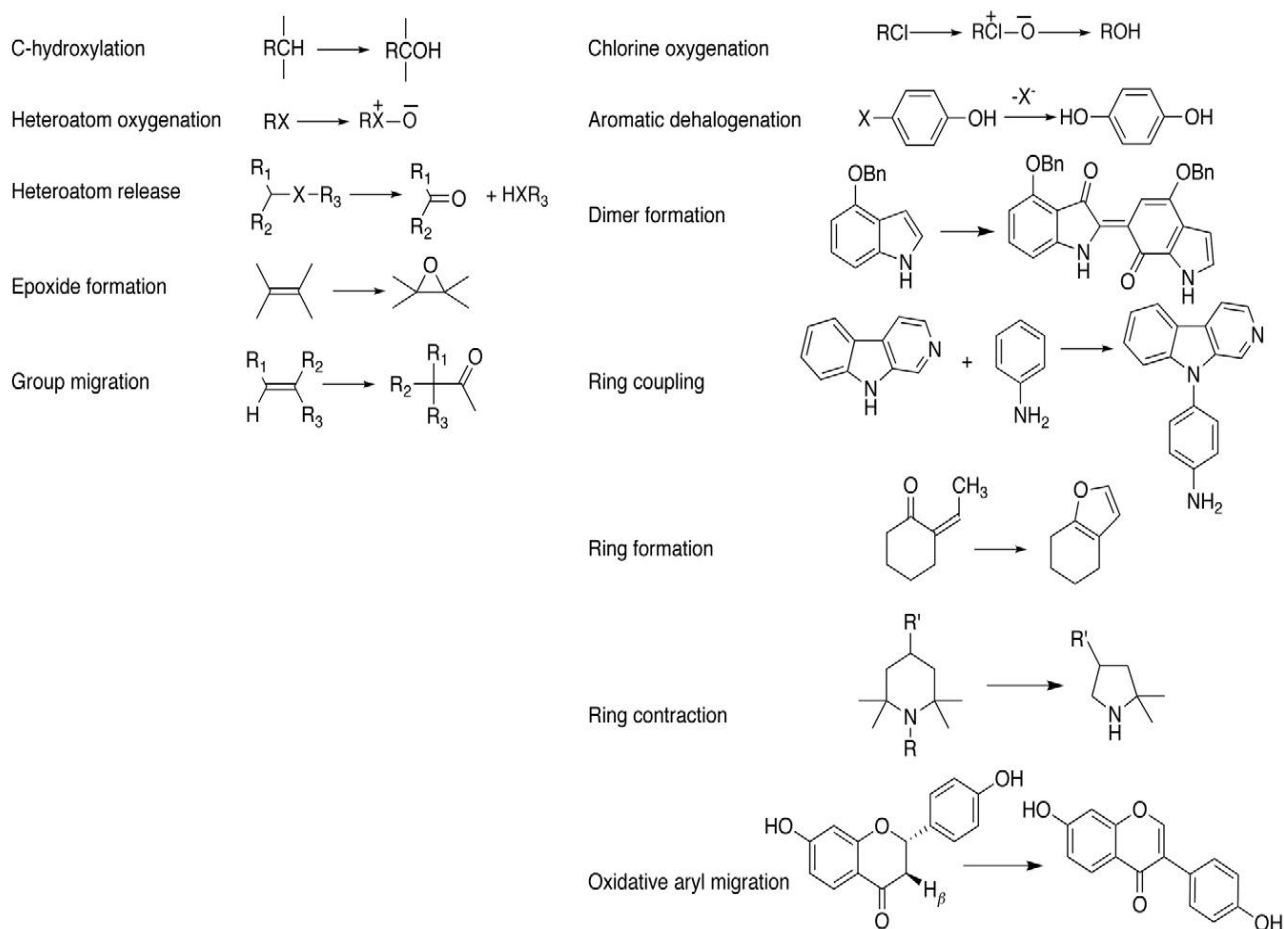


Figure 1.2: Various reactions catalysed by CYP450 enzymes. Reprinted with permission, 4282411152240¹⁹.

The CYP450 enzyme complex is essential in xenobiotic metabolism. The five main metabolizing CYP isoforms (1A2, 2C9, 2C19, 2D6 and 3A4) account for approximately 75% of all drug metabolism⁷. These main isoforms account for about 95% of CYP450 metabolism (CYP1A2: 5%; CYP2C9: 10%; CYP2C19: 5%; CYP2D6: 20-30%; CYP3A4: 40-45%)²⁰. Figure 1.3 illustrates the relative abundance of major CYP450 enzymes, however the abundance does not necessarily correlate to the level of activity in the human body. For instance, CYP3A4, accounting for approximately 30.2% of cytochrome abundance is responsible for 40-45% of metabolism. If abundance or activity of these enzymes become altered, major effects on metabolism can be elicited.

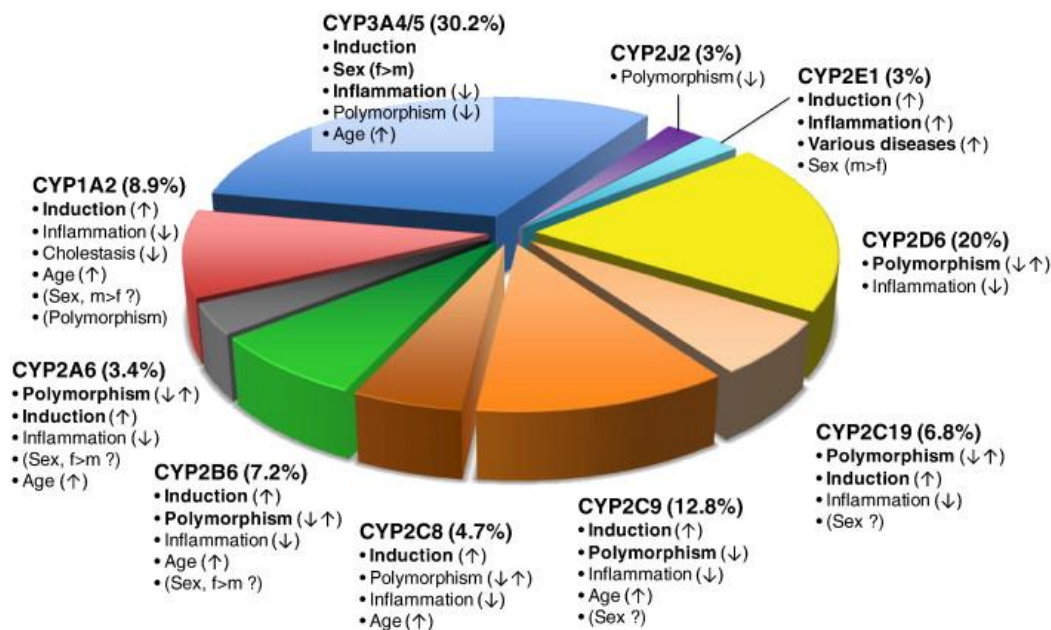


Figure 1.3: Abundance of the main CYP450 enzymes in humans. Arrows describe the effects of different variables on the quantity of these enzymes. Reprinted with permission ²¹.

Cytochrome P450 enzyme metabolism is influenced by numerous variables including the effects of one drug's metabolism on another. These are called drug-drug interactions (DDIs) and can either inhibit or induce CYP450 enzyme expression or activity ²². Inhibition is a reaction which decreases specific drug metabolism due to reduced availability of active enzyme. This is usually a rapid and immediate reaction with a component of the catalytic cycle of the enzyme being inhibited from interacting with a drug. Induction is a response which increases the amount of enzyme or prevents degradation of an enzyme, thereby increasing metabolism. Induction is a slow reaction as it mostly takes place at the level of gene transcription ²³.

These DDIs can alter metabolism and drug clearance, influencing the plasma drug concentration resulting in therapeutic failure or severe adverse reactions. In the case of prodrugs, induction of a CYP450 enzyme can increase the concentration of active metabolites giving rise to toxic effects ²². An example of DDIs is when rifampin (an anti-tuberculosis drug) is given in conjunction with cyclosporine (an immunosuppressive agent). Rifampin induces CYP3A4 thereby increasing metabolism of cyclosporine which can increase the likelihood of organ rejection after a transplant ²⁴. More examples of potential DDIs which occur as a consequence of interactions with the major CYP isoforms are summarised in Table 1.1.

Table 1.1: Significant CYP450 enzymes with their corresponding inhibitors, inducers and substrates. Reprinted/redrawn with permission ²⁵.

Enzyme	Potent inhibitors	Potent inducers	Substrates
CYP1A2	Amiodarone, Cimetidine, Ciprofloxacin, Fluvoxamine	Carbamazepine, Phenobarbital, Rifampin, Tobacco	Caffeine, Clozapine, Theophylline
CYP2C9	Amiodarone, Fluconazole, Fluoxetine, Metronidazole, Ritonavir, Trimethoprim/Sulfamethoxazole	Carbamazepine, Phenobarbital, Phenytoin, Rifampin	Carvedilol, Celecoxib, Glipizide, Ibuprofen, Irbesartan, Losartan
CYP2C19	Fluvoxamine, Isoniazid, Ritonavir	Carbamazepine, Phenytoin, Rifampin	Omeprazole, Phenobarbital, Phenytoin
CYP2D6	Amiodarone, Cimetidine, Diphenhydramine, Fluoxetine, Paroxetine, Quinidine, Ritonavir, Terbinafine	No significant inducers	Amitriptyline, Carvedilol, Codeine, Donepezil, Haloperidol, Metoprolol, Paroxetine, Risperidone, Tramadol
CYP3A4/5	Clarithromycin, Diltiazem, Erythromycin, Grapefruit juice, Itraconazole, Ketoconazole, Nefazodone, Ritonavir, Telithromycin, Verapamil	Carbamazepine, Hypericum Perforatum, Phenobarbital, Phenytoin, Rifampin	Alprazolam, Anlodipine, Atorvastatin, Cyclosporine, Diazepam, Estradiol, Simvastatin, Sildenafil, Verapamil, Zolpidem

1.2.2. *In vitro* hepatotoxicity testing

Different *in vitro*, *in vivo* and *ex vivo* models, which vary in applicability and prediction success rate, are used to predict hepatotoxicity. The ultimate goal of hepatotoxicity testing is longitudinal studies capable of predicting chronic hepatotoxicity of administered compounds. Only *in vitro* and preclinical animal models are commonly used for longitudinal studies due to feasibility, availability and ethical concerns which restrict the research that can be done on humans. Unfortunately, animal models such as rat, mouse, rabbit, monkey, dog and pig cannot conclusively predict hepatotoxicity in humans due to dissimilarity in their CYP450 and pharmacokinetic profiles ²⁶⁻²⁷. Table 1.2 illustrates that there are certain CYP enzymes similarly expressed between humans and animals. The disadvantage is that the effect on these CYP enzymes can only be studied in isolation; corresponding interactions with other CYPs will not reflect those observed in humans.

Table 1.2: Human liver microsomal CYP450 enzymes with potential experimental animal models. Reprinted/redrawn with permission, 4286261202111 ²⁸.

CYP enzyme	Animal model system
1A2	Rat, rabbit, pig, minipig
2C9/10/19	Monkey
2D6	Dog
2E1	Rat, rabbit, pig, minipig
3A4	Pig, minipig

In vitro methods are required to provide safety information for justification of use in preclinical animal models and to ensure entry into clinical trials. Different *in vitro* hepatic models include subcellular fractions such as cellular organelles, liver homogenates and microsomal fractions, primary human hepatocytes (PHH), immortalized cell lines such as HepG2, Fa2N-4, HepaRG, Hep3B, Huh7, PLc/PRF and HBG, induced pluripotent and embryonic stem cells that are differentiated into hepatocyte-like cells, and tissue slices ²⁹⁻³⁰.

PHH are considered the “gold standard” for hepatotoxicity testing as they have the advantage of still resembling *in vivo* cell structure and properties, however results can be dictated by inter-individual variability from donors. PHH sources include deceased donors, not qualified for transplantation, and non-diseased tissue, excised during surgery, which are isolated and either used immediately or cryopreserved. Both variants are expensive and are difficult to culture for extended periods in monolayer cultures as metabolic competence and differentiation state are lost relatively quickly ³¹. However, it has been shown that in spheroid models, PHH can retain their metabolic competency over extended periods ³².

Immortalised cell lines have the potential to grow indefinitely under appropriate cell culture conditions. If immortalised cell lines can accurately predict drug toxicity, potential applications include longitudinal chronic testing - especially as sub-culturing is not a major challenge. A model such as this, could conserve time and improve feasibility as immortalised cells are not as expensive as PHH and do not have to be acquired repeatedly from reliable sources.

The HepG2 cell line is an epithelial hepatoblastoma cell line ³³ that was excised from a 15 year old Argentinian male in 1975. Initially HepG2 cells were used for metabolism studies and isolating common human plasma proteins, such as albumin, plasminogen, fibrinogen and transferrin ³⁴⁻³⁵. These cells are still in use to assess hepatotoxicity through various mechanisms, such as apoptosis and necrosis through ER triggered stress, via mitochondrial pathways as wells as to determine autophagy in hepatocytes ³⁶⁻³⁸.

When comparing HepG2 cells and PHH, significant differences in the genes that regulate cell death, cell cycle checkpoint controls, transport, lipid metabolism and xenobiotic metabolism are evident. Table 1.3 compares the mRNA levels of major CYP450 enzymes in HepG2 cells relative to the expression in PHH. It is evident that HepG2 cells have diminished expression

levels and that the lower expression of CYP450 enzymes can be attributed to a decrease in transcription levels ²³.

Table 1.3: Comparison of relative CYP450 mRNA expression from PHH and HepG2. Reprinted/redrawn with permission, licence number 4478910617077 ²³.

Cell model	1A1	1A2	2A6	2B6	2C9	2C19	2D6	2E1	3A4	3A5
PHH	100	100	100	100	100	100	100	100	100	100
HepG2	6.99	0.03	0.25	0.50	0.01	0.05	1.57	0.04	0.03	1.16

HepaRG cells appear more suitable for hepatotoxicity and CYP450 induction studies as they can be differentiated and thereby better mimic the morphology of PHH and have been shown to express various CYP450 enzymes at higher concentrations than other hepatic cell lines ²⁹. Ramirez *et al.* (2018) observed that differentiation of HepaRG cells isn't fully reproducible and that the differences between slices of PHH cultures make these two sources of hepatic activity less appropriate for metabolomics ³⁹. Despite known limitations, and based on their common use, HepG2 cells were implemented in this study to provide insight into the relevance and competence of potentially driving this less competent cell line towards a phenotype which is applicable for CYP450 studies.

1.2.3. Induction of metabolism

Induction of metabolism is the result of reactions that enlarge the overall expression of CYP450 enzymes *in vivo*, which in turn increases the rate of specific metabolism. This alters the overall metabolism capability and promotes either treatment failure or adverse drug reactions. Induction ensues from different mechanisms such as increased transcription, decreased rate of enzyme degradation and post-translational modifications - stabilizing proteins ⁴⁰. *In vitro* enzyme induction is an appealing approach to consider enhancing CYP450 enzyme activity in certain cell lines with low baseline enzyme expression. Enzyme induction provides the potential to increase expression of selected phase I metabolizing enzymes, which could make these cells more applicable for hepatotoxicity testing.

There are three main metabolism evaluation strategies to assess CYP activity, namely the individual drug analysis, pooled sample analysis and the drug cocktail method. The classic individual drug analysis scrutinizes one drug only. The pooled sample analysis tests multiple individual samples, which are then examined together. The cocktail method inspects multiple drugs that are both tested and analysed within the same sample. A drug cocktail approach is beneficial as it integrates multiple tests, removes replication of work, reduce costs and technical error from experiments ⁴¹.

Individual drugs, such as rifampin, have the ability to induce multiple CYPs simultaneously ¹⁰, but in a cocktail, more specific drug interactions are sought. The advantage of specific, more selective inducers allows for better tailoring of the experimental method, whereby drug and concentration selection can be easily modified, to induce a specific CYP enzyme. As this poses

a major advantage, the induction cocktail approach was selected for this study. The induction cocktail contained phenacetin, diclofenac, omeprazole, dextromethorphan, midazolam and bupropion, each of which are briefly described below.

Phenacetin was introduced in 1887 for therapeutic use as an analgesic and an antipyretic drug. The US FDA banned its use in 1983 due to its carcinogenic and nephrotoxic effects⁴²⁻⁴³. Phenacetin is metabolised through de-ethylation, N-deacetylation, and ring hydroxylation, however the main metabolic pathway is oxidative de-ethylation by CYP1A to form the active metabolite acetaminophen*⁴³⁻⁴⁵.

Diclofenac is a non-steroidal anti-inflammatory drug (NSAID) used for its anti-inflammatory, analgesic and anti-pyretic properties⁴⁶⁻⁴⁷. Alfred Sallmann and Rudolf Pfister first synthesized diclofenac, which was introduced by Novartis (previously Ciba-Geigy) in 1973⁴⁶. Diclofenac undergoes hydroxylation and the main metabolising pathway occurs via CYP2C9 to form 4-hydroxydiclofenac*⁴⁸⁻⁴⁹.

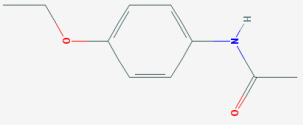
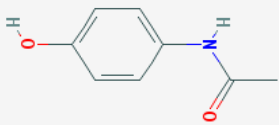
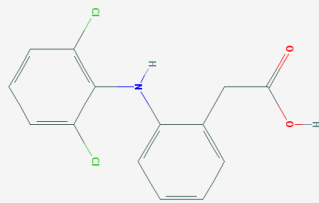
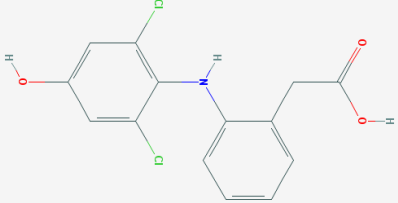
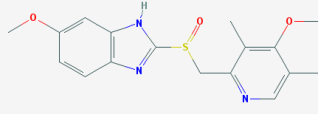
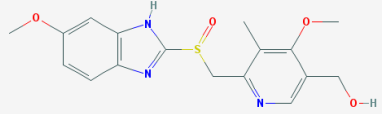
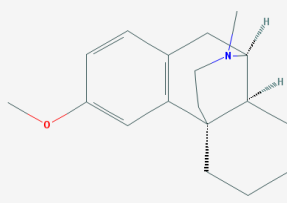
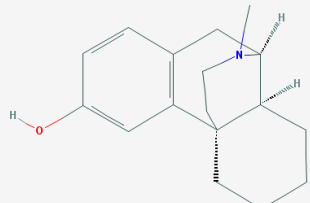
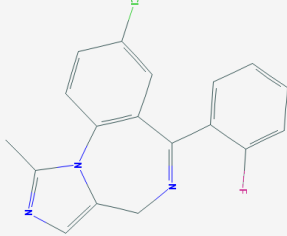
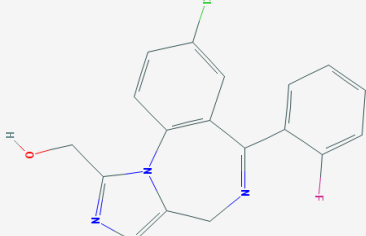
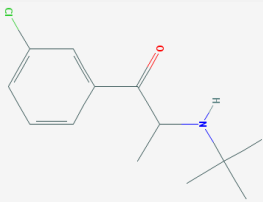
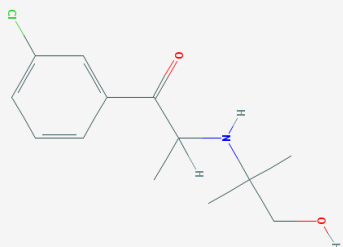
Omeprazole was first synthesized in 1979 and was launched as Losec in Europe in 1988. Omeprazole is used to suppress the production of ions that lower the pH of the stomach, to treat disorders such as peptic ulcers and gastroesophageal reflux disease⁵⁰. Omeprazole is metabolized through sulfoxidation and hydroxylation with the main metabolic pathway occurring via CYP2C19 to form 5-hydroxyomeprazole*⁵¹.

Dextromethorphan was first introduced in 1954 as an antitussive agent and was approved by the US FDA as an over the counter drug in 1958⁵²⁻⁵³. Dextromethorphan is primarily metabolized through oxidative-demethylation to dextrorphan* by CYP2D6. Dextrorphan* has the same pharmacological action as the parent drug, both influencing N-methyl-D-aspartate (NMDA) receptors. However, dextrorphan* is glucuronidated by uridine diphosphate-glucuronosyltransferase to form dextrorphan-O-glucuronide which cannot pass the blood brain barrier and is rapidly excreted through the kidneys⁵³⁻⁵⁴.

Midazolam was first synthesized in 1976 by Armin Walser, Rodney I. Fryer and Louis Benjamin and was patented by Hoffmann La Roche in 1979 as a benzodiazepine derivative⁵⁵. It is used as an anxiolytic to induce amnesia and sedation prior to use of general anaesthetics and is useful in acute seizures⁵⁶. Midazolam is metabolized by CYP3A4/5 to 1-hydroxymidazolam*, 4-hydroxymidazolam, and 1,4-dihydroxymidazolam. 1-hydroxymidazolam* is metabolised to a glucuronide derivative with all metabolites being active and cleared through the urine⁵⁶⁻⁵⁷.

Bupropion was first synthesised by Nariman Mehta and patented by GlaxoSmithKline (GSK) (previously Burroughs Wellcome) in 1974⁵⁸. It was originally withdrawn from market between 1986 and 1989 due to the occurrence of seizures. It has a few off label uses but is mainly prescribed as an antidepressant⁵⁸⁻⁵⁹ and as an aid to help with smoking cessation⁶⁰. CYP2B6 is responsible for metabolism of bupropion to hydroxybupropion*⁶¹, which has the same but less potent pharmacological action as bupropion⁶².

Table 1.4: Summary of the drugs used in a cocktail for CYP450 induction (structures obtained from PubChem ⁶³).

CYP	Drug	Primary reaction	Metabolite
1A2	Phenacetin 	Phenacetin O-deethylation	Acetaminophen* 
2C9	Diclofenac 	Diclofenac 4-hydroxylation	4-Hydroxydiclofenac* 
2C19	Omeprazole 	Omeprazole 5-hydroxylation	5-Hydroxyomeprazole* 
2D6	Dextromethorphan 	Dextromethorphan O-demethylation	Dextrorphan* 
3A4/5	Midazolam 	Midazolam 1-hydroxylation	1-Hydroxymidazolam* 
2B6	Bupropion 	Bupropion hydroxylation	Hydroxybupropion* 

1.3. Monolayer vs. spheroid cultures

Cells growing *in vivo* have certain characteristics which are required for optimal physiological functions. If *in vitro* models are developed to replicate normal physiology, it would allow for more accurate and reliable predictions of xenobiotic toxicities. In order to obtain a high degree of certainty that experimental data is accurate, the phenotype of the tissue studied has to be reproducible. *In vitro* cellular assays provide a cell-type specific prediction of *in vivo* responses. Cell based assays are primarily used as either monolayer (two-dimensional) or various spheroid cultures (three-dimensional). Different cell culturing methods have been developed which are illustrated and describe in Figure 1.4 and Table 1.5 respectively.

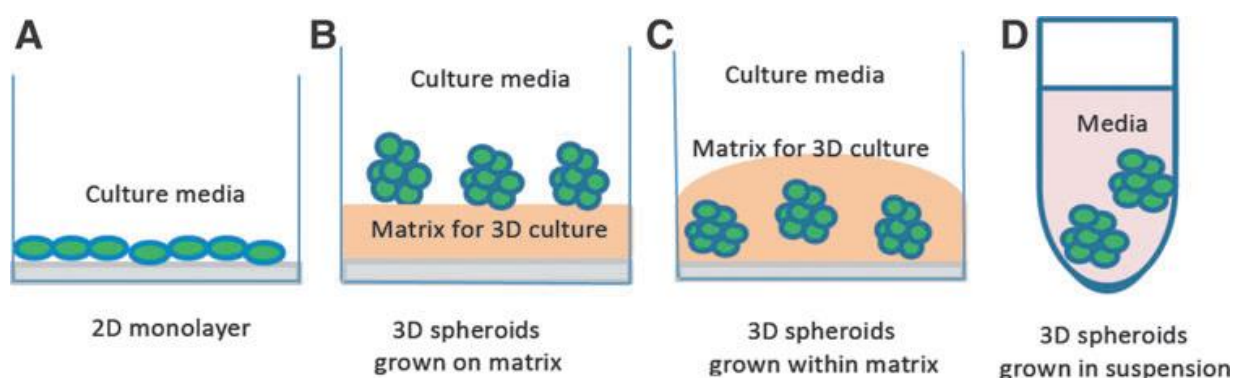


Figure 1.4: Diagrams of cell-based assays in monolayer and spheroid cultures. A) Classic monolayer or two-dimensional (2D) culture. B-D) Commonly used spheroid or three-dimensional (3D) cultures. Reprinted with permission ⁶⁴

Table 1.5: Brief description of monolayer and spheroid cell based assays ⁶⁵⁻⁶⁶.

Culture method	Description
Monolayer	Flat layer of cells grown on a plastic or glass surface
Forced floating	Plates are covered with a thin film to prevent cells from attaching to the surface
Matrices and scaffolds	Extracellular matrix (ECM) is added to promote spheroid formation
Microfluidic cell culture platforms	Micro pillar array stops passing cell suspension to form a spheroid
Hanging drop	Cell suspension overturned to form a drop and cells form a spheroid at the drop apex
Agitation based	Spinner flasks containing a stirring component to keep cells in suspension and form spheroids
	Rotating cell culture where the culture flask is rotated to keep cells in suspension

Evidence over recent years has illustrated that monolayer cultures are not accurate in depicting responses *in vivo*. Spheroid cultures, where cells spatially organise and interact, have been shown to be a more realistic model in their prediction of *in vivo* responses. Some of the major differences between these culture techniques have been summarised in Table 1.6. Examples highlighting the varied responses in monolayers are spheroid cultures include: trastuzumab which has a different effect on cell surface molecules and intracellular signalling in monolayer compared to spheroids ⁶⁷; substantial differences in viability are observed for cells treated with 5-fluorouracil and tirapazamine ⁶⁸; melanoma cells in monolayers upregulate and downregulate different genes, while in spheroids these melanoma cells upregulate the same genes that are upregulated in a tumour ⁶⁹.

Table 1.6: Major differences between monolayer and spheroid culturing ⁶⁴.

Cellular characteristics	Monolayer	Spheroid
Morphology	Sheet-like, flat and stretched cells in single layer	Natural shape in spheroid structure
Proliferation	Often proliferate at a faster rate than <i>in vivo</i>	May proliferate faster/slower than monolayer cultured cells depending on cell type and/or type of spheroid model system
Exposure to medium/drugs	Cells in monolayer are equally exposed to nutrients/growth factors/drugs that are distributed in growth medium	Nutrients/growth factors/drugs may not be able to fully penetrate the spheroid, reaching cells near the core
Stage of cell cycle	More cells are likely to be in the same stage of cell cycle due to being equally exposed to medium	Spheroids contain proliferating, quiescent, hypoxic and necrotic cells
Gene/protein expression	Often display differential gene and protein expression levels compared to <i>in vivo</i> models	Cells often exhibit gene/protein expression profiles more similar to those <i>in vivo</i> tissue origins
Drug sensitivity	Cells often succumb to treatment and drugs appear to be very effective	Cells are often more resistant to treatment compared to those in monolayer culture system, often being better predictions of <i>in vivo</i> drug responses

In a clinical trial performed in 1993, fialuridine was administered to patients to treat hepatitis B. In preliminary studies of 2 and 4 weeks respectively the treatment appeared efficacious in some of the patients and a second longer trial was initiated. After 13 weeks the trial was stopped when a patient who already ceased using the medication at 11 weeks had severe hepatotoxicity and lactic acidosis. This toxicity was not observed preclinically ⁷⁰ however, more recently developed PHH spheroid models have demonstrated this toxicity in an *in vitro* chronic exposure setting. ⁷¹. These examples give an indication that spheroid models can more accurately determine drug effects as it mimics the *in vivo* environment more closely.

1.4. OMICS based biology

Systems biology is a holistic approach considering multiple disciplines such as physics, chemistry, mathematics and biology to determine how a biological system functions. If a specific cell or organ system is considered in isolation, important information may be overlooked or misrepresented from a lack of interactions within the organism studied.

OMICS is a term defining multiple disciplines in biology such as genomics, transcriptomics, proteomics and metabolomics. Genomics is the study of the genome by analysing DNA sequences, structure and composition. Genomics focusses mainly on genetic variance to interpret and predict disease, treatment regimens and possible prognoses. Transcriptomics studies the RNA to determine which transcripts are present and to what extent they are expressed and regulated. Proteomics is the study of the proteins encoded by the genome and transcriptome, to determine their structure, function, abundance and post-translational modifications which determine overall cellular functions⁷²⁻⁷³.

Metabolomics involves the study of metabolites in a given set of conditions and can be used to quantify multiple small type molecules simultaneously. These molecules include vitamins, minerals, amino acids, carbohydrates, fatty acids, drugs, toxins or any other chemical smaller than 2000 Da⁷⁴. Metabolite levels are the measurement of the final effect of an organisms' counter to genetic and environmental changes.

The analysis of all small molecules in a biological system is conducted by a specific sequence of steps including separation, detection, identification and quantification. Separation can be achieved by using techniques such as high-performance liquid chromatography (HPLC), ultra-performance liquid chromatography (UPLC), gas chromatography (GC) and capillary electrophoresis (CE). Mass spectrometry (MS) and nuclear magnetic resonance (NMR) can then be used to detect and identify these molecules. When techniques such as HPLC and MS are combined it enables detection of large amounts of metabolites in a single sample and is called liquid chromatography mass spectrometry (LC-MS).

LC-MS is an analytical technique that can be used to separate, identify and quantify entities in a solution. Principally, UPLC and HPLC are similar separation techniques which take advantage of the slight differences in polarity of compounds to separate them with UPLC utilising a higher pressure during separation. Two phases, the mobile and stationary phase, interact with analytes in a mixture to separate them.

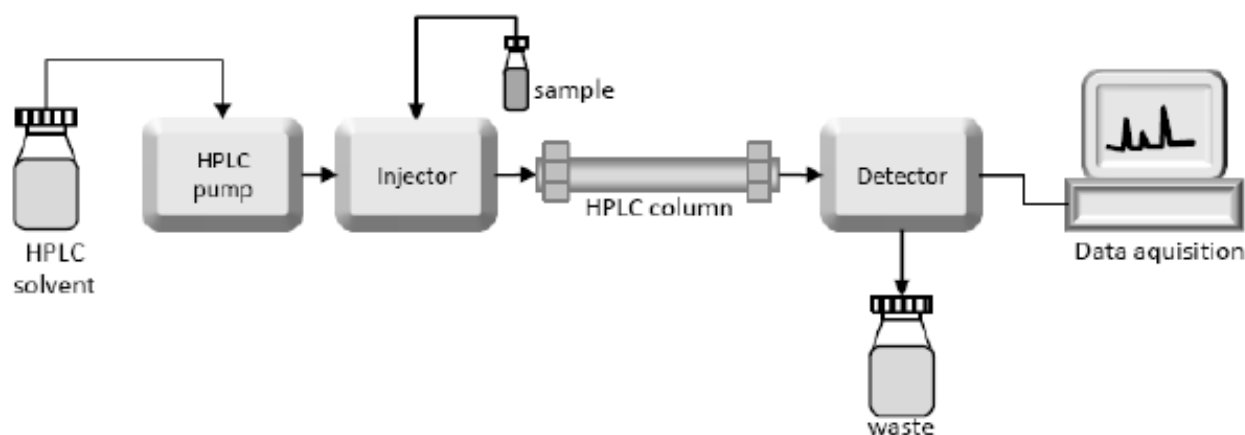


Figure 1.5: A simple diagram of an HPLC system ⁷⁵.

An HPLC system consists of an autosampler, pumps, column and a detector (Figure 1.5). The autosampler introduces the sample, containing analyte mixtures, into the mobile phase and the pumps move the mobile phase through the system to the detector. The flow rate of the mobile phase allows for the analytes to interact with particles in the stationary phase (HPLC column) based on analyte-column chemistry which promotes or retards their movement through the system. There are different types of columns with different particle sizes and chemical compositions for different applications. For example, to conduct reverse phase chromatography, a C18 column contains particles with chains of 18 carbons to attract and bind to non-polar analytes. The particle size influences the amount of backpressure in the system and ultimately the degree of analyte separation.

Mass spectrometry is a qualitative and quantitative method where the concentration of a certain analyte present in a solution can be determined. There are different types of mass spectrometers, however the same basic principles apply for when an analyte enters the MS. These principles dictate that the analyte can be ionised, mass resolved, fragmented, and deflected based on its mass to charge ratio (m/z). An optimised fragmentation pattern is used to detect and analyse deflected ions. Coupling an HPLC to an MS provides a powerful analytical technique for investigating polar soluble small molecules.

MS is advantageous to use with metabolomics as targeted or untargeted approaches can be used. Untargeted metabolomics approaches are used for discovery based research for the identification of analytes. Targeted metabolomics approaches use prior knowledge to detect previously identified metabolites. Sample preparation and the biochemical environment of molecules is a limiting factor for quantification of these molecules. An isotope labelled internal standard equivalent to the analyte in question can be used to overcome this in some scenarios, however, in discovery based research this cannot be applied due to the unknown analytes being investigated ^{73,76}. Using an optimised method, targeted MS has a major

advantage to being highly specific and sensitive and can quantitate very low quantities of an analyte within a sample ⁷⁷⁻⁷⁸.

1.5 Aim and objectives

The aim of this study was to determine the degree to which a tailored cytochrome inducing cocktail could enhance CYP450 activity in both monolayer and spheroid HepG2 cultures at the level of the metabolome.

Objectives

- To optimise procedures for culturing HepG2 spheroids using the 3D Petri Dish[®] using general spheroid morphology and viability as markers
- To determine sub-toxic concentrations of individual CYP-inducing drugs as well the drug cocktail using the sulforhodamine B assay
- To promote metabolic enzyme induction in HepG2 cells over both an acute (short term) and chronic (long term) drug cocktail exposure period
 - Short-term – 72 h exposure to a 6-drug CYP-induction cocktail following monolayer or spheroid culture establishment in cocktail-free medium for 72 h
 - Long-term – 72 h exposure to a 6-drug CYP-induction cocktail after cells were passaged three times (8 days each), as monolayer or spheroid cultures in the continual presence of sub-toxic concentrations of a 5-drug CYP-induction cocktail
- To develop and validate a liquid chromatography tandem mass spectrometry method (LC–MS/MS) for the simultaneous analysis of 12 analytes (6 parent compounds and 6 metabolites) and an internal standard
- To compare the activity of CYP1A2, CYP2C9, CYP2C19, CYP2D6, CYP2B6 and CYP3A4/5 by quantification of CYP inducing drugs and corresponding metabolites using the validated LC-MS/MS method

Chapter 2: Cell culture and spheroid optimization

2.1. Methods and materials

Chemicals, analytical reagents, agarose moulds and cell culture medium were purchased from Sigma-Aldrich (St Louis, USA); Microsep (Waters Corporation; Milford, USA); and Gibco, Lifeline Cell Technology, Thermo Fischer Scientific (Maryland, USA) and stored as per manufacturer's recommendations. Consumables were purchased from Laboratory and Scientific Equipment Company (Cape Town, RSA); Stargate Scientific (Roodepoort, RSA) and Corning Incorporated Life Sciences (Lowell, USA). Items not purchased from the above companies were detailed throughout the materials and methods as required.

2.1.1. Cell culture maintenance

Human hepatoblastoma, HepG2, cells (CHEP-x; Cellonex, South Africa) were cultured using in-house protocols of the Department of Pharmacology, University of Pretoria. Cells were maintained in Eagle's minimum essential medium (EMEM) supplemented with 10% gamma irradiated foetal calf serum (FCS) (Gibco), 2 mM glutamate and 1% penicillin-streptomycin (10 000 U/ml penicillin and 10 000 µg/ml streptomycin). Cells were maintained in a humidified incubator at 37°C, with 5% CO₂ in 75 cm² flasks. Once at 80% confluence, cells were washed with sterilized phosphate buffered saline (PBS) and detached from the flask using TrypLE Express dissociation solution. Dissociated cells were centrifuged at 200 × *g* for 5 minutes to concentrate the cellular pellet and resuspended in 1 ml EMEM with 10% FCS. The cellular concentration was determined using the trypan blue exclusion assay (0.1% w/v) and a haemocytometer. The cell suspension was diluted to the required concentration for each of the respective assays.

2.1.2. Spheroid culture

Spheroids were cultured in an agarose mould (3D Petri Dishes[®]; MicroTissues, Inc: Rhode Island, USA) with an 81 spheroid per well matrix, compatible with 12-well culture plates. A 2% (w/v) agarose solution (A9045; Sigma-Aldrich) was prepared in sterile dH₂O and stored at 4°C. Prior to use, agarose was heated and 500 µl agarose at 60 - 70°C was pipetted into the silicone 3D Petri Dish[®], further referred to as a micro mould (Figure 2.1 A). After 10 minutes of gelling, the solidified agarose, further referred to as an agarose mould (Figure 2.1 D), was gently removed from the micro mould and transferred to a 12-well plate.

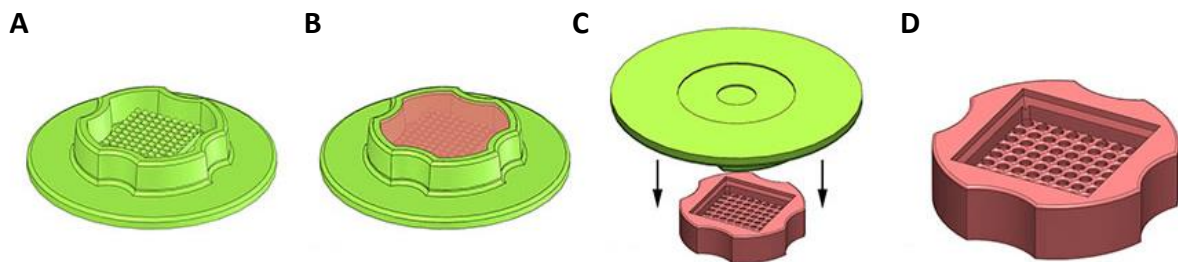


Figure 2.1: Image panel showing the production of a solidified agarose mould from a silicone 3D Petri Dish®. A) Silicone 3D Petri Dish or micro mould, B) Micro mould with agarose gelling, C) Agarose mould being removed from the micro mould and D) Agarose mould with a 9 by 9 matrix for spheroids. Reprinted with permission, ⁷⁹.

Agarose moulds were equilibrated overnight in 12-well plates by covering the agarose mould with 1.3 ml/well EMEM. Following equilibration, media was removed, and cells suspensions were prepared according to the guidelines specified in Table 2.1. Initially, these spheroid sizes were investigated and the most optimal size for this cell type and downstream applications was determined. The desired cell suspension, in 170 μ l medium, was added in a drop wise fashion into the empty cell seeding chamber of the agarose mould. Cells were left to settle into the micro well matrix of the agarose mould for thirty minutes. Each well of the 12-well plate was gently filled along the well edge with 2 ml of supplemented EMEM. The tissue culture plates were incubated at 37°C with 5% CO₂. The medium surrounding the 3D Petri Dish® was exchanged every 72 h.

Table 2.1 Cell numbers per spheroid assessed for HepG2 cells in the 81 spheroids/well matrix as per manufacturer instruction ⁷⁹.

Approximate nominal spheroid diameter (μ m)	~Cells/spheroid	Total cells seeded (cells/170 μ l)
200	1000	8.1×10^4 /well
300	3375	2.73×10^5 /well
400	8000	6.48×10^5 /well
500	15625	1.3×10^6 /well
600	27000	2.2×10^6 /well
700	42875	3.5×10^6 /well

2.1.3. Spheroid morphology and viability

Light microscopy was used to track changes in gross morphology and determine spheroid diameter by imaging every 3 days using a Zeiss AX10 fluorescence microscope with AxioVision SE64 4.9.1 software.

“Live–dead” fluorescent staining was used to determine the viability of cells within spheroids. Fluorescein diacetate (FDA) counterstained with propidium iodide (PI) was used to distinguish

viable cells from dead cells respectively. Stock of 5 mg/ml FDA was prepared in acetone and stored at -20°C while 2 mg/ml PI was prepared in PBS and stored at 4°C. Staining solution (5 ml PBS with 8 µl FDA and 12 µl PI) was made up fresh and used within 2 h. Medium was removed from the agarose mould and spheroids washed with PBS three times. After PBS was removed, 200 µl of the staining solution was added directly to the cell seeding chamber of the agarose mould and incubated for 5 minutes at room temperature in the dark. The staining solution was removed, the sample washed with PBS followed by the addition of PBS to fill the seeding chamber. Spheroids were visualised on a Zeiss AX10 fluorescence microscope each day from Day 4 to 7. Samples were analysed for FDA at an excitation wavelength of 488 nm and emission wavelength of 514 nm and PI at an excitation wavelength of 535 nm and emission wavelength of 617 nm. Image analysis was conducted using AxioVision SE64 4.9.1 and ImageJ 1.51.

2.1.4. Cell cycle analysis

Cell cycle analysis, using flow cytometry, was conducted to assess viability and the approximate distribution of cells, within a spheroid, throughout the cell cycle phases. Spheroids were cultured and harvested at Day 4, 6 and 7 and compared to cells collected at seeding (Day 0). Harvested spheroids were washed with pre-warmed PBS, centrifuged at 200 × *g* for 5 minutes and disaggregated in 1 ml TrypLE Express dissociation solution at 37°C for 30 minutes.

Dissociated cells were centrifuged at 200 × *g* for 5 minutes and resuspended in 200 µl PBS with 1% FCS. Cells were fixed by adding 2 ml of ice cold 70% ethanol in a drop wise manner while being agitated by a vortex spinner. Fixed samples were stored overnight at 4°C. Samples were centrifuged at 200 × *g* for 5 minutes and pellets resuspended in 1 ml PI staining solution (40 µg/ml PI, 0.1% (v/v) Triton X-100 and 100 µg/ml DNase free RNase) and incubated at 37°C for 40 minutes. Samples were analysed using a Beckman Coulter FC500 flow cytometer at an excitation of 488 nm and emission wavelength of 620 nm. Raw cell cycle histograms were analysed using deconvolution software (Wincycle Software; Washington, USA) and the average of each cell cycle phase compared using GraphPad Prism version 6.1. for Windows, GraphPad Software, La Jolla California USA

2.1.5. Protein analysis

Protein quantification analysis was done to characterise the average protein content per spheroid over the time-course. Spheroids from 3 wells (3 × 81 spheroids) were collected per day on Day 0, 4, 5, 6 and 7 of culturing and centrifuged at 200 × *g* for 5 minutes. The supernatant was removed, and protein samples resuspended in lysis buffer (10 mM Tris-Cl (pH 8.0), 1 mM EDTA, 1% (v/v) Triton X-100, 0.1% (w/v) sodium deoxycholate, 0.1% (w/v) SDS, 140 mM NaCl) and Complete™ protease inhibitor cocktail (1/25 ratio of protease inhibitor) with lysis aided by an overnight freeze-thaw cycle at -80°C. Samples were centrifuged at 16000 × *g* for 10 minutes and the supernatant was used for protein quantitation.

The concentration of the solubilised protein per sample was determined by the bicinchoninic acid (BCA) assay⁸⁰. A human serum albumin (HSA) standard curve with eight concentrations ranging between 0 mg/ml and 1.5 mg/ml was used for protein quantification. One part sample or HSA standard was added to 39 parts BCA reagent. The BCA reagent was composed of 50 parts reagent A (1% (w/v) BCA, 2% (w/v) sodium bicarbonate, 0.16% (w/v) sodium tartrate, 0.95% (w/v) sodium bicarbonate, pH 11.25) added to one part reagent B (4% (w/v) cupric sulphate pentahydrate). The plate was placed on a microplate shaker for 2-3 minutes before incubation at 60°C for 1 h. Absorbance was measured at 570 nm on a microplate reader (BioTech ELX 800, WINOOSKI, USA). Gen 5 software was used to extrapolate unknown protein concentrations from the HSA standard curve and results expressed as the mean of internal triplicates and independent triplicate experiments done using GraphPad Prism version 6.1. for Windows, GraphPad Software, La Jolla California USA

2.1.6. Study drugs and preparation of stocks

Stock solutions of all drugs used for induction in cell cultures were prepared in dimethyl sulfoxide (DMSO) at a concentration of 50 mM. Aliquots (5 µl) were stored at -80°C and diluted using medium prior to use. Stock solutions for LC-MS optimization and method development were made up in methanol at 1 mg/ml and stored at -80°C.

2.1.7. Sulforhodamine B (SRB) assay of HepG2 monolayer cells

A 100 µl solution of cells, in 10% FCS supplemented EMEM, was pipetted into a 96-well plate (20 000 cells/well). Cells were incubated overnight at 37°C to allow for cellular attachment. To the cells was added 100 µl negative control (EMEM), vehicle control (0.5% DMSO), and each drug inducer shown in Table 2.2 at 7 half-log dilution concentrations (0.1 µM; 0.32 µM; 1 µM; 3.2 µM; 10 µM; 32 µM; 100 µM) for 72 h or 7 days. Plates for 72 h and 7 days were analysed in technical and biological triplicates. Blanks containing 200 µl 10% FCS-supplemented EMEM were used to account for sterility and background noise.

The SRB assay⁸¹ was modified and used to determine the sub-toxic concentration of each drug inducer selected for the induction cocktail. After 72 h and 7 days in culture respectively, cells were fixed with 50 µl of 50% (w/v) trichloroacetic acid (TCA) overnight at 4°C. TCA was washed off with water three times, dried and then stained with 100 µl of 0.057% (w/v) SRB dissolved in 1% (v/v) acetic acid, for 30 minutes at room temperature. After 30 minutes' incubation, the plate was rinsed four times with 1% acetic acid to remove unbound dye and was allowed to dry at 60°C. Once dried, 200 µl 10 mM Tris-base solution (pH 10.5) was added to each well and the plate was placed on a shaker for 60 minutes. Absorbance was measured using a microplate reader (BioTech ELX 800) at 540 nm. Sub-toxic concentrations were calculated from dose response curves generated in GraphPad version 6.01 using non-linear regression with a non-normalized variable slope.

After sub-toxic concentrations were determined for the individual drugs, the optimal sub-toxic concentration for the six-drug cocktail was determined. Table 2.2 provides concentrations, obtained from literature, that indicate the maximum in-well concentration of

a specific drug where it is suggested that CYP cross-induction is avoided. As IC₅₀ values were not obtained for several of the individual drugs, the concentrations provided in Table 2.2 were used at various dilutions of this suggested maximum (max) concentration. After 72 h of six-drug cocktail exposure the SRB assay was performed and the optimal concentration for the cocktail was determined. The same concentrations for each drug were then used for both the 5-drug cocktail used during enzyme induction phase passaging of HepG2 cells and the 6-drug cocktail used in the monolayer and spheroid cultures. The 5-drug cocktail initially excluded Bupropion, which is specific for CYP2B6, the purpose for which was two-fold. It was included only in the final exposures to ascertain whether extensive cross-induction of CYPs was evident during the passaging of cell stocks or if the 72 h exposure could influence this CYP under 'primed' conditions.

Table 2.2 Drugs contained in the cocktail with their corresponding maximum in well concentrations to prevent loss of CYP specificity ⁴¹.

Drug	CYP	In well concentration
Phenacetin	CYP1A2	50 µM
Diclofenac	CYP2C9	100 µM
Omeprazole	CYP2C19	40 µM
Dextromethorphan	CYP2D6	25 µM
Midazolam	CYP3A4	5 µM
Bupropion	CYP2B6	100 µM

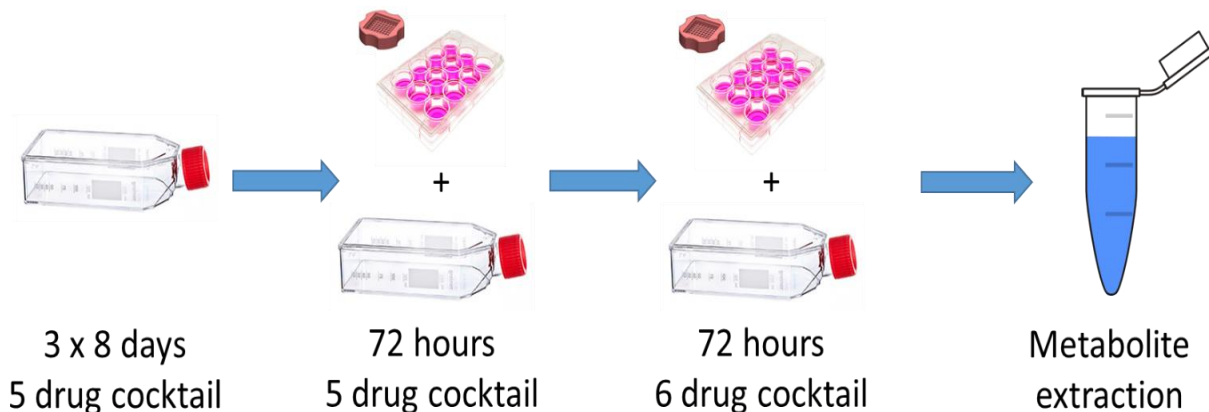
2.1.8. Exposure of cells to the drug cocktail for induction

After determining the sub-toxic concentrations of the enzyme induction cocktail, cells were cultured in the 5-drug cocktail in an attempt to condition HepG2 cells to induce increased baseline cytochrome activity. Cells cultured in induction cocktail were compared to cells prepared in equivalent conditions without any induction drug cocktail. The induction procedure is illustrated in Figure 2.2. HepG2 cells were exposed to the 5-drug cocktail in standard monolayer cultures in a 75 cm² flask for three passages. HepG2 cells (1 x 10⁶ total) were added to a flask for 8 days. After 8 days the flask was passaged equally into two new flasks which was again cultured in the presence of the 5-drug cocktail for 8 days. After 8 days the two flasks were again passaged into three new flasks which were again cultured in the continual presence of the 5-drug cocktail for a further 8 days. These third passage cell cultures were considered induced cells.

Induced cells were then seeded (Day 0) into monolayer or spheroid cultures, in a 75 cm² flask and a 12-well plate respectively, in the continuous presence of the 5-drug induction cocktail at Day 0. After an initial 72 h in which spheroids formed, cells were exposed to the 6-drug cocktail. Bupropion, with specificity for CYP2B6, was added for 72 h only to compare the magnitude of change in short 'primed' cultures between monolayer and spheroid cultures. Additional short-term induction using only the 6-drug cocktail for 72 h with no previous

passaging in induction medium was also done as a control for acute induction. After 72 h the supernatant of each sample (2 ml) was collected for analysis of the parent drug and their respective metabolites.

Figure 2.2 Long-term induction procedure from first induction in flask to where supernatant was



collected and processed before sample preparation for LC-MS.

2.2 Results

2.2.1. Spheroid culturing

The ranges of cell number seeded per spheroid that was under investigation, provided in Table 2.1, included four densities from 8.1×10^4 /well to 1.3×10^6 cells/well (Figure 2.3). The two larger spheroid sizes were not considered for investigation as the nominal diameter appeared too large for diffusion limits in proliferating cells. When seeding at 1.3×10^6 cells/well, spill over of cells from the agarose mould into the well was observed (Figure 2.4A), while seeding at a concentration of 9.7×10^5 cells/well provided spheroids of a similar size to those obtained from higher cell numbers but with negligible spill over (Figure 2.4B). After the optimal seeding density was determined, images were taken on Day 1, 4, 7 and 10 of spheroid culturing to determine how they were maintained and changed over time.

2.2.2. Protein analysis

The BCA assay was done both to determine protein concentration and to obtain a gross overview of the average spheroid protein content over time. Figure 2.6 suggests an increase in protein concentration up to day 5 which decreases at day 7 which could be an indication that cell viability in spheroids is reduced.

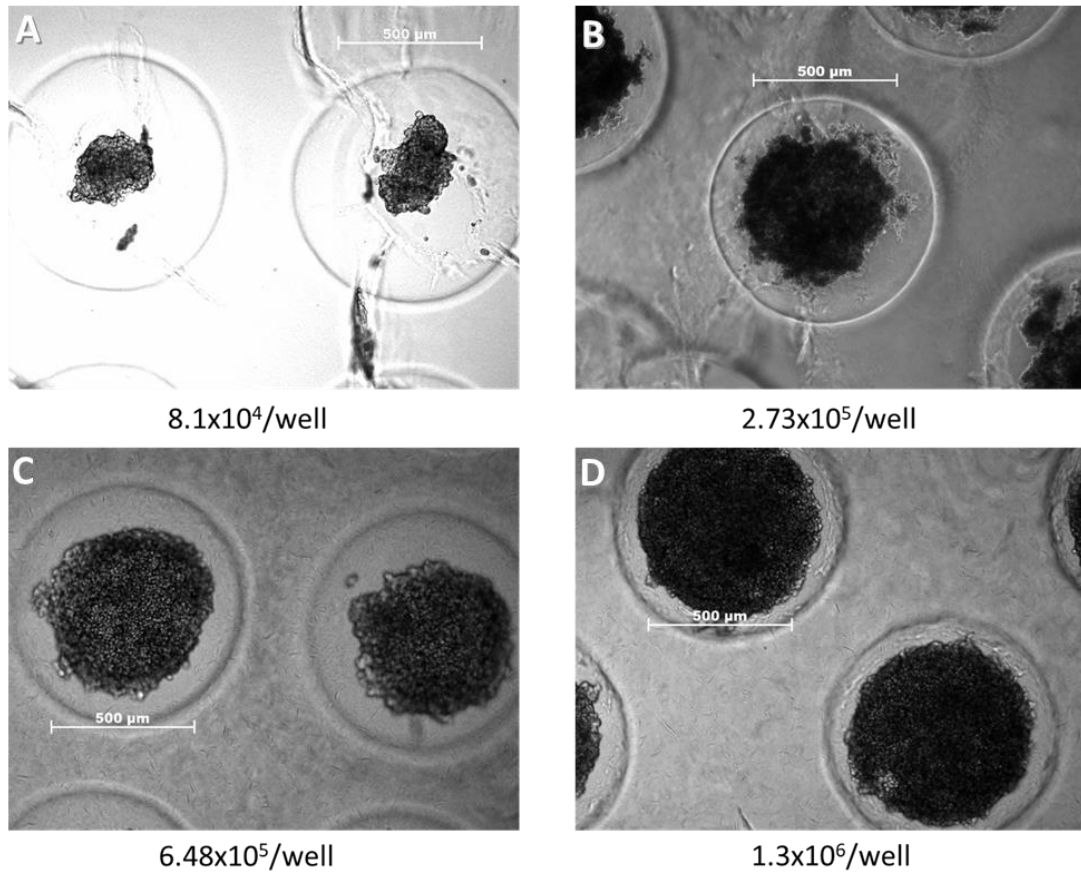


Figure 2.3: Seeding density titration. Images of spheroids within the agarose mould matrix cultured at various seeding densities. Scale bar: 500 μm .

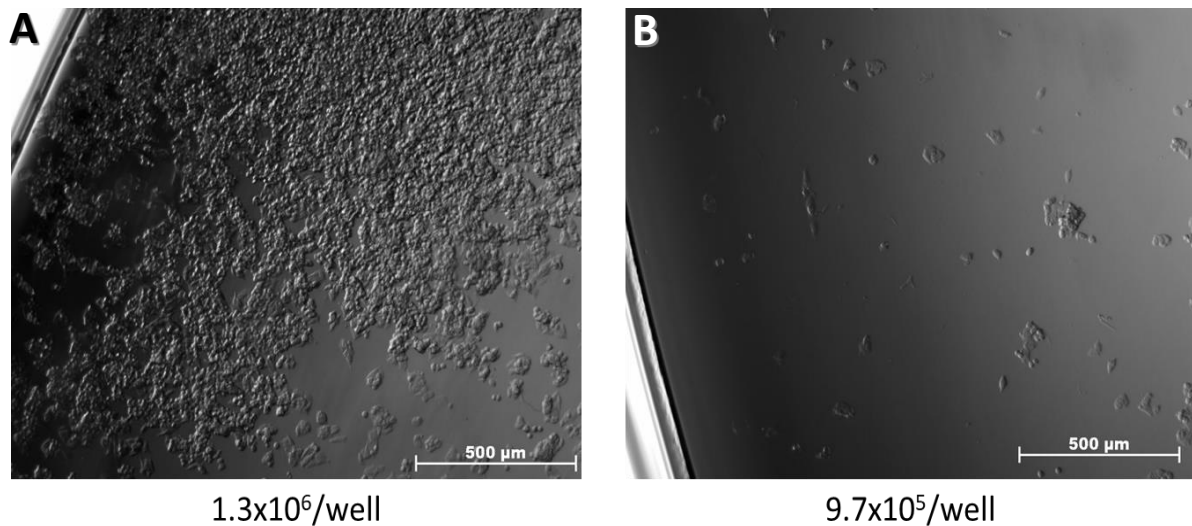


Figure 2.4. Spill over of cells observed 24h post-seeding when seeding at A) Initial seeding density of 1.3×10^6 cells per well and B) The optimised seeding density of 9.7×10^5 cells per well with markedly reduced spill over. Scale bar: 500 μm .

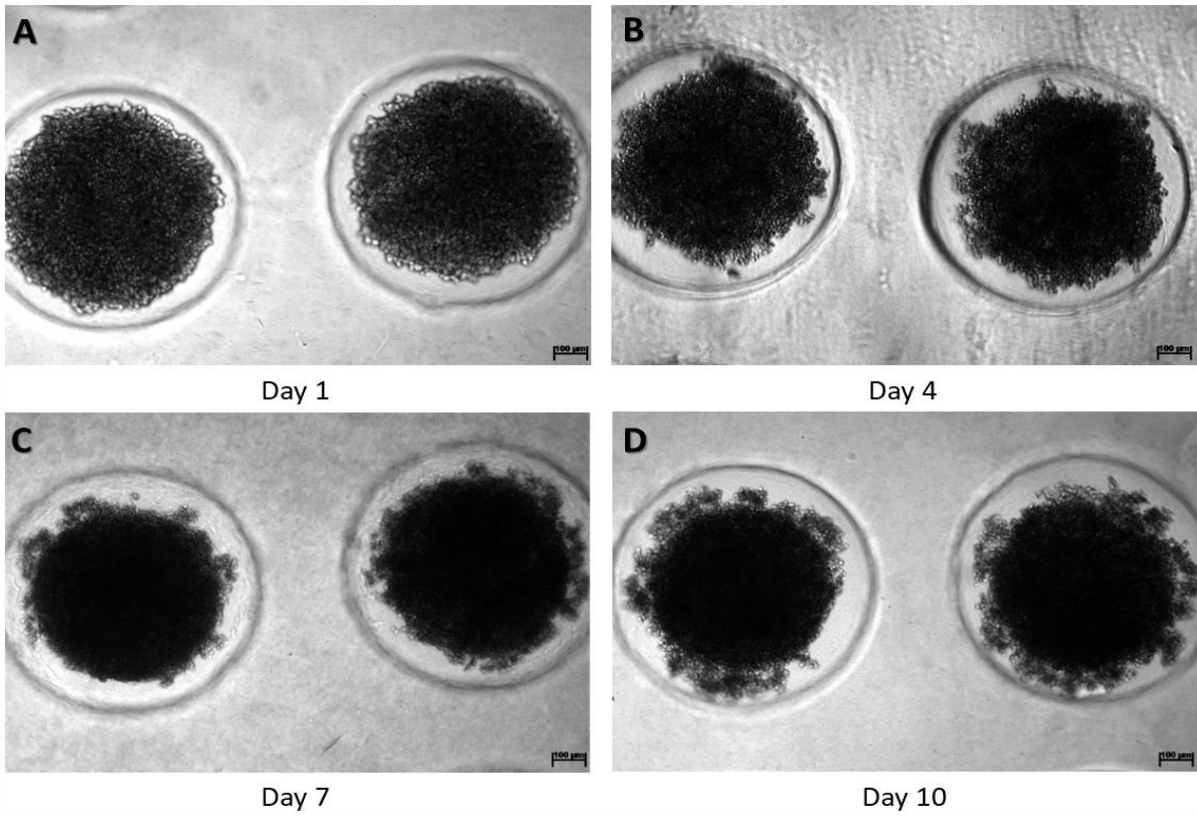


Figure 2.5: Time-course of spheroid formation at a seeding density of 9.7×10^5 cells/well. Scale bar: 100 μ m.

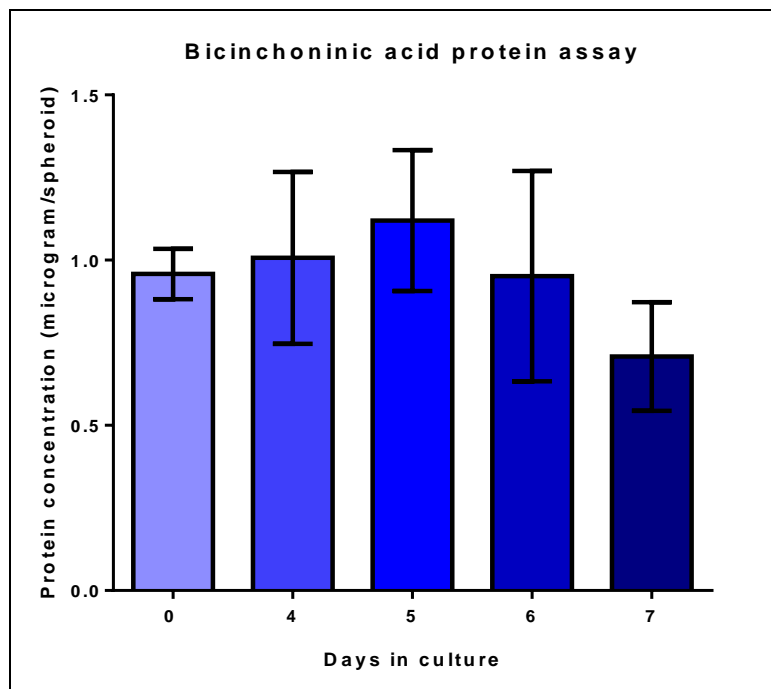


Figure 2.6. Protein concentration changes over time, calculated for a single spheroid in the 81-spheroid matrix, compared to the equivalent number of cells seeded at Day 0.

2.2.3. Live-dead microscopy

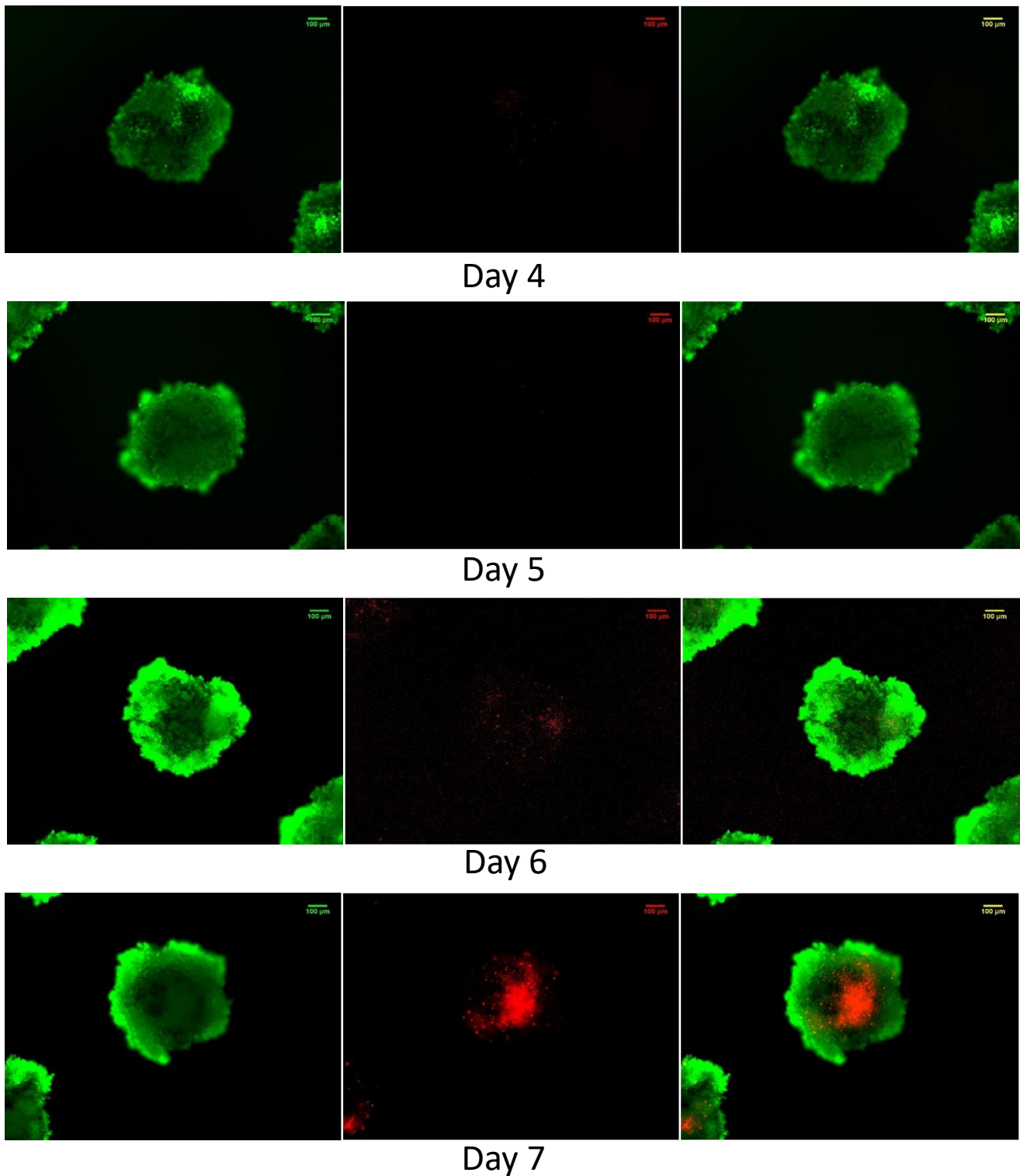


Figure 2.7: Spheroids in agarose moulds were stained with FDA (green, left) and PI (red, centre) to demonstrated viability and membrane integrity respectively with their corresponding dual stained overlay (right). Scale bar: 100 µm.

As illustrated in Figure 2.7 only day 7 had observable PI staining, potentially determining that a necrotic core had formed, as cells in the centre of the spheroid had shown compromised membranes. The other days had non-specific PI staining as very few cells had been compromised from day 4-6.

2.2.4. Cell cycle analysis

A panel of cell cycle histograms is shown in Figure 2.8 for cells on the day of seeding as Day 4, Day 6 and Day 7 of spheroid cultures. The percentages provided are the mean values of triplicate experiments. Data was mostly reproducible, as seen in Table 2.3. Exceptions included the S phase of Day 6 and the Sub-G1 phase of Day 7 which were considered as non-reproducible with the significance values greater than 0.05.

Table 2.3. Cell cycle analysis of HepG2 spheroids. Table divided into sub-G1 (cell debris and DNA fragments), G1 phase, S phase and G2/M phases with the associated percentage mean and SEM across replicates. P (significance) values determined by * = 0.05, ** = 0.01 and * = >0.001.**

	% G1		% G2		% S		% Sub-G1	
	Mean	SEM	Mean	SEM	Mean	SEM	Mean	SEM
Day 0	81,34***	1,69	11,26***	1,20	7,40***	1,14	0,15**	0,09
Day 4	80,58***	0,25	10,82***	0,17	8,60***	0,23	1,65*	0,41
Day 6	64,99*	2,04	15,58*	0,50	19,43	1,55	2,53***	0,01
Day 7	79,51***	1,81	5,47*	0,61	15,02**	1,35	2,64	0,97

2.2.5. SRB assay

The SRB assay was performed to determine the concentration at which the drug cocktail could be used to induce cytochromes while adequately maintaining limited cytotoxicity. An initial single drug determination was done to see if the drugs were non-toxic at their respective maximum concentrations, as provided in Table 2.2. No IC₅₀ was determined for Phenacetin, Bupropion, Diclofenac and Omeprazole in monolayer cultures (Figure 2.9). The IC₅₀ determined for Dextromethorphan was greater than 100 µM for 72h and 48.75 µM for 7 days which was higher than the 25 µM max value from Table 2.2. The IC₅₀ determined for Midazolam was 81.35 µM for 72h and 73.85 µM for 7 days which was also higher than the corresponding 5 µM max value from literature.

The combination of the maximum values was then tested at various dilutions in order to assess a non-toxic threshold for the six-drug cocktail. Initially the combination was assessed at max, max/2 and max/10 (Figure 2.10), In this initial SRB 100% safety was not obtained as even the max/10 showed a 10% reduction in viability. A more comprehensive dilution series was generated, for further assessment (Figure 2.11), and a safe concentration was determined to be max/20 as there was no observable toxicity and the effect plateaued

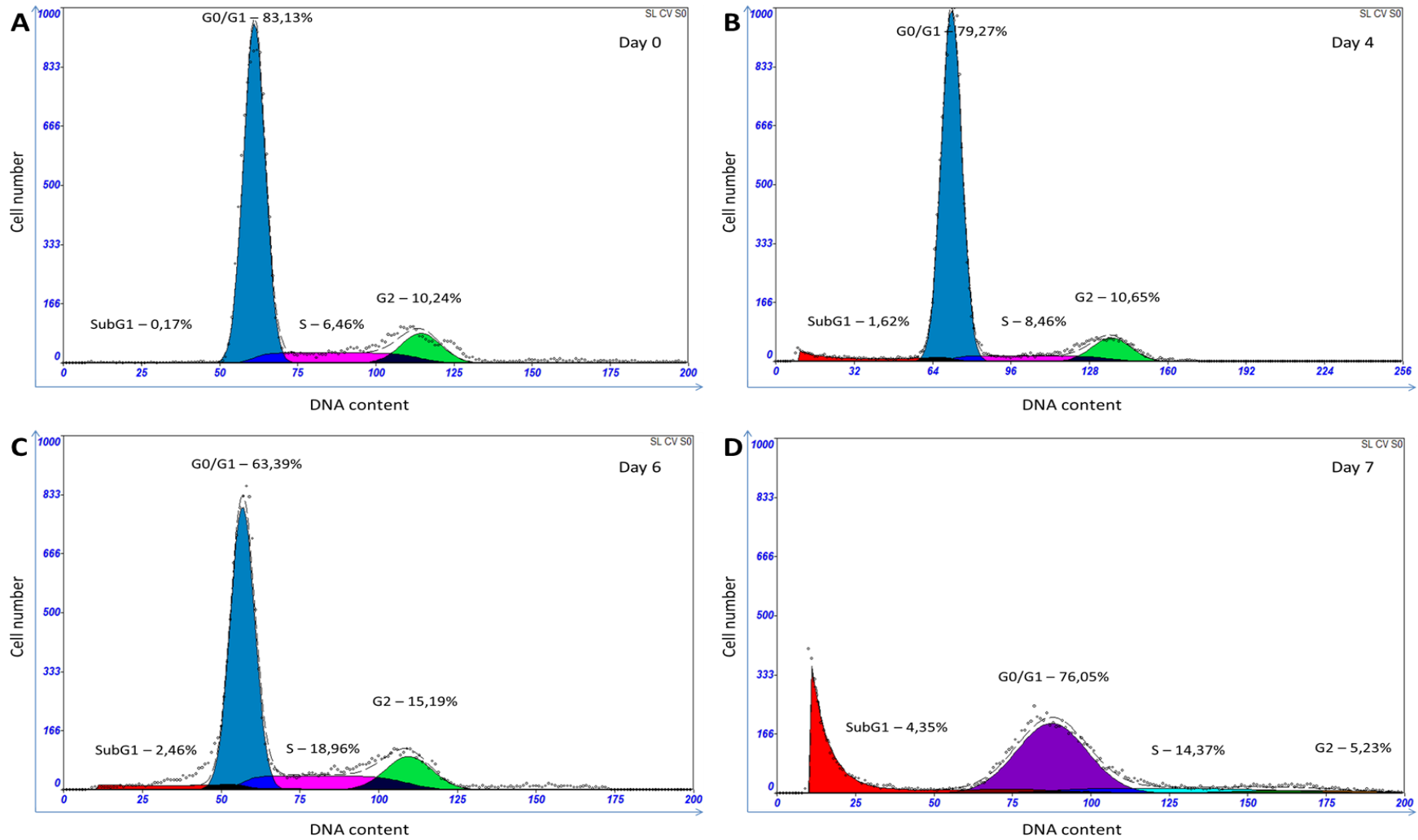


Figure 2.8 Cell cycle analysis of spheroids over 7 days. A) analysed on day of seeding, B) after 4 days in culture, C) after 6 days in culture, D) after 7 days in culture. Sub-G1 indicates apoptotic cell death; G0/G1 indicates normal, resting or not yet dividing cells; S is the replication phase; G2 is the phase just prior to mitosis. Images A-C have the same colours and D has different colours to highlight the difference in the histogram as all the phases have shifted to the right.

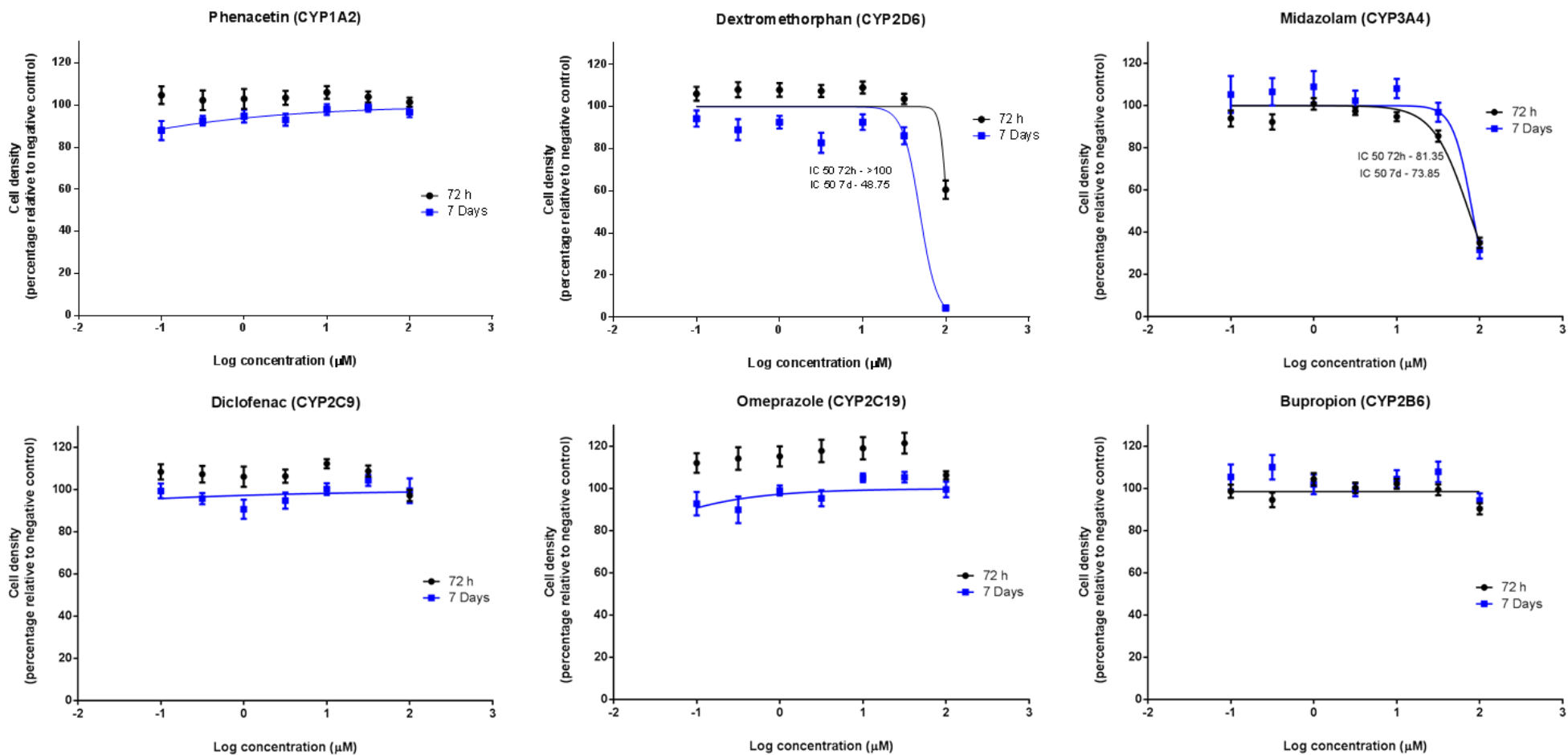


Figure 2.9 Dose response curves of each drug in the 6-drug cocktail individually generated using the SRB assay.

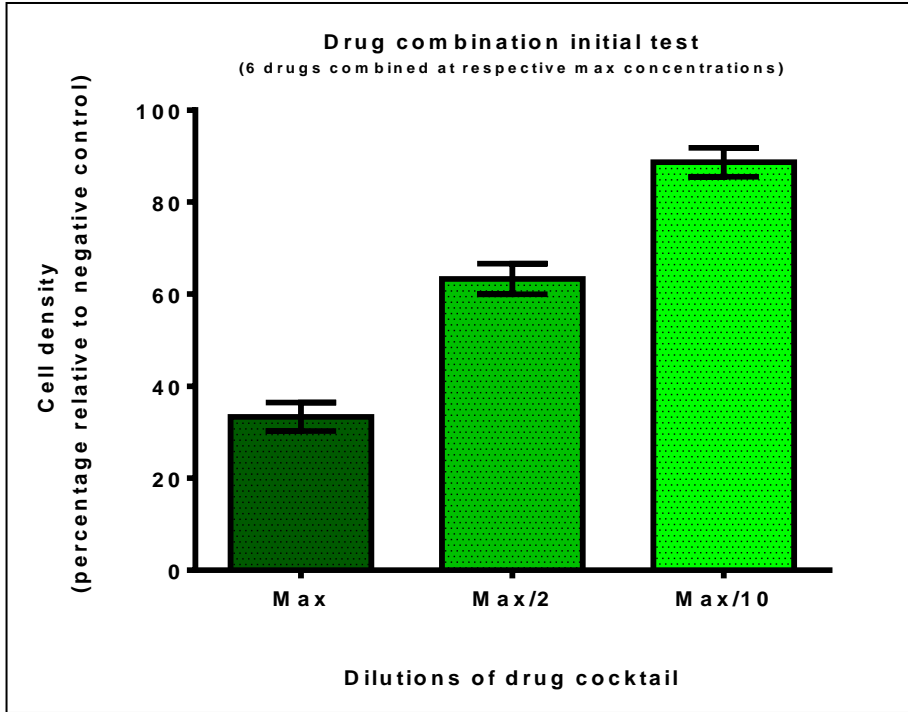


Figure 2.10: Comparative cell survival during the first pilot study following 72 h exposure to different concentrations of the six-drug cocktail to determine the concentration range relative to the maximum non cross inducing concentration and untreated negative controls.

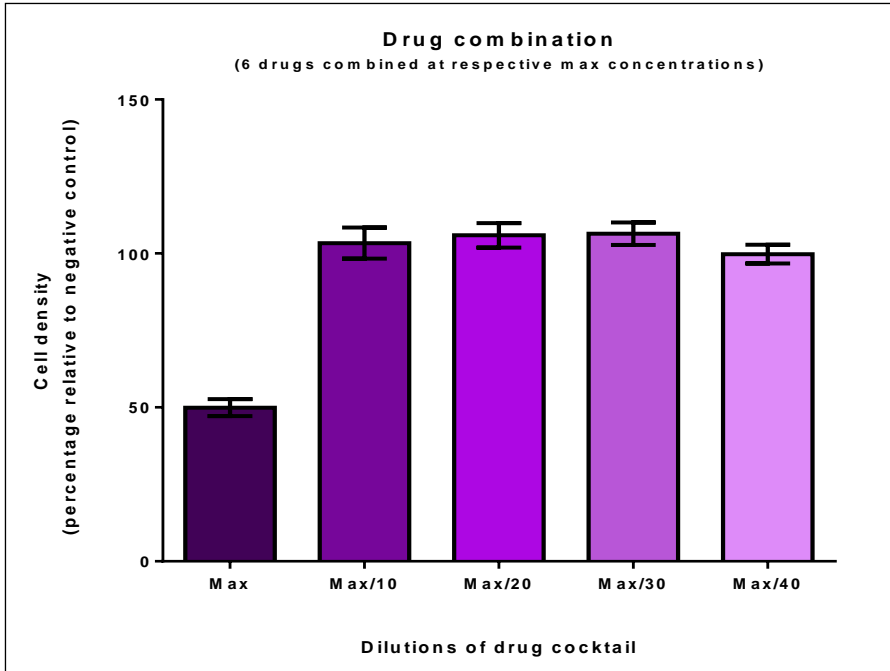


Figure 2.11 Cell survival after 72 h exposure to various concentrations of the six drugs combination compared to the maximum concentration, indicating the plateau of response for dilutions to less than max/10.

As the micro mould technique for spheroid cultures had not been previously performed by the laboratory, the growing conditions and seeding densities required optimization before finally performing drug exposure assays. It was determined that reproducible spheroids could be generated and formed optimally at a seeding density of 9.7×10^5 cells per micro mould when seeded in 170 μ l medium. This yielded up to 81 spheroids with a diameter of approximately 450 μ m. Live dead staining, cell cycle analysis and protein content indicated that HepG2 cells, cultured as spheroids of this diameter using the micro moulds, were viable till only Day 6. Therefore, all cell-based work that followed was conducted at a seeding density of 9.7×10^5 cells/170 μ l and culturing was carried out until Day 6.

With the use of the SRB assay, a concentration of drug cocktail was determined to prevent cross-induction of the CYP450 enzymes and to allow continual passaging in the presence of low concentrations of all the drugs in this drug cocktail. This analysis was done in monolayer cultures only since the passaging of enzyme induced cells, prior to the formation of spheroids, was done in monolayers. Table 2.3 shows the final in-well concentration of each drug for subsequent experiments.

Table 2.4 Final in-well concentration of the six drug combination cocktail used when inducing metabolic enzymes during HepG2 cells in culture.

Drug	CYP	In-well concentration
Phenacetin	CYP1A2	2.5 μ M
Diclofenac	CYP2C9	5 μ M
Omeprazole	CYP2C19	2 μ M
Dextromethorphan	CYP2D6	1.25 μ M
Midazolam	CYP3A4	0.25 μ M
Bupropion	CYP2B6	5 μ M

Chapter 3: LC-MS/MS method development and cocktail analysis

3.1 Materials and methods

3.1.1. Standards

Phenacetin, diclofenac sodium salt, omeprazole, bupropion hydrochloride, dextromethorphan hydrobromide, imipramine hydrochloride as well as the metabolites acetaminophen*, 4-hydroxydiclofenac* and Dextrorphan* were purchased from Sigma Aldrich (St Louis, USA). Midazolam (extracted from dormicum ampoules 15 mg/3 ml) was purchased from Roche. The metabolites hydroxybupropion* and 1-hydroxymidazolam* were purchased from Cerilliant (Texas, USA). The metabolite 5-hydroxyomeprazole* was purchased from Caymen chemical company (Ann Arbor, USA).

MS grade methanol and acetonitrile was purchased from Romil (Cambridge, UK). Double deionised water (>18 MΩ) as produced in-house at the Department of Pharmacology using an Elga Genetics water purification system. LC-MS grade formic acid was purchased from Sigma Aldrich (St Louis, USA).

3.1.2 Sample preparation and LC-MS/MS instrumentation

The same methodology was used for both samples and controls, within the method development phase, concerning sample preparation for a single injection, multi-analyte, LC-MS/MS analysis method. A 200 µl aliquot of medium was harvested from each sample of HepG2 cells, grown for 72 h as monolayers or spheroids, in the presence of the six-drug combination cocktail. Protein precipitation was performed using methanol with 0.1% formic acid (FA) which was added in four sequential steps with 1 minute vortex mixing and 5 minute ultrasonic extraction after each addition. The starting volume of sample was 200 µl and 200 µl methanol was added at each step, that yielded a final mixture containing 80% methanol by volume. The sonication of the sample after each addition of methanol ensured maximum analyte recovery. The solution was centrifuged at 16 000 × *g* for 10 min and the supernatant was used to further develop the clean-up and analytical method. Imipramine hydrochloride (1 µg/ml) was added to each sample as an internal standard (IS).

The LC-MS/MS system consisted of an Agilent 1100 series autosampler, binary pump, degasser and column oven coupled to a Sciex 4000 QTrap mass spectrometer with a Turbo V electrospray ionisation (ESI) source. The complete system was centrally controlled, and data collected and analysed using Analyst Software, Version 1.5.2.

3.1.2.1. Chromatographic conditions

The initial chromatographic separation of the combination of 13 analytes was conducted using standards for each analyte in methanol/water injected onto a Kinetex Biphenyl (100 × 2.10 mm,

2.6 μm) analytical column with the column temperature set to 30°C. After obtaining an acceptable basic separation, other types of reverse phase analytical columns were screened to assess the best conditions to ensure resolution between critical pairs of analytes. The autosampler tray was set to a temperature of 20°C. The aqueous mobile phase A consisted of 0.1% formic acid in double deionised water, whereas the organic mobile phase B consisted of 0.1% formic acid in methanol. A gradient elution program was employed and used an initial high aqueous concentration which changed to a high organic concentration. A method and gradient program, initially over 15 minutes, was modified and optimized to achieve the best chromatographic resolution of each analyte, although some coelution was acceptable for non-crosstalk compounds. The method had to be sensitive, robust, reduce matrix effects and provide accurate quantitation. The chromatographic parameters that were optimized included peak shape, analyte resolution and retention times. The stability of some analytes was also of concern and this was taken into account.

3.1.2.2. Mass spectrometer conditions

Analytes were analysed using the Sciex 4000 QTrap mass spectrometer system which was initially set to scan from 100 - 1000 m/z units in positive mode. Several scan modes were used to optimise the MS parameters for each individual analyte and included Q1 scans, high resolution scans, product ion scans and MRM scans. The optimised ionisation source parameters as well as the precursor-product transitions for each analyte were determined during infusion assays of solutions of approximately 50 $\mu\text{g}/\text{ml}$ infused at 10 $\mu\text{l}/\text{min}$. The following parameters were optimized for each of the analytes: ESI voltage, nebulising and desolvation gas flows, desolvation temperature, source temperature, declustering potential and extraction voltages by monitoring specific ions for each analyte and optimising the signal intensities. Collision energy was optimised for the specific precursor masses to obtain the best intensity of the major and unique product ions. Optimizing these conditions ensured the best sensitivity by maximising transfer of analytes to the detector and limiting noise through use of multiple reaction monitoring, increasing the method sensitivity and selectivity which is required for a quantitative multi-analyte method.

3.1.2.3. Method validation

The analytical method was validated according to the International Conference on Harmonization (ICH) Q2(R1) guidelines, using different assays to meet the following criteria: linearity, dynamic range, accuracy, precision, specificity, detection limit, quantitation limit, robustness, recovery, stability and system suitability testing.

Recovery was determined by the ratio of the slopes obtained from solvent matrix based calibration curves versus cell growth medium matrix matched calibration curves. Calibration curves were made up on three different days with intra-day triplicate runs being performed. Calibration curves were produced by diluting accurately known concentrations of analyte

mixtures into extracted cell growth medium and solvent. Seven different standard concentrations and two separately prepared quality control (QC) standards were used for each specific drug or metabolite, with Imipramine added to all standard mixtures as an internal standard at a constant concentration of 1 µg/ml.

Specificity and robustness were determined during method development through: extraction of the analytes from cell growth media; optimization of the mass spectrometer to individually identify and quantitate each analyte; optimising chromatographic conditions and minimising matrix effect. Recovery, linearity, range, accuracy, precision, detection limit and the quantitation limit were determined using replicate calibration curves. The optimized method, detailed in the results and discussion, was used to analyse the metabolic changes of the short-term and long-term drug induced enzyme induction in monolayer and spheroid cultures.

3.2. Results

3.2.1. Mass spectrometer optimization

Each analyte was individually assessed using low flow infusion during which the source parameters were optimised. As some parameters cannot easily be changed during the mass spectrometric analysis, the most acceptable compromises were taken for use of static parameters during the analysis. These parameters are set out in (Table 3.1 and 3.2) below and formed the basis for all subsequent LC-MS/MS analysis.

Table 3.1 Optimised parameters for mass spectrometry

Optimised source conditions for the 6-drug cocktail and their metabolites	
Parameter	Value
Capillary voltage	+5000 V
Drying gas temperature	450°C
Ion source gas 1	35
Ion source gas 2	35

Table 3.2 Final MRM pairs used for the analysis of the CYP cocktail.

Optimised multiple reaction monitoring (MRM) pairs for the 6-drug cocktail, the metabolites, and the internal standard				
Analytes	Q1 Mass (Da)	Q3 Mass (Da)	Collision energy (volts)	Declustering potential (volts)
Phenacetin	180.3	110.3	28	65
Acetaminophen*	152.2	110.2	23	60
Dextromethorphan	272.5	213.3	38	90
Dextrorphan*	258.4	199.3	36	95
Diclofenac	296.3	215.1	26	60
4-OH-Diclofenac*	312.3	231.3	27	50
Midazolam	326.4	291.4	39	100
1-OH-Midazolam*	342.4	324.3	30	80
Omeprazole	346.6	284.5	32	100
5-OH-Omeprazole*	362.6	300.5	33	90
Bupropion	240.4	184.2	18	55
OH-Bupropion*	256.4	238.5	17	60
Imipramine	281.4	86.3	50	50

3.2.2. Chromatography

After MS parameter optimisation, the chromatographic method was optimised by evaluating different mobile phases, columns and gradient profiles. The Kinetex Biphenyl (100 × 2.10 mm, 2.6 µm) column and the Phenomenex C18 (100 × 2.10 mm, 2.6 µm) column were tested using a gradient elution method and by changing mobile phase B from methanol (MeOH) to acetonitrile (MeCN). Organic mobile phase compositions, tested for each column, included 100% MeOH, 80:20 MeOH:MeCN, 50:50 MeOH:MeCN, 20:80 MeOH:MeCN and 100% MeCN.

Figure 3.1 and Figure 3.2 each display a chromatogram where the most optimal gradient elution and mobile phase composition were selected for the Biphenyl column and C18 column, respectively. The Biphenyl column was chosen as the most appropriate column as the selectivity and sensitivity was improved when compared to that obtained from the C18 column. For simultaneous analysis of multiple analytes in a single sample, the most optimal separation and sensitivity had to be achieved with the aqueous mobile phase A consisting of 0.1% formic acid (FA) in deionised water with the organic mobile phase B consisting of 0.1% FA in 20:80 MeOH:MeCN.

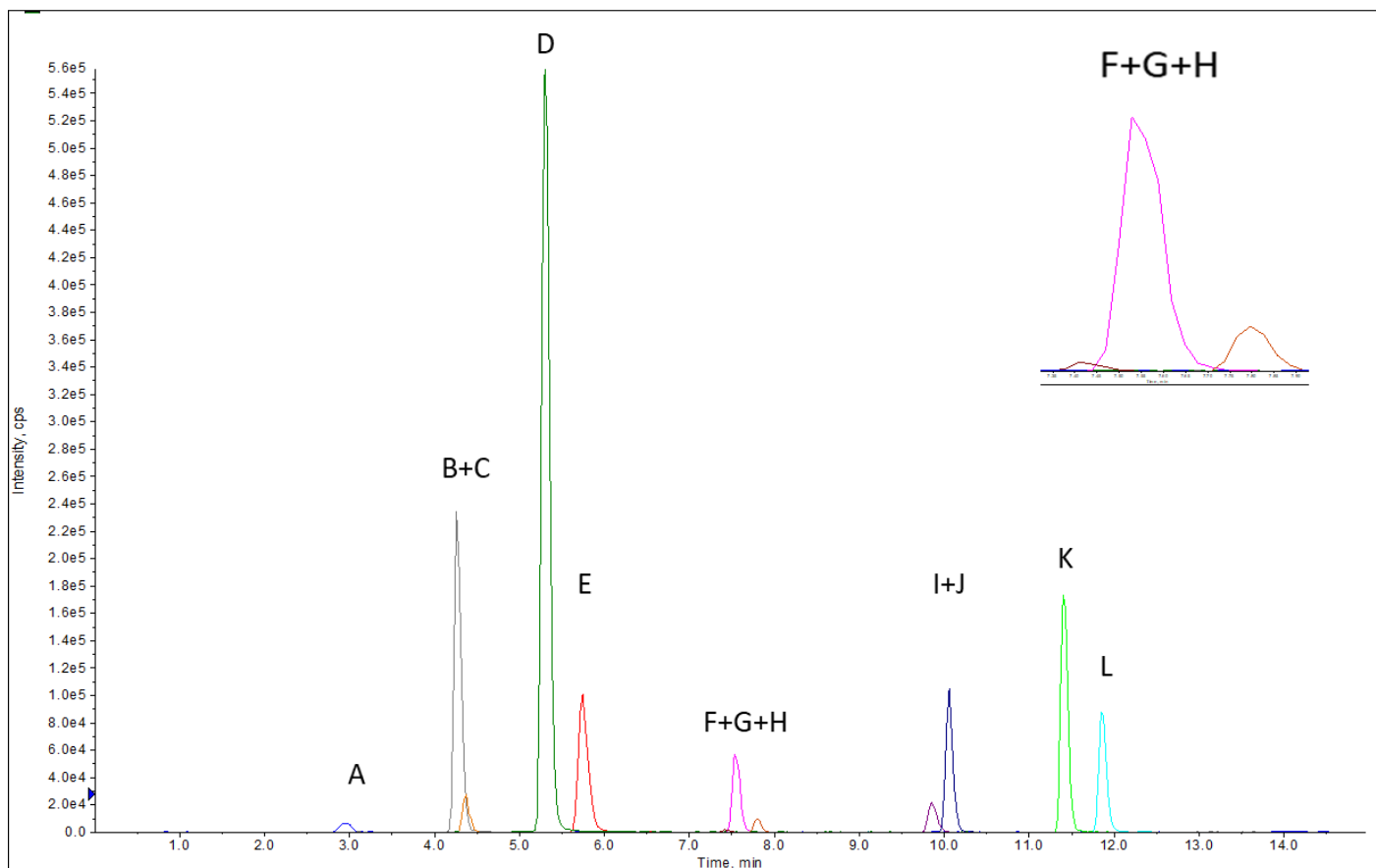


Figure 3.1 Optimised biphenyl phase chromatography using mobile phase A of 0.1% FA in H₂O and mobile phase B of 0.1% FA 20:80 MeOH:MeCN, with all 12 analytes described by retention times (from left to right): A) Acetaminophen*, B) OH-Bupropion*, C) Dextrophan*, D) Bupropion, E) Phenacetin, F) 1-OH-Midazolam*, G) Dextromethorphan, H) Midazolam, I) 4-OH-Diclofenac*, J) 5-OH-Omeprazole*, K) Omeprazole, L) Diclofenac. Inset: enlarged version of F) 1-OH-Midazolam*, G) Dextromethorphan, H) Midazolam to visualise smaller peaks.

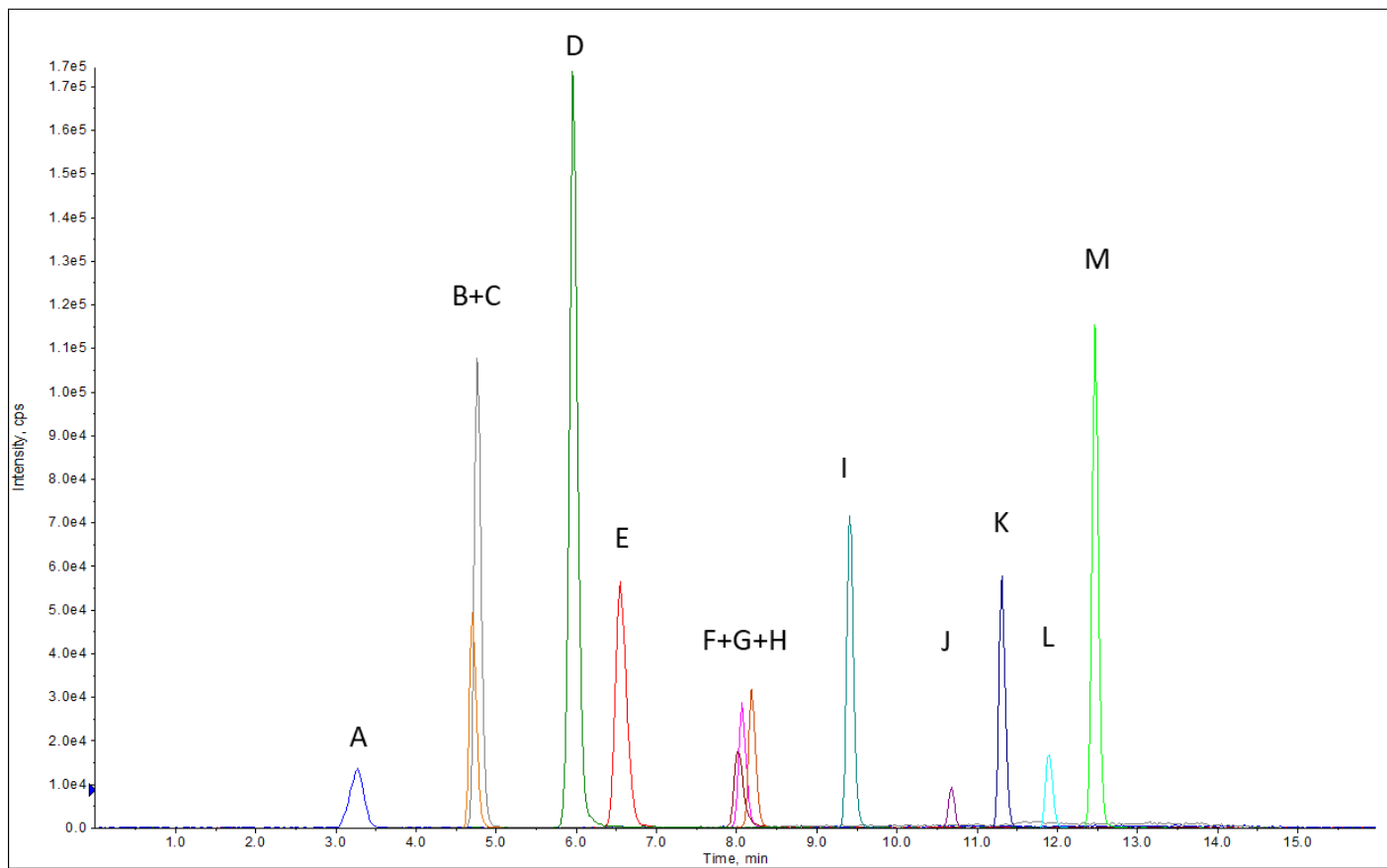


Figure 3.2 Optimized C18 chromatogram using Mobile phase A of 0.1% FA in H₂O and Mobile phase B of 0.1% FA 20:80 MeOH:MeCN) with all 12 analytes and IS described by retention time order (from left to right): A) Acetaminophen*, B) OH-Bupropion*, C) Dextrophan*, D) Bupropion, E) Phenacetin, F) 1-OH-Midazolam*, G) Dextromethorphan, H) Midazolam, I) 4-OH-Diclofenac*, J) 5-OH-Omeprazole*, K) Omeprazole, L) Diclofenac and M) Imipramine.

Table 3.3 Chromatography gradient optimised for the best separation for all analytes

Step	Total Time (min)	Flow Rate ($\mu\text{l}/\text{min}$)	A (%)	B (%)
0	0	300	95	5
1	0.5	300	75	25
2	2	300	75	25
3	3	300	72	28
4	4	300	71	29
5	4.5	300	68	32
6	5.5	300	65	35
7	6	300	60	40
8	6.5	300	52	48
9	7.5	300	51	49
10	8.5	300	50	50
11	9	300	40	60
12	9.5	300	37.5	62.5
13	11.5	300	15	85
14	11.6	300	95	5
15	15	300	95	5

After finalising the most optimal chromatography conditions (Table 3.3), and running the method using blank samples, peaks were observed at elution times thought to be for omeprazole and 5-hydroxyomeprazole* (Figure 3.3). Contaminants with apparently similar MRM transitions were found to be the cause of these unexpected peaks and thereby showed that the original conditions selected during tuning were, in fact, not for omeprazole. This resulted in exclusion of both omeprazole and 5-hydroxyomeprazole* during the analysis of experimental samples (Figure 3.4 and Figure 3.5).

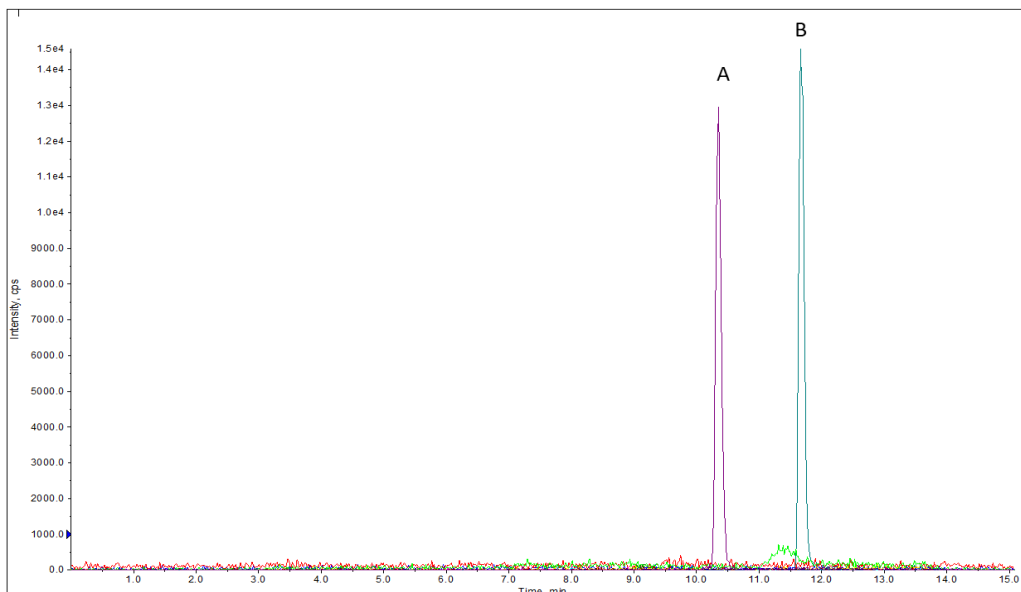


Figure 3.3: Chromatogram that displays contamination at retention times thought to be for Omeprazole and 5-OH-omeprazole*

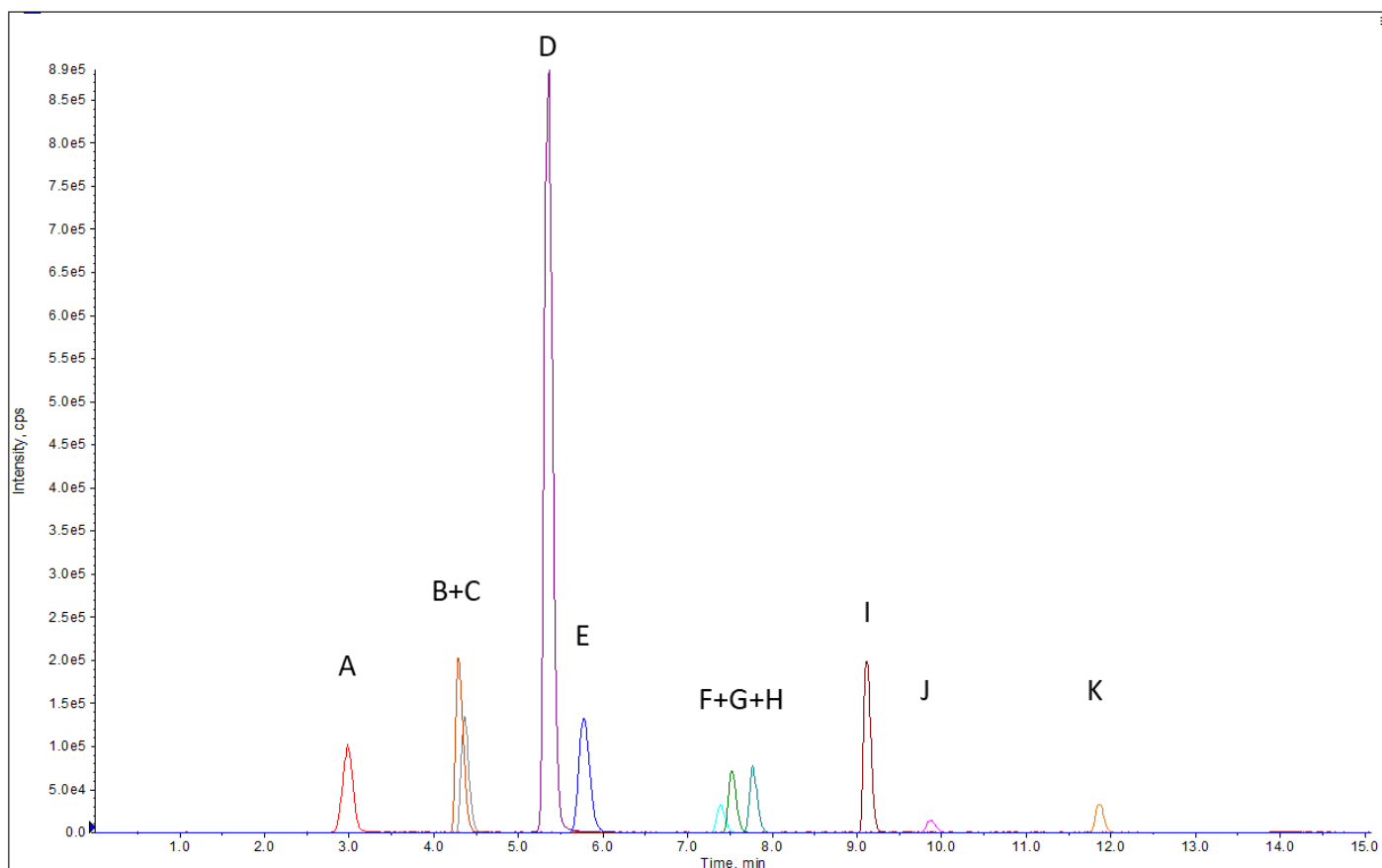


Figure 3.4 Chromatogram with contaminants removed which consists of 5 parent drugs and 5 metabolites along with the internal standard described by retention times (from left to right): A) Acetaminophen*, B) OH-Bupropion*, C) Dextrophan*, D) Bupropion, E) Phenacetin, F) 1-OH-Midazolam*, G) Dextromethorphan, H) Midazolam, I) Imipramine, J) 4-OH-Diclofenac*, K) Diclofenac.

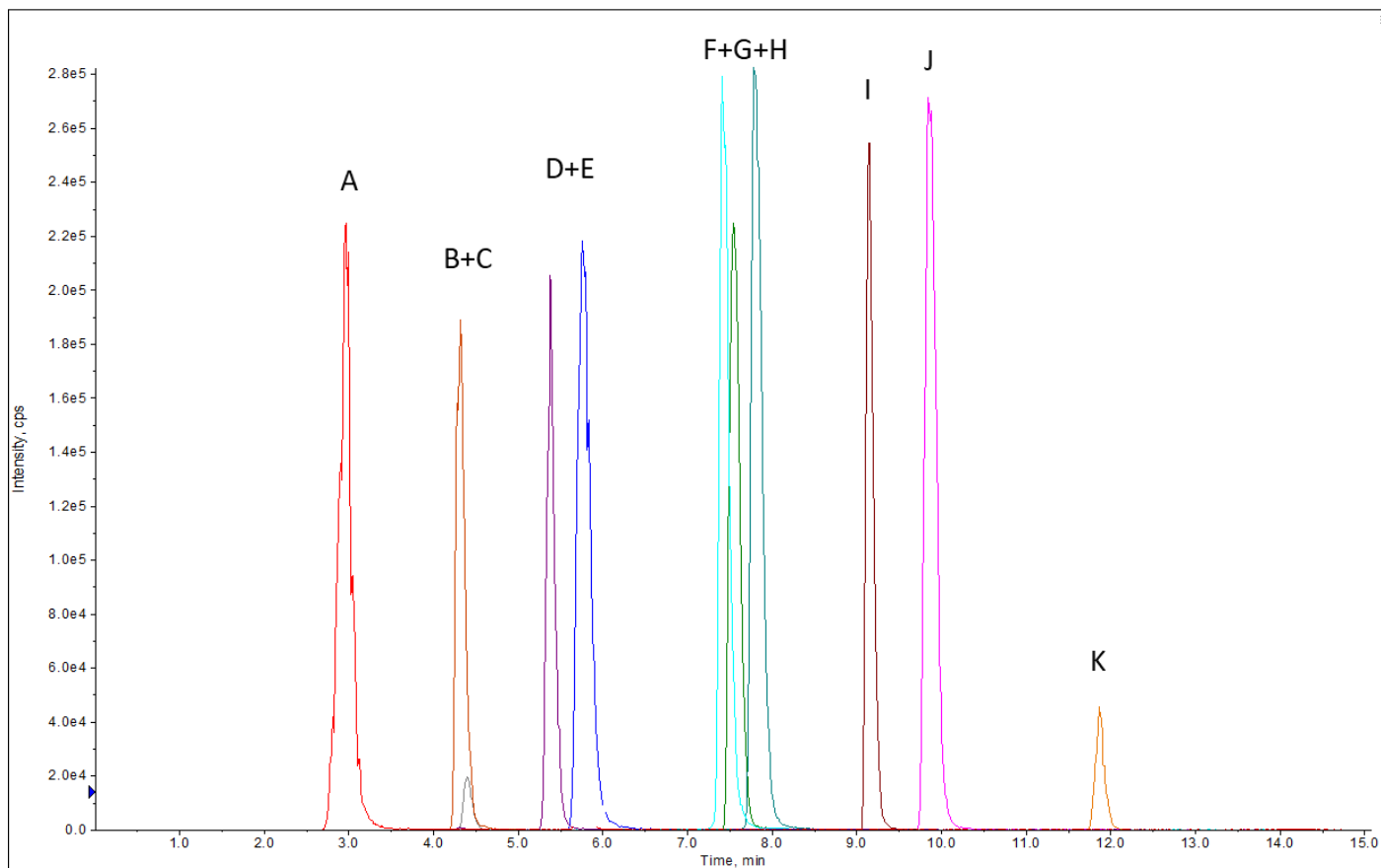


Figure 3.5 Chromatogram with final parameters normalised to show peaks at more or less the same height labelled by retention times (from left to right): A) Acetaminophen*, B) OH-Bupropion*, C) Dextrorphan*, D) Bupropion, E) Phenacetin, F) 1-OH-Midazolam*, G) Dextromethorphan, H) Midazolam, I) Imipramine, J) 4-OH-Diclofenac*, K) Diclofenac.

Resolution was considered good with the exception of two analyte pairs which were limited in observable separation between hydroxybupropion* and dextrorphan* as well as 1-hydroxymidazolam* and dextromethorphan. These peaks are shown in Figure 3.6 where 1-hydroxymidazolam* and dextromethorphan partially overlap.

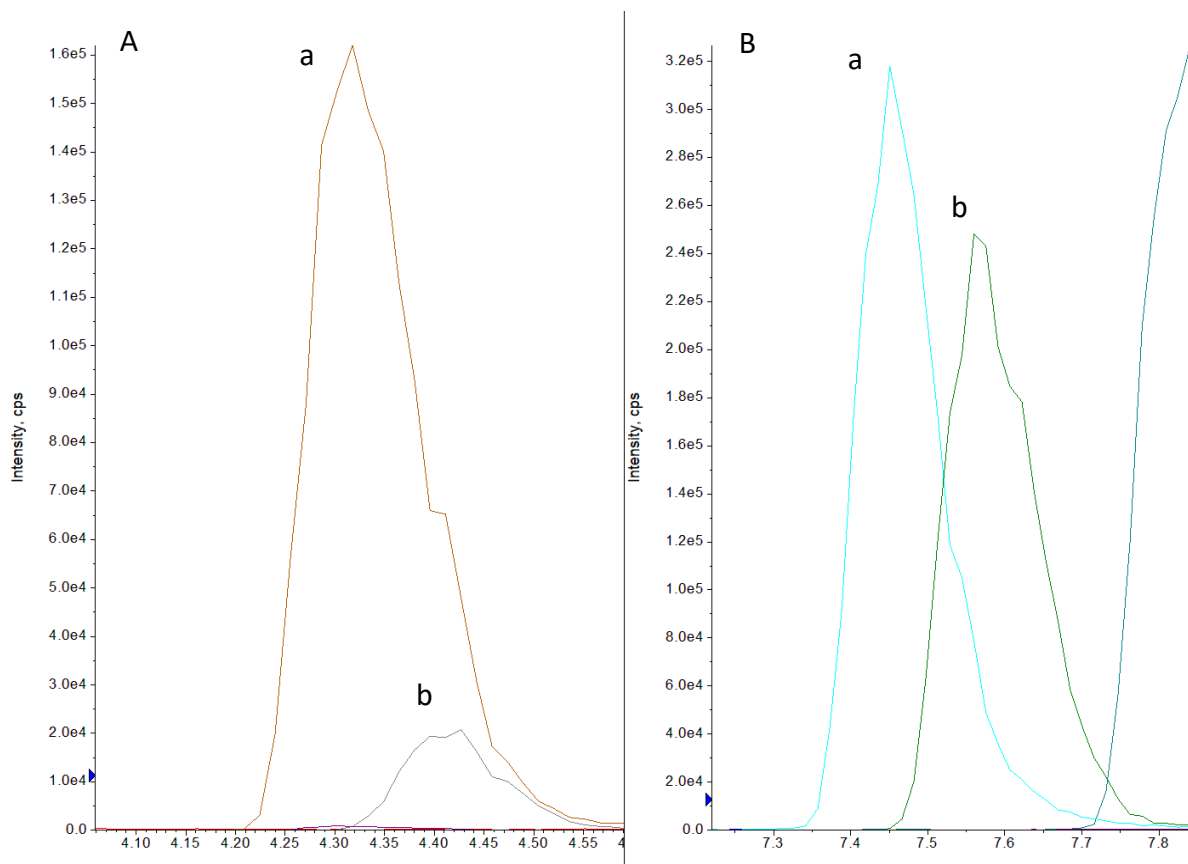


Figure 3.6 Enlarged areas of the chromatograms showing the peaks of A) a: OH-bupropion* and b: dextrorphan* and B) a: 1-OH-midazolam* and b: dextromethorphan showing poor analyte resolution which could indicate ion suppression

3.2.3. Recovery

Recovery was determined to test for any detrimental effects which cell growth media could have had on analyte quantitation. Water, which was spiked with the analytes, was compared to cell growth media also spiked with the analytes. The concentrations spiked into the different corresponding matrices and were the same as those used to calculate the calibration curve. Table 3.4 shows the calculated percentage by which the medium had changed the calculated concentrations of the analytes. A general trend of suppression was seen when using the cell growth media as only two analytes, acetaminophen* and diclofenac, signals were enhanced by roughly 1%. This suppression of the analytes was not high, except for Phenacetin and Bupropion where approximately 11% signal suppression was observed. These effects were not substantial enough to be considered limiting to quantification of these analytes as they still fall within the 15% acceptable change.

Table 3.4. Recovery determined by the ratio of solvent matrix calibration curve versus cell growth medium matrix calibration curves.

Drug	Recovery
Phenacetin	88.99%
Acetaminophen*	100.72%
Dextromethorphan	98.20%
Dextrorphan*	94.83%
Diclofenac	101.12%
4-OH-Diclofenac*	98.62%
Midazolam	93.86%
1-OH-Midazolam*	97.50%
Bupropion	89.15%
OH-Bupropion*	93.39%

3.2.4 Calibration curves

Once MS, chromatography conditions and sample preparation altogether were optimised, calibration curves for the multiple analyte method were constructed. The calibration curves allowed simultaneous determination of linearity, linear dynamic range, accuracy, precision and the quantitation limit. Table 3.5 displays the concentrations used for each analyte in setting up the calibration curves. A large linear range was required so each analyte concentration was tailored specifically for that analyte based on instrument sensitivity.

Table 3.5. Each drug and metabolite's concentration used for calibration curves

Drug	Concentration (ng/ml)						
Phenacetin	1	5	10	50	100	500	1000
Acetaminophen*	5	25	50	250	500	2500	5000
Diclofenac	1	5	10	50	100	500	1000
4-OH-Diclofenac*	10	50	100	500	1000	5000	10000
Dextromethorphan	2.5	12.5	25	125	250	1250	2500
Dextrorphan*	0.1	0.5	1	5	10	50	100
Midazolam	0.4	2	4	20	40	200	400
1-OH-Midazolam*	5	25	50	250	500	2500	5000
Bupropion	0.050	0.25	0.5	2.5	5	25	50
OH-Bupropion*	1	5	10	50	100	500	1000

A 7-point calibration curve was generated for each analyte, however, each analyte saturated the MS at the highest concentrations and was subsequently removed from the calibration curves. Figure 3.7 displays a calibration curve of Dextromethorphan and shows linearity from 2.5 ng/ml to 1250 ng/ml with an r^2 -value of >0.99 . Calibration curves for the rest of the analytes followed a similar trend (data not shown) with the linearity of all analytes provided in Table 3.6.

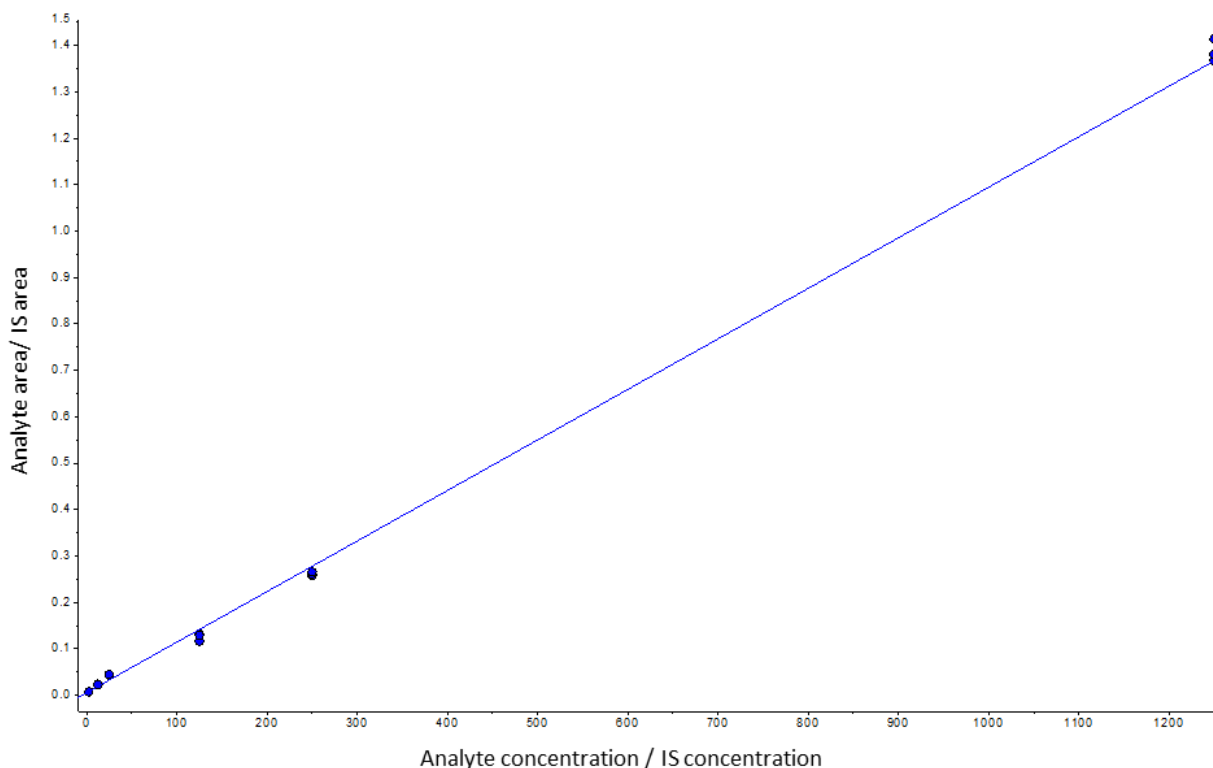


Figure 3.7 Calibration curve of dextromethorphan with linearity between 2.5 ng/ml and 1250 ng/ml

The linear range for each analyte was established, calculating the lowest concentration by using the lower limit of quantitation (LLOQ) and ascertaining the highest concentration via the maximum concentration used for each drug in the drug cocktail. Figure 3.8 displays the chromatogram of dextromethorphan at its lowest concentration (2.5 ng/ml) to indicate the signal to noise ratio for determination of the LLOQ. Signal to noise was similarly determined for each analyte (data not shown). LLOQ was then calculated using the lowest concentration that has a signal to noise ratio of at least 10. Once the signal to noise for each analyte was established to be greater than 10, the linear range was tabulated (Table 3.7).

Table 3.6. List of all analytes showing linear regression, r-values and r²-value

Drug	Linear regression	r value	r ² -value
Phenacetin	$y = 0.0028 x + 0.0019$	0.9957	0.9914
Acetaminophen*	$y = 0.0007 x + 0.0052$	0.9945	0.9890
Dextromethorphan	$y = 0.0011 x + 0.0058$	0.9972	0.9944
Dextrophan*	$y = 0.0017 x + 0.0002$	0.9961	0.9922
Diclofenac	$y = 0.0005 x + 0.0002$	0.9858	0.9718
4-OH-Diclofenac*	$y = 0.0004 x + 0.0075$	0.9912	0.9825
Midazolam	$y = 0.0095 x + 0.0181$	0.9958	0.9916
1-OH-Midazolam*	$y = 0.0007 x + 0.0180$	0.9942	0.9884
Bupropion	$y = 0.0337 x + 0.0027$	0.9850	0.9702
OH-Bupropion*	$y = 0.0021 x + 0.0066$	0.9958	0.9916

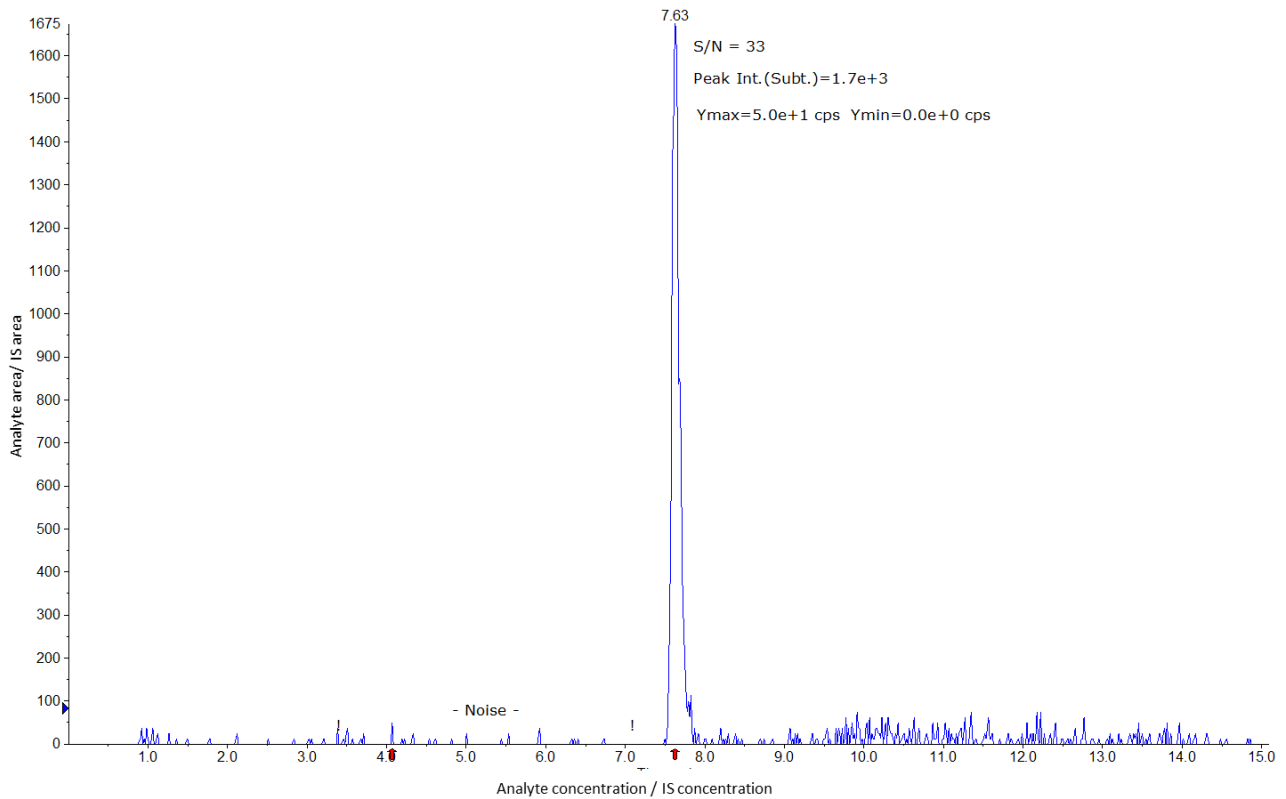


Figure 3.8: Signal to noise ratio (S/N) of 2.5 ng/ml dextromethorphan to indicate the LLOQ

Table 3.7. Signal to noise ratio of each analyte used to establish their LLOQ concentration and confirmation of the linear range of each analyte

Drug	Signal to noise ratio	LLOQ concentration (ng/ml)	Linear range
Phenacetin	10.6	1	1 ng/ml - 500 ng/ml
Acetaminophen*	14.3	5	5 ng/ml - 2500 ng/ml
Dextromethorphan	33	2.5	2.5 ng/ml - 1250 ng/ml
Dextrorphan*	10.5	0.5	0.5 ng/ml - 50 ng/ml
Diclofenac	21.5	5	5 ng/ml - 500 ng/ml
4-OH-Diclofenac*	23.7	10	10 ng/ml - 5000 ng/ml
Midazolam	191.5	0.4	0.4 ng/ml - 200 ng/ml
1-OH-Midazolam*	72.9	5	5 ng/ml - 2500 ng/ml
Bupropion	24.2	0.05	0.05 ng/ml - 25 ng/ml
OH-Bupropion*	29.7	1	1 ng/ml - 500 ng/ml

Accuracy and precision were determined from the calibration curves set up for each analyte. Accuracy and precision were determined by using nine replicates per analyte. The nine points were obtained from three intra-day and three inter-day calibration curve repeats, where the inter-day repeats were carried out at least one day apart. Allowed variation in accuracy and precision across replicates is 15% for mid concentrations and 20% at the LLOQ. All of the analytes were found to be within these acceptable limits for accuracy and precision.

The variability of the internal standard represents the minimum variability that can be expected from any given analysis. The average variance of imipramine, used as the internal standard during this study, was 5.99%. This allows the assumption that the technical variability is at least 5.99%.

The variability, observed for the individual analytes in the QC standards, was calculated and is shown in Table 3.9 where variability for both solvent and cell growth media, based QC standards, are shown for both the high and low QC standards. A general trend is seen where the variability of the lower QC standards are greater than that of the high QC standards and the cell growth media has a higher variability in the low QC than that of the solvent low QC.

Table 3.8. Mean peak areas and standard deviation of the internal standard and the most sensitive (Midazolam) and the least sensitive (Dextrophan*) compound 1 is the lowest concentration run with the most diluted spiked sample up to 5 which contain the highest concentration of spiked analytes.

Sample	Internal Standard (Imipramine)		Midazolam		Dextrophan*	
	Mean	StDev	Mean	StDev	Mean	StDev
1	1,70E+06	4,36E+04	3,13E+04	1,93E+03	6,40E+02	2,27E+02
2	1,64E+06	1,72E+05	7,35E+04	4,59E+03	2,05E+03	1,92E+02
3	1,59E+06	1,03E+05	1,22E+05	8,39E+03	3,70E+03	5,74E+02
4	1,61E+06	9,61E+04	3,20E+05	1,48E+04	1,15E+04	1,25E+03
5	1,68E+06	8,66E+04	6,69E+05	6,73E+04	2,51E+04	2,52E+02
QC 0.75	1,66E+06	1,27E+05	7,33E+04	9,11E+03	2,20E+03	1,52E+03
QC 7.5	1,62E+06	7,57E+04	4,69E+05	1,88E+04	2,54E+04	1,44E+03

Table 3.9. Percentage variability for the different QC samples for each analyte.

Sample	Low QC Std Solvent	High QC Std Solvent	Low QC Std Cell growth Media	High QC Std Cell growth Media
Phenacetin	11,00%	5,40%	16,00%	3,36%
Acetaminophen*	12,04%	5,56%	17,22%	6,70%
Dextromethorphan	5,32%	8,37%	12,05%	3,46%
Dextrophan*	9,33%	3,34%	4,59%	5,68%
Diclofenac	8,24%	8,28%	7,03%	7,11%
4-OH-Diclofenac*	9,27%	6,67%	13,31%	5,25%
Midazolam	2,35%	5,79%	12,43%	4,00%
1-OH-Midazolam*	5,42%	11,94%	17,79%	7,45%
Bupropion	3,21%	13,45%	11,74%	2,36%
OH-Bupropion*	13,00%	12,93%	12,21%	9,09%

Figure 3.9 had been generated to show the relative consistency of the injection volume, using the internal standard as a constant. Figure 3.10 and Figure 3.11 had been produced to visualise the general trend the optimised calibration curves had followed using the most sensitive and least sensitive compound respectfully.

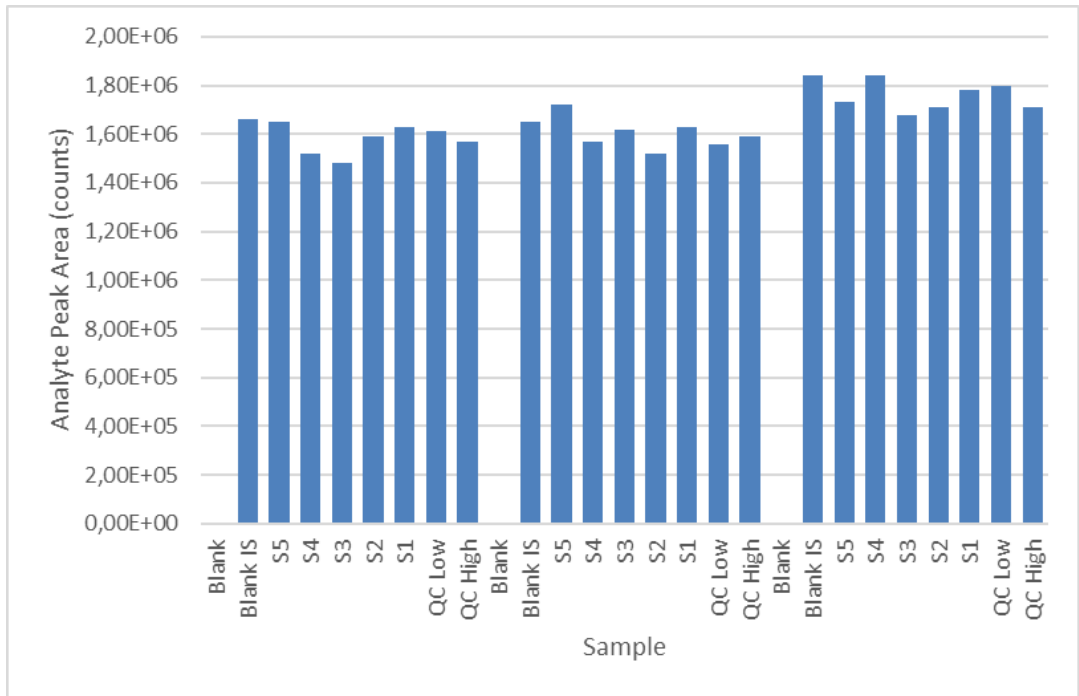


Figure 3.9. Bar graph to show the relatively stable injection volume of the internal standard Imipramine, shown for peak area. S1 – S5 are the increasing concentrations of the mixed analytes.

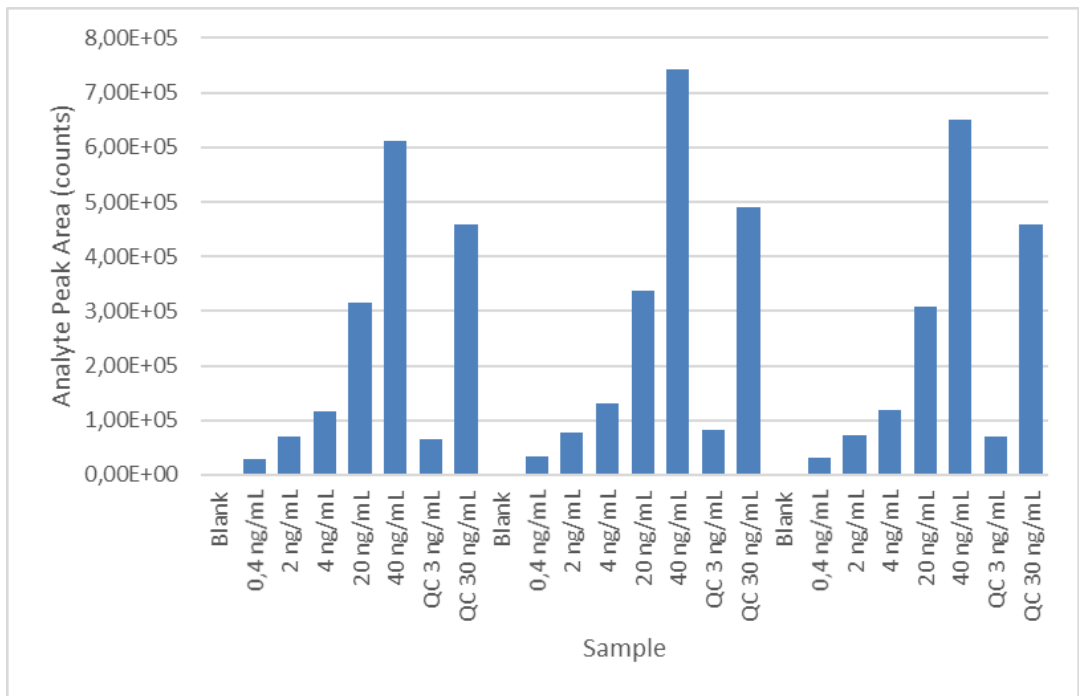


Figure 3.10. Bar chart of Midazolam peak areas from a calibration curve series indicating the general trend that the most sensitive compound follows.

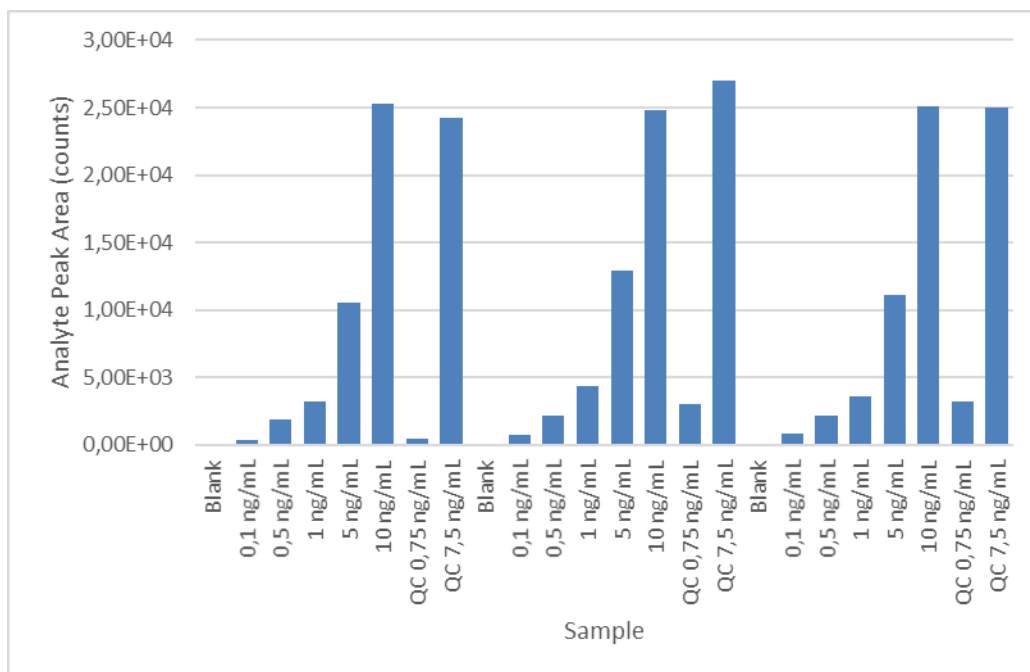


Figure 3.11. Bar chart of Dextrorphan* peak areas from a calibration curve to indicate the general trend followed by the least sensitive compound.

3.2.5. Induction results

The developed and validated LC-MS/MS method was used to quantify the 10 analytes in the induction experiments where HepG2 cells were cultured in the presence of the six-drug combination cocktail. The metabolism in monolayer and spheroid cultures were compared. Figure 3.12 provides the analyte concentration after long-term exposure to the drug cocktail, where neither diclofenac or bupropion exhibited any metabolised. Phenacetin, dextromethorphan and midazolam were found to be metabolised in both monolayer and spheroid models.

Figure 3.13 describes how much metabolism has taken place after only 72 h of exposure to the drug cocktail. No metabolism was evident for phenacetin, bupropion or diclofenac. Dextromethorphan was metabolised in the monolayer format but not in the spheroid format and no midazolam (notably, neither parent drug nor metabolite) was detected after only 72 h of culturing.

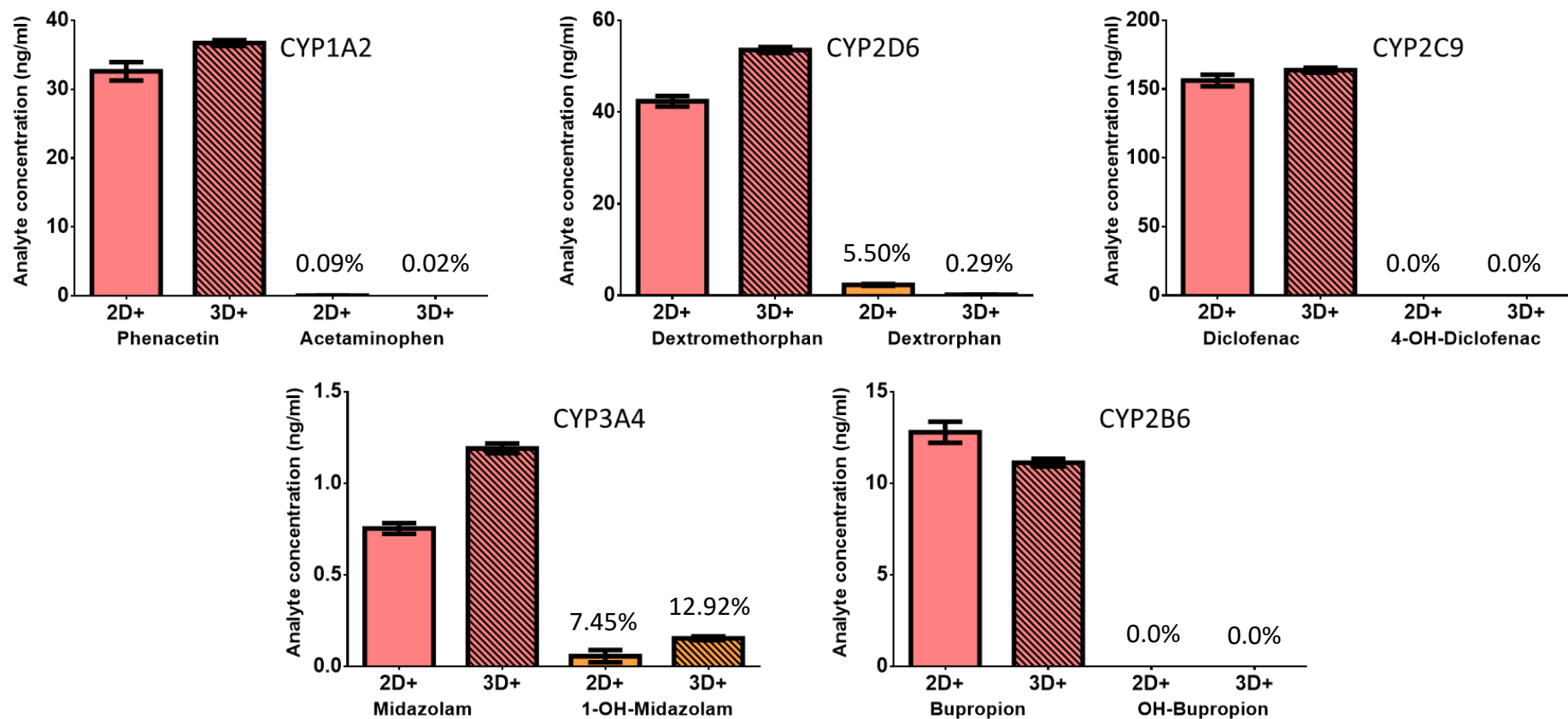


Figure 3.12 Bar graphs displaying the calculated analyte concentration of each parent drug used in the drug cocktail and the corresponding metabolite for both monolayer(2D+) and spheroids(3D+) after long term culturing (30 days) under continual exposure to low dose of the drug cocktail. Metabolism is calculated as a percentage of the parent analytes.

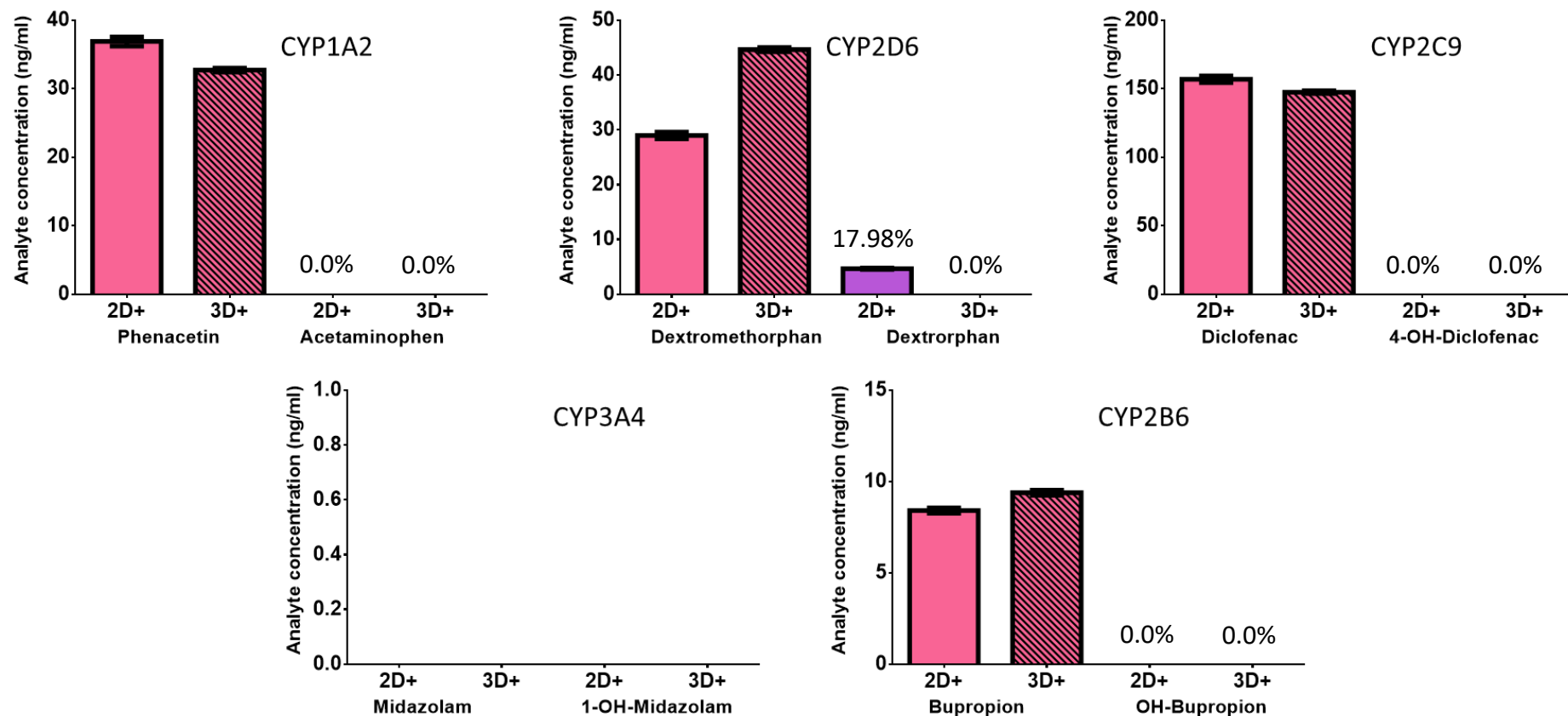


Figure 3.13 Bar graphs displaying the calculated analyte concentration of each parent drug used in the drug cocktail and the corresponding metabolite for both monolayer(2D+) and spheroids(3D+) after a single 72 h exposure. Metabolism calculated as a percentage of the parent analytes. Midazolam showed no response for parent so no percentage was calculated.

Chapter 4: Discussion and Conclusion

4.1. Discussion

As a lack of metabolic competence has been attributed to HepG2 *in vitro* models mainly due to an inherent reduction of phase I metabolizing enzymes (Gomez-Lechon *et al.*, 2008), this project was conducted in an attempt to counter such limitations. Studies on *in vitro* models have indicated the observed decrease in such enzymes to be a consequence of HepG2 cells being utilized as an immortalized cell line and being passaged in a xenobiotic-free, artificial cell culture microenvironment. These factors were targeted for investigation by comparing the inductive capacity potential of phase I enzymes in conventional monolayers and as 3D spheroid cultures. This was to be determined with the use of a novel cocktail combination using a single acquisition LC-MS/MS method.

By using a drug cocktail method to potentially improve the metabolic competency of HepG2 cells more active cytochromes would provide a more suitable model for hepatotoxicity screening. An *in vitro* model with fully competent metabolic enzymes will be advantageous as it will more accurately depict what happens in the body and minimize the need for animal testing and possibly reduce adverse reactions that might be observed during clinical trials or after release on the market.

HepG2 cells have shown some promise in being induced by culturing spheroids with the use of a basement membrane matrix as a scaffold. Ramaiahgari *et al.* 2014 was able to increase the transcription factors of various phase I and phase II enzymes as well as some drug transporters. The transcription factors of some of these increased to indicate some level of metabolic competency of the phase I enzymes, however not all CYP450s that showed an increase in mRNA translated into functional metabolism⁸².

Metabolic competency in long-term cultures is most efficient in PHH. There are drawbacks to the use of PHH in that they are expensive and are donor dependent. The advantage of donor dependent samples can help by improving our understanding of genetic responses and to help promote the correct use of personalised medicine³². However, when it comes to determining a drug's mechanism and possible toxicity profile, a standardised method is required.

The first objective was designed for the optimizing of the spheroid culture methodology, undertaken with the 3D Petri Dish, to determine a timeline of spheroid viability. Seeding density was chosen to yield the largest spheroid size and maintained viability; establishing comparable parameters between monolayer and spheroid cultures for proceeding objectives. Generally compacted, round spheroids were formed by the third day of culturing.

Hence, when the method was initiated different seeding densities were tested to establish the spheroid sizes. Spheroids formed using 1.3×10^6 cells/well (Figure 2.3D) had suitable morphology and were originally considered optimal. However, when seeding at this high cell density, some cells did not settle into the agarose mould matrix and were found in a monolayer at the bottom of the well (Figure 2.4A). This reduced the reproducibility of the assays and new cell concentrations between 6.48×10^5 cells/well and 1.3×10^6 cells/well were assessed. This seeding density was calculated at 9.7×10^5 cells/well and generated spheroids of a similar size with enhanced reproducibility and reduced spill-over into the cell culture plate wells (Figure 2.4B).

The general morphology of spheroid culture over time (Figure 2.5) illustrated that spheroids decrease in diameter over time. This could be due to progression in the three-step spheroid formation process. Cells aggregate before subsequent integrin-ECM and cadherin up-regulation with final spheroid compaction from cadherin-cadherin binding between cells⁸³. The advantage of culturing spheroids in this agarose mould format is that aggregation is forced via seeding high cell numbers per well as this may reduce the time between spheroid aggregation and compaction. Spheroids, after 10 days in culture, were of a similar size to Day 7 but presented with some loss of sharpness around the spheroidal border. This may be indicative of cell stress experienced between Day 7 and Day 10.

Three different assessments; BCA protein quantitation, live-dead staining microscopy and cell cycle analysis were done to determine spheroid viability and resulted in day 7 being considered the maximum culture duration for proceeding experiments.

BCA established the increase or decrease in protein content for indicative correspondence to cell growth or cell death, respectively. Protein concentration, calculated per spheroid of the 9 by 9 matrix, increased up to Day 5 but had decreased by Day 7, which may implicate that there was a reduction in cell viability. The relatively small difference presented between Day 0 and Day 4 may be accredited to a spill over error of cells whilst seeding. For future approximation of protein content up to Day 4, estimations using Day 1 protein content may increase accuracy as this would include only the cells captured within the mould. The high variability in results, indicated by the error bars in Figure 2.6, represent that changes in protein over time are non-significant. The large error bars could be due to seeding inefficiency, the assumption that every microwell forms a spheroid of similar size or simply that experimental design/ conduct did not allow for adequate insight into relevant protein changes. The decrease in protein content on Day 7 was seemingly definitive and reproducible.

From the live-dead staining results (Figure 2.7), it was observed that the spheroids were thoroughly stained with FDA dye, indicating the presence of metabolically active cells. The absence of PI staining confirmed that membranes of few cells were compromised within the spheroids on Days 4 and 5. On Day 6, some non-specific PI staining were observed while, on

Day 7, an apparent prominent necrotic core formed as deduced by high localisation of PI at the spheroid centres. On Day 6 there is a central, sparsely stained region of the spheroid which could be associated with poor depth penetration of dyes, potentially underestimating cell death at this time point. From the combination of reduced protein content and PI staining it was suggested that spheroids, grown with approximated 12 000 cells per spheroid, were compromised by Day 7.

Cell cycle analysis between Day 4 to Day 6 showed a slight decrease in the G0/G1 phase as well as an increase in the sub-G1, S and G2 phases (Table 2.3). Overall, the growth kinetics of cells in spheroids seemed substantially unaltered in early 3D culture. The Day 7 histogram profile (Figure 2.8D) differs greatly across all phases being shifted to the right on the x-axis and the peak areas spread out wider. When comparing percentages of cells in G0/G1 phase peak of Day 7 to that in G0/G1 phase peaks of any other time point, it calculated at least three times lower.

The changes observed on Day 7, as the sub-G1 phase has increased substantially, may indicate cell death. The shifting and widening of the other peaks could indicate that these cells have been ineffectively disaggregated and was, therefore, clumping together. This could also indicate that additional ECM deposition has occurred and that the method for normal disaggregation was insufficient.

The combination of protein content, fluorescent staining and cell cycle analysis indicated that HepG2 cells, seeded at 9.7×10^5 cells/well, should not be cultured for longer than 6 days for sufficient viability to be retained. Longer culture times have been reported when using this format, where C3A cells were able to be cultured for 14 days at a spheroid size of about 200–250 μm ⁸⁴ and where a single H35 cell formed a micro tumour after 21 days⁸⁵. As investigations on HepG2 culture periods in this format are limited in literature, it is perhaps only a speculation that the high seeding density was the main reason for the short culturing time achieved in this objective. The largest possible spheroids maintained without a necrotic core for a long duration were sought for further assays. As spheroids above 500 μm in diameter are more likely to form a necrotic core⁸⁶, it should be taken into consideration that a model vulnerable to this limitation was used. Here, a high seeding density where the spheroids displayed both good morphology and viability for a time duration, considered to be adequate, was chosen.

In order to meet the objective of passaging cells in the presence of a drug cocktail, two factors were required. Firstly, a cell density for monolayers to be cultured for long term in flasks and, secondly, establishing a suitable concentration of drug cocktail for continual passaging. For continual passaging in the presence of drug cocktail, cells were cultured as monolayers in flasks. This was performed for determination of the longest viable time necessary for the induction period between passages. This was determined to be eight days between each passage as the cells, still viable at Day 8, reached a state of high confluence in the flask. Seeding density when passaged was 1×10^6 cells per 75 cm^2 flask.

The next objective was to set up a drug cocktail exposure method for metabolic enzyme induction and to develop an LC-MS/MS multi-analyte method. A known drug cocktail, targeting various specific CYPs, was selected to attempt an increase in the metabolic competency of HepG2 cells. This method required the correct drug compounds at suitable non-toxic concentrations. The analytical method had to be sensitive enough to analyse all of the parent drugs and the common metabolites of these drugs in the same sample.

First a cocktail was established based on reviewing the literature. Spaggiari et al. 2014, compared all the drug cocktail studies investigating the phase I drugs *in vitro* up to 2013 and included the preferred drugs for inducing the most abundantly active cytochromes ⁴¹. These main CYP isoforms (CYP1A2, CYP2B6, CYP2C9, CYP2C19, CYP2D6 and CYP3A4) account for about 95% of CYP450 metabolism. Parameters considered when selecting this cocktail was limited to cross-induction between drugs, specificity of individual drugs to individual CYPs, ability of drugs to be used in a single method, preferred use of the drug in a cocktail, the ability to set up a valid LC-MS/MS method with the maximum ranges possible for each drug and their corresponding metabolites.

Phenacetin was used for CYP1A2 as preference drug in 68% of the cocktails. Its interaction with CYP1A2 is very specific and its potential to be metabolised by other CYPs, such as CYP2C9 and CYP2C19, only occurs at concentrations above 50 μ M. Hence, the maximum limit of phenacetin deemed desirable in the cocktail was 50 μ M. Safety of phenacetin was determined using the SRB cell enumeration assay and it was found to be safe even at concentrations beyond 100 μ M (Figure 2.9). After determining viability thresholds for the drug combination cocktail, a final concentration for phenacetin of 2.5 μ M was included (Figure 2.11). This allowed for the assumption that no cross-induction will have taken place between phenacetin and any non-targeted CYPs once the cocktail was introduced to the cells. The maximum range for phenacetin determined by LC-MS/MS was found to be between 1 ng/ml - 500 ng/ml and its metabolite acetaminophen* 5 ng/ml - 2500 ng/ml. This allowed for a sensitive method that was able to detect these two analytes.

In 95% of the drug cocktails bupropion was used to induce CYP2B6. It is very specific to CYP2B6 metabolism but has potential for interactions with CYPs such as CYP2C19, CYP2D6 and CYP3A4 at concentrations higher than 50 μ M. The final concentration of 5 μ M bupropion used in the drug cocktail was below the 50 μ M threshold (Figure 2.11), allowing for the assumption that there was no cross-induction potential and that bupropion was specifically metabolised only by CYP2B6. The maximum range for Bupropion determined by LC-MS/MS was found to be between 0.05 ng/ml - 25 ng/ml and its metabolite hydroxybupropion* 1 ng/ml - 500 ng/ml. This allowed for a sensitive method able to detect both analytes.

Diclofenac and tolbutamide were almost equally preferred as CYP2C9 inducers. Diclofenac was preferred in 51% of the cocktails used and tolbutamide was preferred in 49% of the cocktails. Diclofenac was selected due to its availability. Its interaction with CYP2C9 is very specific and its potential to be metabolised by other CYPs, such as CYP2C19 and CYP3A4, only occurs at concentrations above 100 μ M. Diclofenac safety was tested up to 100 μ M via the SRB cell enumeration assay and it was found that cell toxicity was limited even at excess concentrations of 100 μ M (Figure 2.9). For the drug cocktail combination, a final concentration for diclofenac of 5 μ M was used which maintained its specificity to CYP2C9 (Figure 2.11). The LC-MS/MS determination of maximum range found it for diclofenac to be between 5 ng/ml - 500 ng/ml and for its metabolite 4-hydroxydiclofenac* to be 10 ng/ml - 5000 ng/ml. Therefore, developing a method sensitive enough to detect both.

Dextromethorphan was used as it was the preferred drug for induction of CYP2D6 in 63% of the probe cocktails. Its potential to be metabolised by other CYPs, such as CYP2C9, only occurs above the threshold of 25 μ M dextromethorphan. Cell toxicity was evaluated to validate the use of dextromethorphan in the cocktail at its maximum restriction of 25 μ M. The SRB cell enumeration assay indicated IC_{50} to be greater than 100 μ M after 72 h and 48.75 μ M after 7 days (Figure 2.9) – neither disputing the threshold of 25 μ M above which cross-induction is reported to occur. The final concentration for dextromethorphan of 1.25 μ M (Figure 2.11), determined by SRB, was combined in the cocktail and assumed to maintain specificity for CYP2D6. The maximum range for dextromethorphan determined by LC-MS/MS was between 2.5 ng/ml - 1250 ng/ml and its metabolite dextrophan* was 0.5 ng/ml - 50 ng/ml, allowed a quantifying method to be designed with sensitivity for both dextromethorphan and its associated metabolite.

Midazolam is reported as the preferred substrate of CYP3A4 in 70% of the cocktails reviewed. Its interaction is most specific to CYP3A4, though potential to be metabolised by other CYPs, such as CYP2B6 and CYP2C8, already increases from a concentration of 5 μ M. The IC_{50} determined for Midazolam was 81.35 μ M after 72 h and 73.85 μ M after 7 days (Figure 2.9). After determining SRB for the cocktail as a combination, a final concentration for Midazolam of 0.25 μ M was implemented (Figure 2.11). The LC-MS/MS method was developed to be sensitive according to the concentration range of 0.4 ng/ml - 200 ng/ml for midazolam and 5 ng/ml - 2500 ng/ml for 1 - hydroxymidazolam*.

Omeprazole, as the CYP2C19 substrate, was combined in 21% of reported drug cocktails. The true drug of preference, when considering CYP2C19 metabolism, is (S)-mephenytoin. This was reportedly metabolized to 4-hydroxymephenytoin during its use in 49% of the perused drug cocktails. However, due to the lack of availability of the preference drug, omeprazole was favoured for use in this study. The interaction of omeprazole with CYP2C19 is considered specific up to concentrations of 40 μ M before specificity may be lost to CYP1A2, CYP2C9 and CYP2D6. To

confirm that 40 μM of omeprazole is a sub-toxic dose in HepG2 cells, the SRB cell enumeration assay assessed omeprazole concentrations between 0 μM – 100 μM and relevant cell toxicity was only found above the cross-induction threshold of 40 μM (Figure 2.9). After determining the safety threshold for the cocktail as a combination, a final concentration for omeprazole, of 2 μM was used (Figure 2.11).

All the analytes, with the exception of omeprazole, displayed optimal stability in a low pH environment. Omeprazole is known to degrade fairly rapidly and, therefore, differs in experimental preference, tending for alkaline conditions. During the performance of long-term stability testing, omeprazole was analysed using the same sample every hour for 2 days. A single full experiment analysis was calculated to be less than 48 h and was accepted as sufficient time for quantification. Omeprazole and 5-hydroxyomeprazole* have MRM transition pairs reported in literature with omeprazole at 198 m/z⁸⁷⁻⁸⁸ and 5-hydroxyomeprazole* at 214 m/z⁸⁸⁻⁸⁹. However, during LC-MS/MS optimisation in this study, the sensitivity evidently appeared higher for tested MRM pairs, both the pair selected from literature and the pair found in optimization in this study. During long term stability testing, results indicated that the tested MRM pair (chosen from literature) showed rapid degradation over time while the apparent MRM pair, obtained in this study and originally accredited to omeprazole, did not. This warranted further investigational optimization.

Contaminants with similar MRMs transition, determined for omeprazole and its metabolite (such as stearamide and dibutyl phthalate, respectively) was found after finalising the optimal chromatography conditions, and running the method using blank samples. The peaks observed at elution times, may therefore not have been for Omeprazole and 5-hydroxyomeprazole* The rapid degradation of omeprazole may have already been initiated in the injection vials prior to the acquisition of the cocktail. As the optimized methodology allowed for only single acquisitions, analysis of omeprazole, with its metabolite, was excluded from further experimentation in this study.

When initially testing for the potential toxicity of the cocktail, all of the drugs were confirmed safe to use at the concentrations reported in literature to avoid cross-induction of alternative CYPs. After individual toxicity was determined the combination was assessed at each drugs' respective max, max/2 and max/10 (Figure 2.10). In the initial SRB experiment of the combined cocktail, even the max/10 showed approximately 10% reduction in viability. Further dilutions were therefore selected and a viability threshold was determined at max/20 where no significant toxicity was displayed and the cytotoxic effect plateaued (Figure 2.11). Concentrations of max/10 presented as a viable option, however max/20 was selected to provide a margin of safety against cellular accumulation of drug/metabolite over multiple exposures in the downstream experiments.

The single-acquisition analytical LC-MS/MS method was developed by combining liquid chromatography with the use of a triple quadrupole mass spectrometer. Mass spectrometry parameters were optimized for the 10 chosen analytes of interest and for the internal standard, chosen to be imipramine (Table 3.1 and Table 3.2).

For the liquid chromatography segment of the method, the C18 and Biphenyl columns were considered for selection (Figure 3.1 and Figure 3.2). Optimization procedures involved comparison of both to opt for the column with most appropriate chemistry with analytes. Though the C18 column is most commonly used for reversed phase chromatography, the Biphenyl column was investigated as it presents hydrophobic interactions as well as π - π interactions. The property of containing phenyl moieties allows the capability of π - π interactions with compounds containing double bonds and increases separation ability for compounds with similar structure⁹⁰⁻⁹¹. As all of the analytes under investigation contain at least one aromatic ring, these potential π - π interactions may allow for better selectivity and better separation of the aromatic compounds relative to the C18 column.

When working with multiple analytes, the optimal chromatographic method often negatively impacts peak sensitivity/resolution of other analytes while attempting to improve a particular analyte. The C18 and Biphenyl columns were compared by running a spiked sample, at the same concentration of each of the combined drugs in the cocktail (100 ng/ml), using the best optimised method for each respective column. The hydrophobic particles of the C18 column provided increased peak sizes for acetaminophen, dextromethorphan, midazolam and OH-midazolam, indicating greater sensitivity of these analytes relative to the Biphenyl column. The resolution of OH-bupropion and dextromethorphan was also slightly higher in the C18 column. However, the overall best method was selected by taking all analytes into account and, even though the C18 performed better in some cases, most analytes responded clearer in the Biphenyl column. The distinctive π - π interactions formed by the Kinetex Biphenyl column may have allowed the increased selectivity and sensitivity which proved the column overall superior for this tailored drug cocktail.

Resolution is defined as the separation between two adjacent peaks on a chromatogram and is a fundamental characteristic to enable accurate quantification. Resolution is determined by the difference in retention time between two peaks. Retention time, selectivity and column efficiency affect resolution. For baseline separation between two peaks, a resolution of 1.5 is required. However, for quantitation a resolution value of 1 (where two peaks overlap by approximately 25%) is considered the minimum resolution for quantitation if relatively low ion suppression can be confirmed.

Despite acceptable separation between most of the analytes, peak overlap was observed between hydroxybupropion* and dextrorphan* as well as for 1-hydroxymidazolam* and

dextromethorphan. The chromatogram in Figure 3.6 displays that 1-hydroxymidazolam* and dextromethorphan overlapped just below their peak half height. 1-hydroxybupropion* and dextrophan* overlapped completely, indicating the likelihood of some ion suppression occurring for these peaks. These compounds are difficult to separate under the conditions used to separate multiple analytes. This is one challenge faced when separating multiple analytes in one method. Different chromatographic conditions were attempted to separate these specific analytes but with detrimental effects on the sensitivity and selectivity of the other analytes in the mixture.

Calibration curves were set up from which linearity, concentration dynamic range, accuracy, precision and the quantitation limit were determined. All analytes yielded a linear regression correlation of >0.985 (Table 3.6) which indicates that linearity is well established for all of the analytes. A flat gradient was found for all of the analytes. This is because the curve is generated by taking the AUC of the analyte over the AUC of the internal standard. The internal standard was spiked at a higher concentration (1 µg/ml) than the analytes, which gave excessively high peak areas for the internal standard.

Two similar studies were performed with a cocktail which included the six drugs of interest in addition to three others specific to CYPs not targeted in this study. Pooled human liver microsomes were used for inhibition studies, exposing the cells for only 60 min,⁹²⁻⁹³. This contrasts the study under current discussion where HepG2s cells were induced with continual exposure to low concentrations of the drug cocktail for 30 days. Other reports on methods have been stipulated the use of same number, but different types, of drugs. Such objectives involved assaying for one specific CYPs activity or made use of drugs targeting CYPs not assessed in this study. The objective of this project was to be able to detect any increase in metabolic potential of pre-treated HepG2 cells, therefore specific CYPs involved in a wide spectrum of drug metabolism were targeted. Hence, this project is the first to implement methodology, using these specific analytes below their maximum selective CYP induction ranges, for measuring the induction degree of the dominant drug-metabolising CYPs in cultured HepG2 cells.

The cytochrome enzymes responsible for metabolism of more than 95% of commonly prescribed drugs are CYP1A2, CYP2C9, CYP2C19, CYP2D6, CYP2B6 and CYP3A4/5. Therefore, the final objective after complete development of the drug cocktail methodology, was to assess the activities of these enzymes in the cells, after exposure to this drug cocktail when cultured in long and short-term inductions.

In the long-term induction procedure, potential induction was investigated by exposing cells to the drug cocktail at multiple points over a time frame of 30 days. From Figure 3.12 it was observed that constituents of diclofenac and bupropion were not metabolised to concentrations above the LLOQ in either monolayer or in spheroid culturing formats. Phenacetin, dextromethorphan and midazolam were found to be metabolised in both monolayer and

spheroid models. Phenacetin’s metabolism appeared specifically low as its associated metabolite, acetaminophen*, was detected in concentrations close to the LOQ, for both cell culture formats. Furthermore, dextromethorphan metabolism appeared higher in the monolayer than in its corresponding spheroid culture. Midazolam was metabolised to a greater extent in its spheroid format when compared to its monolayer format.

The short-term induction procedure of a single exposure drug cocktail (Figure 3.13), for only one 72 h cycle, yielded phenacetin, bupropion and diclofenac metabolite concentrations below the LLOQ in both cell culturing formats. In contrast, dextromethorphan was metabolised in the monolayer format but not in the spheroid format and no midazolam (notably, neither parent drug nor metabolite) was detected after only 72h of culturing.

As bupropion is not interactive with the enzymes of interest, it was included in the cocktail for only 72 h in both induction-time experiments (long-term and short-term procedures) as an intended control for cross-induction. Its associated metabolite did not form, indicating that no metabolic response occurred in either induction-time experiments and that no cross-induction was apparent. Once results between long-term and short-term experiments were compared, the ability of drugs to induce enzymes could be better inferred from metabolite formation between induction-time experiments. Overall apparent lack of metabolism in diclofenac indicated that no induction of CYP2C9 took place. The very low metabolite levels, associated with phenacetin, weakly suggestive of some metabolism possibly performed by induced CYP1A2, was noted after the long-term exposure as this minimal response caused uncertainty with regards to significance.

Table 4.1: Comparison of relative CYP450 mRNA expression from PHH and HepG2. Reprinted/redrawn with permission, licence number 4478910617077 ²³.

Cell model	1A1	1A2	2A6	2B6	2C9	2C19	2D6	2E1	3A4	3A5
PHH	100	100	100	100	100	100	100	100	100	100
HepG2	6.99	0.03	0.25	0.50	0.01	0.05	1.57	0.04	0.03	1.16

Dextromethorphan caused a metabolic increase for both monolayer time-induction experiments. This may potentially be due to successful induction. However, dextromethorphan induction was specifically directed to CYP2D6 which is an enzyme inherently expressed at relatively large volumes in HepG2 cells, when compared to the other main CYPs. Therefore, monolayer results may also have been influenced by CYP2D6 still present in the cells instead of only induced CYP2D6 enzyme. This is indicated in Table 4.1 first seen in the introduction and re-inserted above (Table 1.3), where inherent metabolic competency of HepG2 is compared to PHH, it confirmed that CYP2D6 has the highest inherent capacity among the five CYPs investigated in this study.

Although a capacity of 1.57% appears low it may still explain why the cell sustains the ability of its CYP2D6 to metabolise within monolayer cultures. As this study in the short-term conversion resulted in high metabolism of 17.98%, while only resulting in 5.5% metabolism in the long-term conversion, it may also be because of the suspected 1.57% having an influence and further proposes that this influence possibly decreased over time. The difference observed between the spheroidal and monolayer models when compared in both time induction experiments may be due to monolayer culture properties, being increased surface area, which allows for the relative ease with which drugs are imported. Thereby, potentially explaining why more dextromethorphan was able to reach monolayer cells. The increase in spheroid metabolism apparent in the long-term induction procedure (0.29%), appearing absent in the short-term culture, may still be too low for the change to significantly infer induction. Confirmation of this possible insignificance would require a spheroid model capable of a longer culture time.

The complete absence of midazolam results in the short-term induction with resulting lack of overall quantification of midazolam (or time-related degradation) prevented the comparison to long-term studies, complicating definitive interpretations (for example, as induction or accumulation) for the increase in metabolite formation in both monolayer and spheroid cultures. The implemented concentration, as determined for midazolam, may have been too low for investigations of the short-term response as the single exposure study, which may explain why midazolam presented with no detectable response. If the increase is assumed to be interpretable as an induction of CYP3A4, results indicate a higher response in spheroids (12.92%) relative to response achieved in the monolayer culture (7.45%). Drawing attention back to Table 4.1, midazolam is seen to only have a 0.03% inherent metabolism left in culture, substantiating enzyme induction as a possibility found in this studies' results. However, the CYP3A4 is the most abundant of the human CYP450 enzymes. Therefore, the number of CYP3A4 enzymes left within HepG2 cells before induction may yield enough basal activity to introduce bias in activity level results observed in this study, regardless of its metabolism capacity being only 0.03%. The ambiguity of induction would be countered if midazolam showed any quantifiable results in short term culture.

Metabolism capacity was not different when comparing spheroid and monolayer cultures using the complete induction and assay methods described for analysis, as the two drugs that were metabolised showed differing results, where monolayer showed improved metabolism in dextromethorphan and spheroid showed improved metabolism in midazolam. Phase III metabolism, involved in transport functions necessary for metabolism, may be decreased in HepG2 cells. As phase III metabolism is necessary for the transport of hydrophilic molecules out of the cells, there may still be some of the parent drugs and their metabolites within the cells. Therefore, absent from the supernatant and not seen due to a lack of extraction. Lysing cells may improve extraction and deter such bias.

HepG2 cell lines are still frequently used for toxicity testing, however if the phase I metabolic enzymes functionality was able to be increased, the model will have a greater application for determining hepatotoxicity.

4.2. Conclusion

Given the desire of modelling a HepG2 culture which may offer a closer resemblance to the human body, experiments observing CYP enzyme induction via specific drugs were performed in cells developed as spheroids for comparison to monolayers. The procedure of spheroid culturing was targeted to maintain both good morphology and viability over time, which resulted in a culture time of 6 days.

A drug cocktail dosage was sought that could provide a concentration able to elicit an induction response of specific cytochromes (given the condition of avoiding cross-induction) as well as being below cytotoxic levels. An appropriate dose was determined for each drug with the exception of midazolam. The relatively low concentration of midazolam, adhering to the parameters stated, potentially lead to the prevention of certain observations to be confirmed.

The study design intended for developing a single acquisition LC-MC/MS method, containing 12 analytes and an internal standard, which may allow the determination of parent drug vs metabolite for inferring active metabolism. The developed method was considered successful for evaluating a combination of 10 of the analytes. Complications with regards to the internal standard caused all analyte calibration curve gradients to be lowered, limiting the power of the method to identify small fluctuations in analyte concentrations.

Long- and short-term exposure to a drug cocktail containing phenacetin, dextromethorphan, diclofenac, midazolam and bupropion was finally assessed using the validated method established during this study. Metabolism was not consistent for the enzyme combination, as implemented in this study, as only certain drugs were sufficiently metabolised to quantify the metabolites. It is unclear whether or not the measured metabolism is because of enzyme induction, from inherent phase I metabolism potential or from problems regarding abnormalities of other inherent metabolism (such as possible phase III transporter inactivity) of the cells.

The overall aim of this study was to determine the degree to which long term exposure, to a tailored cytochrome inducing drug cocktail, could enhance CYP450 activity in both traditional monolayer and spheroid cell cultures at the level of the metabolome. This required establishing and characterising a 3D spheroid model for the HepG2 cells, determining a non-toxic dose of a drug cocktail that is selectively metabolised by six different CYPs, developing a quantitative LC-

MS/MS method for analysing these drugs and their respective CYP metabolites, culturing the HepG2 cells in the presence of the drug cocktail and final analysis of the drug metabolites.

Metabolism capacity was not different when comparing spheroid and monolayer cultures, as midazolam and dextromethorphan - the only sufficiently metabolised drugs - showed differing results. This may be due to possible phase III metabolism inactivity in *in vitro* models, leading to accumulation of hydrophilic metabolites within cells if extraction processes are not improved (for example, in this study this may have influence as cells were not lysed after induction for analysis). All the required objectives were successfully achieved and the finding was that the overall phase I metabolic capacity of the HepG2 cells were not increased for a drug cocktail as a whole for cells cultured in either the monolayer or the 3D spheroid format. It is encouraged to expand on this project with the extension of objectives to peruse the proteome and transcriptome (in conjunction with the metabolome) and with increased optimization as per suggestion listed under considerations.

4.3 Considerations

A constructive discussion of certain limitations and/or complications is necessary to consider prior to using this project as a framework for similar or derivative topics.

It is suggested that downstream complications in this study may be linked to limitations of culture outcomes in the first objective. Considerations that could allow for enhanced reproducibility include optimising cell culture methodology, improving induction experiments and broadening LC-MS/MS methodology for the full spectrum of drugs. Furthermore, recommendations are included here for expanding the possibilities to investigate.

With regards to cell culturing, the length of culturing time achieved by the spheroidal model was brief when compared to the viability established by the monolayer model in long-term culturing. This restricts the models capability to compare spheroidal and monolayer data. Therefore, further culturing optimisation should aim to increase the lifespan of spheroids. The optimal seeding density was chosen to produce compact spheroids at maximum size while maintaining viability. However, a publication by Curcio et al. 2007 indicated that spheroids have a nutrient diffusion limitation of 150 – 200 μm , therefore the selection of a lower seeding density spheroid would allow for a spheroid model of medium size but with a longer lifespan. Optimization parameters of spheroid culture methodology may be better determined by prioritising time of spheroid viability rather than volume of the spheroid.

As stated in the discussion, potential aberrations in results is introduced by possibilities such as the phenomenon of drugs and metabolites remaining within the cells instead of being excreted

into supernatant. Results obtained in induction, or drug related culturing, of the monolayers may overcome such limitations if the end-point analysis is exchanged for a kinetic study which increases observation. Such modulation at various time-points throughout the induction phase would require minimal alterations of the project design. It is recommended that cells and supernatant be collected during each passage for exposure to the drug metabolism assay and analysed to allow modulation of metabolic activity over time. However, for this advantageous enhancement to be applied to a spheroid model, methodology must diverge from what is described in this study to decrease spheroidal size nearing 200 μm . This will delay the necrotic core formation and diffusion limitations. As spheroid and supernatant collection is only possible after every 72 h, when media exchange takes place, modulation of the spheroids in this project would have been too sparse for a practical kinetic study. Additionally, precautions such as cell lysis or bullet-blending of the collected supernatant before analysis will aid in the extraction of intracellular parent drugs and metabolites.

The complication of the initial drug cocktail combination's cell toxicity, was reduced in this study by dividing the concentration of each individual drug by 20. The initial cocktail concentration of each individual drug, ascertained from literature as the maximum concentration to avoid cross-induction, was independently confirmed to be below the IC_{50} via SRB toxicity testing. A derivative study should also aim to evaluate every combinational drug-drug relationship acting on cells, as this could provide an improved cocktail using highest concentrations possible for each constituent drug to prevent toxicity as well as focusing on cross-induction. However, if this is considered as a secondary objective, it is suggested that the final drug cocktail could only modify the midazolam concentration used in this study. A midazolam modification is suggested as the concentration after uniform division (by 20) appeared to be potentially low enough to introduce bias. As seen from results, short term induction yielded no response from midazolam and its associated metabolite in both monolayer and spheroid formats. The long-term and short-term experiments was compared to determine if an increased exposure time is needed or may be useful in promoting CYP induction. The lack of response from midazolam creates ambiguity as to whether induction truly occurred or if a response was seen due to slow accumulation. Other limitations were potentially caused by a delay in the implementation of short-term induction culturing. This delay potentially provided adequate time for degradation of midazolam within the medium. To avoid this potential limitation short-term induction should be done either prior to or simultaneously with long-term induction.

For LC-MS/MS methodology utilised in this study, the internal standard of imipramine will have to be optimised to a lower concentration. This is necessary to allow for sensitive and accurate calibration curves, as the high concentration of imipramine in this study yielded points lying outside the analyte concentration range. This pushed analyte calibration curve gradients below a sensitive detection level. Optimisation would involve reducing the internal standard

concentration to mid-range concentrations for the analytes to improve the power of the method to identify small fluctuations in concentrations of analytes.

Omeprazole was removed from cocktail analysis as it did not adhere to the parameters set in the study design. If future studies would benefit from including omeprazole in a drug cocktail, some optimisation is needed, given that some extra steps be considered. The biggest problem encountered using omeprazole is that it degrades in acidic conditions. A separate method will have to be constructed, to analyse omeprazole alone, as all the other analytes require an acidic environment. This separate method could be done by using, for example, ammonium bicarbonate. This may increase the pH used during the extraction process as well as in the mobile phases. This would prevent a single high throughput method from being developed, as used in this study is to determine metabolic outcome, and possibly justify the use of two separate methods that allows all of the analytes to be analysed.

Outcomes of the study have the potential to be broadened by not just analysing the metabolome, but also including the proteome and the transcriptome of the HepG2 cells. By utilising a more encompassing study design, the overall picture generated will provide insight into where problems may occur. For example, surveying the mRNA expression or applying selected protein analysis to quantify CYP expression may provide for more robust investigations in the future.

Chapter 5: References

1. FDA [Internet] The drug development process. U.S. Food and Drug Administration; 2015 [updated 24/06/2015; cited 2016 10/06/2016]. Available from: <http://www.fda.gov/ForPatients/Approvals/Drugs/default.htm>.
2. Willmann JK, Van Bruggen N, Dinkelborg LM, Gambhir SS. Molecular imaging in drug development. *Nature reviews Drug discovery*. 2008; 7(7):591.
3. Morgan S, Grootendorst P, Lexchin J, Cunningham C, Greyson D. The cost of drug development: A systematic review. *Health Policy*. 2011; 100(1):4-17.
4. Walker D. The use of pharmacokinetic and pharmacodynamic data in the assessment of drug safety in early drug development. *Br J Clin Pharmacol*. 2004; 58(6):601-8.
5. Onakpoya IJ, Heneghan CJ, Aronson JK. Post-marketing withdrawal of 462 medicinal products because of adverse drug reactions: A systematic review of the world literature. *BMC Med*. 2016; 14(1):10.
6. Muller M, Muller-Zellenberg U, Hochhaus G, Derendorf H. Current concepts in pharmacokinetics and their implications for clinical medicine. *Wien Klin Wochenschr*. 2001; 113(15/16):565-72.
7. Langmajerová M, Řemínek R, Pelcová M, Foret F, Glatz Z. Combination of on-line ce assay with ms detection for the study of drug metabolism by cytochromes p450. *Electrophoresis*. 2015; 36(11-12):1365-73.
8. Weinshilboum R. Inheritance and drug response. *N Engl J Med*. 2003; 348(6):529-37.
9. Westerink WM, Schoonen WG. Phase ii enzyme levels in hepg2 cells and cryopreserved primary human hepatocytes and their induction in hepg2 cells. *Toxicol In Vitro*. 2007; 21(8):1592-602.
10. Xu C, Li CY-T, Kong A-NT. Induction of phase i, ii and iii drug metabolism/transport by xenobiotics. *Archives of pharmaceutical research*. 2005; 28(3):249-68.
11. Shen G, Kong AN. Nrf2 plays an important role in coordinated regulation of phase ii drug metabolism enzymes and phase iii drug transporters. *Biopharm Drug Dispos*. 2009; 30(7):345-55.
12. Klingenberg M. Pigments of rat liver microsomes. *Arch Biochem Biophys*. 1958; 75(2):376-86.
13. Hasler JA, Estabrook R, Murray M, Pikuleva I, Waterman M, Capdevila J, et al. Human cytochromes p450. *Mol Aspects Med*. 1999; 20(1):1-137.
14. Denisov IG, Makris TM, Sligar SG, Schlichting I. Structure and chemistry of cytochrome p450. *Chem Rev*. 2005; 105(6):2253-78.
15. Nelson DR. Cytochrome p450 nomenclature. *Cytochrome P450 Protocols*. 2006:1-10.
16. Nelson DR. The cytochrome p450 homepage. *Human Genomics*. 2009; 4(1):59.
17. Guengerich FP. Common and uncommon cytochrome p450 reactions related to metabolism and chemical toxicity. *Chem Res Toxicol*. 2001; 14(6):611-50.
18. Bernhardt R. Cytochromes p450 as versatile biocatalysts. *J Biotechnol*. 2006; 124(1):128-45.

19. Lamb DC, Waterman MR, Kelly SL, Guengerich FP. Cytochromes p450 and drug discovery. *Curr Opin Biotechnol*. 2007; 18(6):504-12.
20. Ingelman-Sundberg M, Rodriguez-Antona C. Pharmacogenetics of drug-metabolizing enzymes: Implications for a safer and more effective drug therapy. *Philosophical Transactions of the Royal Society of London B: Biological Sciences*. 2005; 360(1460):1563-70.
21. Zanger UM, Schwab M. Cytochrome p450 enzymes in drug metabolism: Regulation of gene expression, enzyme activities, and impact of genetic variation. *Pharmacol Ther*. 2013; 138(1):103-41.
22. Kamel A, Harriman S. Inhibition of cytochrome p450 enzymes and biochemical aspects of mechanism-based inactivation (mbi). *Drug Discovery Today: Technologies*. 2013; 10(1):e177-e89.
23. Gomez-Lechon M, Donato M, Lahoz A, Castell J. Cell lines: A tool for *in vitro* drug metabolism studies. *Current drug metabolism*. 2008; 9(1):1-11.
24. Hebert MF, Roberts JP, Prueksaritanont T, Benet LZ. Bioavailability of cyclosporine with concomitant rifampin administration is markedly less than predicted by hepatic enzyme induction. *Clin Pharmacol Ther*. 1992; 52(5):453-7.
25. Lynch T, Price A. The effect of cytochrome p450 metabolism on drug response, interactions, and adverse effects. *Am Fam Physician*. 2007; 76(3):391.
26. Martignoni M, Groothuis GM, de Kanter R. Species differences between mouse, rat, dog, monkey and human cyp-mediated drug metabolism, inhibition and induction. *Expert Opin Drug Metab Toxicol*. 2006; 2(6):875-94.
27. Bogaards J, Bertrand M, Jackson P, Oudshoorn M, Weaver R, Van Bladeren P, et al. Determining the best animal model for human cytochrome p450 activities: A comparison of mouse, rat, rabbit, dog, micropig, monkey and man. *Xenobiotica*. 2000; 30(12):1131-52.
28. Zuber R, Anzenbacherova E, Anzenbacher P. Cytochromes p450 and experimental models of drug metabolism. *J Cell Mol Med*. 2002; 6(2):189-98.
29. LeCluyse EL, Witek RP, Andersen ME, Powers MJ. Organotypic liver culture models: Meeting current challenges in toxicity testing. *Crit Rev Toxicol*. 2012; 42(6):501-48.
30. Costa A, Sarmiento B, Seabra V. An evaluation of the latest *in vitro* tools for drug metabolism studies. *Expert Opin Drug Metab Toxicol*. 2014; 10(1):103-19.
31. LeCluyse EL, Alexandre E, Hamilton GA, Viollon-Abadie C, Coon DJ, Jolley S, et al. Isolation and culture of primary human hepatocytes. *Basic Cell Culture Protocols*. 2005:207-29.
32. Vorrink SU, Ullah S, Schmidt S, Nandania J, Velagapudi V, Beck O, et al. Endogenous and xenobiotic metabolic stability of primary human hepatocytes in long-term 3d spheroid cultures revealed by a combination of targeted and untargeted metabolomics. *The FASEB Journal*. 2017; 31(6):2696-708.
33. López-Terrada D, Cheung SW, Finegold MJ, Knowles BB. Hepg2 is a hepatoblastoma-derived cell line. *Hum Pathol*. 2009; 40(10):1512-5.
34. Vouros P. Human hepatocellular carcinoma cell lines secrete the major plasma proteins and hepatitis b surface antigen. *Biomed Mass Spectrom*. 1975; 2:215.
35. Knowles BB, Aden DP. Human hepatoma derived cell line, process for preparation thereof, and uses therefor. *Google Patents*; 1983.

36. Yang Y, Tang X, Hao F, Ma Z, Wang Y, Wang L, et al. Bavachin induces apoptosis through mitochondrial regulated er stress pathway in hepg2 cells. *Biol Pharm Bull.* 2018; 41(2):198-207.
37. Tomas-Hernández S, Blanco J, Rojas C, Roca-Martínez J, Ojeda-Montes MJ, Beltrán-Debón R, et al. Resveratrol potently counteracts quercetin starvation-induced autophagy and sensitizes hepg2 cancer cells to apoptosis. *Molecular Nutrition and Food Research.* 2018.
38. Paech F, Mingard C, Grünig D, Abegg VF, Bouitbir J, Krähenbühl S. Mechanisms of mitochondrial toxicity of the kinase inhibitors ponatinib, regorafenib and sorafenib in human hepatic hepg2 cells. *Toxicology.* 2018; 395:34-44.
39. Ramirez T, Strigun A, Verlohner A, Huener H-A, Peter E, Herold M, et al. Prediction of liver toxicity and mode of action using metabolomics in vitro in hepg2 cells. *Arch Toxicol.* 2018; 92(2):893-906.
40. Sinz M, Wallace G, Sahi J. Current industrial practices in assessing cyp450 enzyme induction: Preclinical and clinical. *The AAPS journal.* 2008; 10(2):391-400.
41. Spaggiari D, Geiser L, Daali Y, Rudaz S. A cocktail approach for assessing the *in vitro* activity of human cytochrome p450s: An overview of current methodologies. *J Pharm Biomed Anal.* 2014; 101:221-37.
42. Dubach UC, Rosner B, Stürmer T. An epidemiologic study of abuse of analgesic drugs: Effects of phenacetin and salicylate on mortality and cardiovascular morbidity (1968 to 1987). *N Engl J Med.* 1991; 324(3):155-60.
43. Grosse Y, Baan R, Straif K, Secretan B, El Ghissassi F, Bouvard V, et al. A review of human carcinogens--part a: Pharmaceuticals. *The Lancet. Oncology.* 2009; 10(1):13.
44. Distlerath L, Reilly P, Martin M, Davis G, Wilkinson G, Guengerich F. Purification and characterization of the human liver cytochromes p-450 involved in debrisoquine 4-hydroxylation and phenacetin o-deethylation, two prototypes for genetic polymorphism in oxidative drug metabolism. *J Biol Chem.* 1985; 260(15):9057-67.
45. Tassaneeyakul W, Birkett DJ, Veronese ME, McManus ME, Tukey RH, Quattrochi LC, et al. Specificity of substrate and inhibitor probes for human cytochromes p450 1a1 and 1a2. *J Pharmacol Exp Ther.* 1993; 265(1):401-7.
46. Altman R, Bosch B, Brune K, Patrignani P, Young C. Advances in nsaid development: Evolution of diclofenac products using pharmaceutical technology. *Drugs.* 2015; 75(8):859-77.
47. Gan TJ. Diclofenac: An update on its mechanism of action and safety profile. *Curr Med Res Opin.* 2010; 26(7):1715-31.
48. Leemann T, Transon C, Dayer P. Cytochrome p450tb (cyp2c): A major monooxygenase catalyzing diclofenac 4'-hydroxylation in human liver. *Life Sci.* 1993; 52(1):29-34.
49. Tang W, Stearns RA, Wang RW, Chiu S-HL, Baillie TA. Roles of human hepatic cytochrome p450s 2c9 and 3a4 in the metabolic activation of diclofenac. *Chem Res Toxicol.* 1999; 12(2):192-9.
50. Olbe L, Carlsson E, Lindberg P. A proton-pump inhibitor expedition: The case histories of omeprazole and esomeprazole. *Nature reviews drug discovery.* 2003; 2(2):132-9.

51. Andersson T, Miners JO, Veronese ME, Tassaneeyakul W, Tassaneeyakul W, Meyer UA, et al. Identification of human liver cytochrome p450 isoforms mediating omeprazole metabolism. *Br J Clin Pharmacol*. 1993; 36(6):521-30.
52. Griissner A. Process for the manufacture of. Google Patents; 1950.
53. Siu A, Drachtman R. Dextromethorphan: A review of n-methyl-d-aspartate receptor antagonist in the management of pain. *CNS drug reviews*. 2007; 13(1):96-106.
54. Canning BJ. Central regulation of the cough reflex: Therapeutic implications. *Pulmonary Pharmacology and Therapeutics*. 2009; 22(2):75-81.
55. Walser A, Fryer RI, Benjamin L. Imidazo [1, 5- α][1, 4] benzodiazepines. Google Patents; 1979.
56. Arcangeli A, Antonelli M, Mignani V, Sandroni C. Sedation in pacu: The role of benzodiazepines. *Curr Drug Targets*. 2005; 6(7):745-8.
57. Bauer TM, Ritz R, Haberthür C, Haefeli W, Scollo-Lavizzari G, Ha H, et al. Prolonged sedation due to accumulation of conjugated metabolites of midazolam. *The Lancet*. 1995; 346(8968):145-7.
58. Mehta N. Meta chloro substituted-alpha-butylamino-propiofenones. Google Patents; 1974.
59. Golden RN, DeVane C, Laizure S, Rudorfer M, Sherer M, Potter W. Bupropion in depression. *Arch Gen Psychiatry*. 1988; 45:145-9.
60. Stahl SM, Pradko JF, Haight BR, Modell JG, Rockett CB, Learned-Coughlin S. A review of the neuropharmacology of bupropion, a dual norepinephrine and dopamine reuptake inhibitor. *Prim Care Companion J Clin Psychiatry*. 2004; 6(4):159.
61. Hesse LM, Venkatakrisnan K, von Moltke LL, Duan SX, Shader RI, Greenblatt DJ. Cyp2b6 mediates the in vitro hydroxylation of bupropion: Potential drug interactions with other antidepressants. *Drug Metabolism and Disposition*. 2000; 28(10):1176-83.
62. Horst WD, Preskorn SH. Mechanisms of action and clinical characteristics of three atypical antidepressants: Venlafaxine, nefazodone, bupropion. *J Affect Disord*. 1998; 51(3):237-54.
63. Kim S, Thiessen PA, Bolton EE, Chen J, Fu G, Gindulyte A, et al. Pubchem substance and compound databases. *Nucleic Acids Res*. 2015; 44(D1):1202-13.
64. Edmondson R, Broglie JJ, Adcock AF, Yang L. Three-dimensional cell culture systems and their applications in drug discovery and cell-based biosensors. *Assay and drug development technologies*. 2014; 12(4):207-18.
65. Pampaloni F, Reynaud EG, Stelzer EH. The third dimension bridges the gap between cell culture and live tissue. *Nature reviews Molecular cell biology*. 2007; 8(10):839-45.
66. Breslin S, O'Driscoll L. Three-dimensional cell culture: The missing link in drug discovery. *Drug discovery today*. 2013; 18(5):240-9.
67. Pickl M, Ries C. Comparison of 3d and 2d tumor models reveals enhanced her2 activation in 3d associated with an increased response to trastuzumab. *Oncogene*. 2009; 28(3):461-8.
68. Tung Y-C, Hsiao AY, Allen SG, Torisawa Y-s, Ho M, Takayama S. High-throughput 3d spheroid culture and drug testing using a 384 hanging drop array. *Analyst*. 2011; 136(3):473-8.

69. Ghosh S, Spagnoli GC, Martin I, Ploegert S, Demougin P, Heberer M, et al. Three-dimensional culture of melanoma cells profoundly affects gene expression profile: A high density oligonucleotide array study. *J Cell Physiol.* 2005; 204(2):522-31.
70. McKenzie R, Fried MW, Sallie R, Conjeevaram H, Di Bisceglie AM, Park Y, et al. Hepatic failure and lactic acidosis due to fialuridine (fiau), an investigational nucleoside analogue for chronic hepatitis b. *New England Journal of Medicine.* 1995; 333(17):1099-105.
71. Bell CC, Hendriks DF, Moro SM, Ellis E, Walsh J, Renblom A, et al. Characterization of primary human hepatocyte spheroids as a model system for drug-induced liver injury, liver function and disease. *Scientific Reports.* 2016; 6:25187.
72. Hasin Y, Seldin M, Lusic A. Multi-omics approaches to disease. *Genome Biol.* 2017; 18(1):83.
73. Karahalil B. Overview of systems biology and omics technologies. *Curr Med Chem.* 2016; 23(37):4221-30.
74. Wishart DS, Jewison T, Guo AC, Wilson M, Knox C, Liu Y, et al. Hmdb 3.0—the human metabolome database in 2013. *Nucleic Acids Res.* 2012; 41(D1):D801-D7.
75. Czaplicki S. Chromatography in bioactivity analysis of compounds. *Column chromatography: InTech;* 2013.
76. Zhang A, Sun H, Wang P, Han Y, Wang X. Modern analytical techniques in metabolomics analysis. *Analyst.* 2012; 137(2):293-300.
77. Aretz I, Meierhofer D. Advantages and pitfalls of mass spectrometry based metabolome profiling in systems biology. *International Journal of Molecular Sciences.* 2016; 17(5):632.
78. Emwas A-HM. The strengths and weaknesses of nmr spectroscopy and mass spectrometry with particular focus on metabolomics research. *Metabonomics: Springer;* 2015. p. 161-93.
79. Microtissues I [Internet] 3d petri dish®. Microtissues, Inc.; [cited 2016 01/05/2016]. Available from: <https://www.microtissues.com/>.
80. Smith PK, Krohn RI, Hermanson G, Mallia A, Gartner F, Provenzano M, et al. Measurement of protein using bicinchoninic acid. *Anal Biochem.* 1985; 150(1):76-85.
81. Vichai V, Kirtikara K. Sulforhodamine b colorimetric assay for cytotoxicity screening. *Nat Protoc.* 2006; 1(3):1112.
82. Ramaiahgari SC, Den Braver MW, Herpers B, Terpstra V, Commandeur JN, van de Water B, et al. A 3d in vitro model of differentiated hepg2 cell spheroids with improved liver-like properties for repeated dose high-throughput toxicity studies. *Archives of Toxicology.* 2014; 88(5):1083-95.
83. Lin R-Z, Chou L-F, Chien C-CM, Chang H-Y. Dynamic analysis of hepatoma spheroid formation: Roles of e-cadherin and β 1-integrin. *Cell Tissue Res.* 2006; 324(3):411-22.
84. Zhang B, Li Y, Wang G, Jia Z, Li H, Peng Q, et al. Fabrication of agarose concave petridish for 3d-culture microarray method for spheroids formation of hepatic cells. *Journal of Materials Science: Materials in Medicine.* 2018; 29(5):49.
85. Napolitano AP, Dean DM, Man AJ, Youssef J, Ho DN, Rago AP, et al. Scaffold-free three-dimensional cell culture utilizing micromolded nonadhesive hydrogels. *Biotechniques.* 2007; 43(4):494-500.

86. Curcio E, Salerno S, Barbieri G, De Bartolo L, Drioli E, Bader A. Mass transfer and metabolic reactions in hepatocyte spheroids cultured in rotating wall gas-permeable membrane system. *Biomaterials*. 2007; 28(36):5487-97.
87. Sudha T, Reddy KK, Hemalatha P, Ravikumar V. An lc-ms/ms method for the determination of omeprazole on proton pump inhibitor in human plasma. *INDONESIAN JOURNAL OF PHARMACY*. 2016; 27(2):80.
88. Ishii M, Sato M, Ogawa M, Takubo T, Hara Ki, Ishii Y. Simultaneous determination of omeprazole and its metabolites (5'-hydroxyomeprazole and omeprazole sulfone) in human plasma by liquid chromatography-tandem mass spectrometry. *Journal of Liquid Chromatography and Related Technologies*. 2007; 30(12):1797-810.
89. Gor P, Alnouti Y, Reed GA. Buspirone, fexofenadine, and omeprazole: Quantification of probe drugs and their metabolites in human plasma. *J Pharm Biomed Anal*. 2011; 55(5):1127-35.
90. Reubsaet JLE, Vieskar R. Characterisation of π - π interactions which determine retention of aromatic compounds in reversed-phase liquid chromatography. *J Chromatogr A*. 1999; 841(2):147-54.
91. Long W, Mack A. Comparison of selectivity differences among different agilent zorbax phenyl columns using acetonitrile or methanol. Agilent Technologies Publication. 2009.
92. Kim H, Choi HK, Jeong TC, Jahng Y, Kim DH, Lee S-H, et al. Selective inhibitory effects of mollugin on cyp1a2 in human liver microsomes. *Food and Chemical Toxicology*. 2013; 51:33-7.
93. Jahng Y, Kwon OK, Lee S. In vitro inhibitory effect of luotonin a on human cyp1a. *Archives of Pharmacal Research*. 2012; 35(12):2199-203.

Chapter 6: Addendum

Addendum 1: Original ethics letter

The Research Ethics Committee, Faculty Health Sciences, University of Pretoria complies with ICH-GCP guidelines and has US Federal wide Assurance.

- FWA 00002567, Approved dd 22 May 2002 and Expires 28 August 2018.
- IRB 0000 2235 IORG0001762 Approved dd 22/04/2014 and Expires 22/04/2017.



UNIVERSITEIT VAN PRETORIA
UNIVERSITY OF PRETORIA
YUNIBESITHI YA PRETORIA

Faculty of Health Sciences Research Ethics Committee

24/11/2016

Approval Certificate New Application

Ethics Reference No.: 438/2016

Title: Comparison of metabolome attenuation in monolayer and three dimensional hepatocyte cultures

Dear Mr Gerben de Koker

The **New Application** as supported by documents specified in your cover letter dated 17/10/2016 for your research received on the 17/10/2016, was approved by the Faculty of Health Sciences Research Ethics Committee on its quorate meeting of 23/11/2016.

Please note the following about your ethics approval:

- Ethics Approval is valid for 1 year
- Please remember to use your protocol number (**438/2016**) on any documents or correspondence with the Research Ethics Committee regarding your research.
- Please note that the Research Ethics Committee may ask further questions, seek additional information, require further modification, or monitor the conduct of your research.

Ethics approval is subject to the following:

- The ethics approval is conditional on the receipt of **6 monthly written Progress Reports**, and
- The ethics approval is conditional on the research being conducted as stipulated by the details of all documents submitted to the Committee. In the event that a further need arises to change who the investigators are, the methods or any other aspect, such changes must be submitted as an Amendment for approval by the Committee.

We wish you the best with your research.

Yours sincerely

Dr R Sommers: MChB; MMed (Int); MPharMed, PhD
Deputy Chairperson of the Faculty of Health Sciences Research Ethics Committee, University of Pretoria

The Faculty of Health Sciences Research Ethics Committee complies with the SA National Act 61 of 2003 as it pertains to health research and the United States Code of Federal Regulations Title 45 and 46. This committee abides by the ethical norms and principles for research, established by the Declaration of Helsinki, the South African Medical Research Council Guidelines as well as the Guidelines for Ethical Research: Principles Structures and Processes, Second Edition 2015 (Department of Health).

☎ 012 356 3084 ✉ deepeka.behari@up.ac.za / fnsethics@up.ac.za 🌐 <http://www.up.ac.za/healthethics>
✉ Private Bag X323, Arcadia, 0007 - Tswelopele Building, Level 4, Room 60, Gezina, Pretoria

Addendum 2: Ethics extension letter



UNIVERSITEIT VAN PRETORIA
UNIVERSITY OF PRETORIA
YUNIBESITHI YA PRETORIA

Faculty of Health Sciences Research Ethics Committee

29/03/2018

Mr Gerben de Koker
Department of Pharmacology
University of Pretoria

Dear Mr Gerben de Koker

RE.: 438/2016 ~ Letter dated 12 March 2018

438/2016 de Koker	
Protocol Title	Comparison of metabolome attenuation in monolayer and three dimensional hepatocyte cultures
Principal Investigator	Mr Gerben de Koker, Tel: Email: Dept: Pharmacology

We hereby acknowledge receipt of the following document:

- Extension of study until the end of December 2018

which has been approved at 28 March 2018 meeting.

With regards

Dr R Sommers; MBChB; MMed (Int); MPharm; PhD
Deputy Chairperson of the Faculty of Health Sciences Research Ethics Committee, University of Pretoria

☎ 012 356 3085 📧 fhsethics.up.ac.za 🌐 <http://www.up.ac.za/healthethics>
✉ Private Bag X323, Arcadia, 0007 - Tswelopele Building, Level 4-59, Gezina, Pretoria